



**Fakultät für Medizin**

**Abteilung für Diagnostische und Interventionelle Neuroradiologie**

# **Tractography of language pathways based on navigated transcranial magnetic stimulation in patients with brain tumors**

**Nico Sollmann**

Vollständiger Abdruck der von der Fakultät für Medizin der Technischen Universität München zur Erlangung des akademischen Grades eines

**Doctor of Philosophy (Ph.D.)**

genehmigten Dissertation.

**Vorsitzender:** Prof. Dr. Arthur Konnerth

**Betreuer:** Prof. Dr. Claus Zimmer

**Prüfer der Dissertation:**

1. Priv.-Doz. Dr. Sandro M. Krieg
2. Prof. Dr. Florian Heinen

Die Dissertation wurde am 03.07.2017 bei der Fakultät für Medizin der Technischen Universität München eingereicht und durch die Fakultät für Medizin am 17.08.2017 angenommen.



## PUBLICATIONS INCLUDED IN THIS THESIS

---

1. Feasibility of nTMS-based DTI fiber tracking of language pathways in neurosurgical patients using a fractional anisotropy threshold.  
Sollmann N, Negwer C, Ille S, Maurer S, Hauck T, Kirschke JS, Ringel F, Meyer B, Krieg SM. J Neurosci Methods. 2016 Jul 15;267:45-54. doi: 10.1016/j.jneumeth.2016.04.002. Epub 2016 Apr 6.
2. Language pathway tracking: comparing nTMS-based DTI fiber tracking with a cubic ROIs-based protocol.  
Negwer C, Sollmann N, Ille S, Hauck T, Maurer S, Kirschke JS, Ringel F, Meyer B, Krieg SM. J Neurosurg. 2017 Mar;126(3):1006-1014. doi: 10.3171/2016.2.JNS152382. Epub 2016 May 27.
3. Interhemispheric connectivity revealed by diffusion tensor imaging fiber tracking derived from navigated transcranial magnetic stimulation maps as a sign of language function at risk in patients with brain tumors.  
Sollmann N, Negwer C, Tussis L, Hauck T, Ille S, Maurer S, Giglhuber K, Bauer JS, Ringel F, Meyer B, Krieg SM. J Neurosurg. 2017 Jan;126(1):222-233. doi: 10.3171/2016.1.JNS152053. Epub 2016 Apr 1.

# TABLE OF CONTENTS

---

<b>1. INTRODUCTION</b> .....	<b>1</b>
1.1. Models of human language organization .....	1
1.1.1. Classical concept .....	1
1.1.2. Contemporary models .....	2
1.2. Mapping language function .....	6
1.2.1. Direct electrical stimulation.....	6
1.2.2. Transcranial magnetic stimulation .....	7
1.3. Objectives of the included publications.....	9
<b>2. MATERIALS AND METHODS</b> .....	<b>10</b>
2.1. Ethics approval.....	10
2.2. Patients .....	10
2.3. Setup and procedures .....	10
2.4. Clinical assessment.....	11
2.5. Magnetic resonance imaging.....	12
2.6. Navigated transcranial magnetic stimulation.....	12
2.6.1. Experimental setup .....	12
2.6.2. Determination of the resting motor threshold.....	15
2.6.3. Object-naming task and baseline .....	17
2.6.4. Mapping procedure .....	19
2.6.5. Mapping analysis .....	22
2.7. Diffusion tensor imaging fiber tracking.....	24
2.7.1. Experimental setup .....	24
2.7.2. Tractography procedure .....	24
2.7.3. Tractography analysis .....	26
2.8. Surgical procedure .....	27
2.9. Statistical analysis .....	28
<b>3. RESULTS</b> .....	<b>30</b>
3.1. Feasibility of nTMS-based DTI fiber tracking of language pathways in neurosurgical patients using a fractional anisotropy threshold .....	30
3.1.1. Key findings .....	30
3.1.2. Own contribution .....	33
3.2. Language pathway tracking: comparing nTMS-based DTI fiber tracking with a cubic ROIs-based protocol .....	34
3.2.1. Key findings .....	34

3.2.2. Own contribution .....	37
3.3. Interhemispheric connectivity revealed by diffusion tensor imaging fiber tracking derived from navigated transcranial magnetic stimulation maps as a sign of language function at risk in patients with brain tumors .....	37
3.3.1. Key findings .....	37
3.3.2. Own contribution .....	40
<b>4. DISCUSSION.....</b>	<b>41</b>
4.1. Tractography based on nTMS data .....	41
4.2. Feasibility and superiority of nTMS-based DTI FT of language-related pathways.....	43
4.3. Risk stratification by nTMS-based DTI FT of language-related pathways .....	44
4.4. Significance and implications .....	45
4.5. Limitations.....	48
4.6. Outlook.....	50
<b>5. SUMMARY.....</b>	<b>53</b>
<b>6. REFERENCES.....</b>	<b>54</b>
<b>7. LIST OF ABBREVIATIONS.....</b>	<b>70</b>
<b>8. LIST OF FIGURES AND TABLES.....</b>	<b>72</b>
8.1. Figures.....	72
8.2. Tables .....	73
<b>9. ACKNOWLEDGEMENTS.....</b>	<b>74</b>
<b>10. PUBLICATIONS .....</b>	<b>76</b>
10.1. Original Articles .....	76
10.2. Case Reports .....	81
<b>11. APPENDIX: ORIGINAL PUBLICATIONS.....</b>	<b>82</b>
11.1. Feasibility of nTMS-based DTI fiber tracking of language pathways in neurosurgical patients using a fractional anisotropy threshold .....	83
11.2. Language pathway tracking: comparing nTMS-based DTI fiber tracking with a cubic ROIs-based protocol .....	93
11.3. Interhemispheric connectivity revealed by diffusion tensor imaging fiber tracking derived from navigated transcranial magnetic stimulation maps as a sign of language function at risk in patients with brain tumors .....	102

# 1. INTRODUCTION

---

## 1.1. Models of human language organization

### 1.1.1. Classical concept

“The limits of my language mean the limits of my world.”

*Ludwig J. J. Wittgenstein (1889 – 1951), Austrian-British philosopher*

This quote by Ludwig J. J. Wittgenstein depicts the fundamental role of language for the human being as appropriately and aesthetically as possible. Language function does not only allow us to communicate with other people and understand the context of words, but is also the universal vehicle used to transport meaning and knowledge over centuries of human development. The birth of this great philosopher fell in the period of the first evolving theories of language organization and representation within the human brain, later referred to as the classical model. This model is inextricably linked to Paul Broca and Karl Wernicke (Broca, 1861; Wernicke, 1874).

The early observations of Broca, Wernicke, and others were primarily based on lesion studies (Berker et al., 1986; Broca, 1861; Chang et al., 2015; Stookey, 1963; Wernicke, 1874). Thus, most of the patients studied by Broca had lesions spatially overlapping with parts of the inferior frontal gyrus (IFG), which were mainly constituted by the pars triangularis of the IFG (trIFG) and the pars opercularis of the IFG (opIFG) of the left hemisphere (LH), or were located in adjacent perisylvian areas (Berker et al., 1986). These patients presented with a loss of the ability to speak or articulatory errors, which presumably occurred due to the specific localizations of the lesions (Berker et al., 1986). The work of Broca later resulted in the naming of these cortical areas after him (Figure 1).

In contrast, Wernicke studied patients who presented with lesions within the posterior superior temporal lobe (pSTL) that he associated with paraphasic errors, impaired naming, and disrupted comprehension, but with fluent articulation and speech (Wernicke, 1874). This region subsequently became known as the Wernicke's area (Figure 1). Furthermore, Wernicke proposed that the pSTL might be connected to the anteriorly located perisylvian regions described by Broca (Wernicke, 1874). Based on the findings by Broca and Wernicke, the classical model of language organization and representation is known to be composed of 2 discrete language sites (Broca's and Wernicke's area) which are involved in 2 distinct functions (motor language processing and sensory language processing) and are interconnected by subcortical fibers (Figure 1) (Chang et al., 2015).

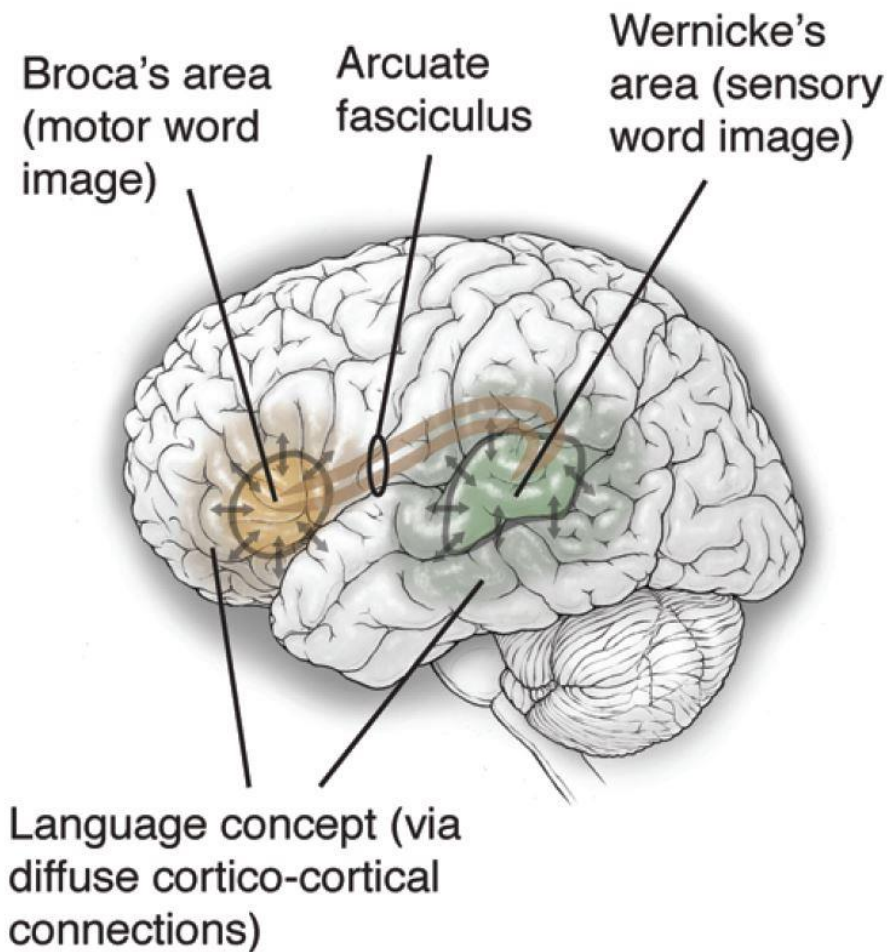


**Figure 1: Classical model of language organization**

The classical model is primarily composed of the Broca's area (brown), Wernicke's area (green), and a fiber tract interconnecting both sites (later referred to as the arcuate fascicle; brown) (Chang et al., 2015). Both cortical areas were already thought to be involved in different aspects of language function during early research (Chang et al., 2015).

### 1.1.2. Contemporary models

In subsequent research, the classical model was repeatedly challenged, with 2 main issues arising, which had not been sufficiently addressed in the early concept (Chang et al., 2015; Friederici and Gierhan, 2013). First, Broca's or Wernicke's aphasia have been shown to not only result from circumscribed lesions to the Broca's or Wernicke's area, thus probably underscoring the impact of isolated or combined damage to subcortical structures (Anderson et al., 1999; Bogen and Bogen, 1976; Chang et al., 2015; Mohr et al., 1978). Second, inherent linguistic complexities were not considered to a sufficient degree (e.g., differences between lexical, semantic, and phonological processing) (Poeppel and Hickok, 2004). These and other issues led to a stepwise and still ongoing development of the classical model into

more contemporary models that are in better agreement with modern findings on language organization and representation.

The currently existing, contemporary models arise from the theories on dual streams of language processing, which are reflected by dorsal and ventral streams (Chang et al., 2015; Friederici and Gierhan, 2013; Hickok and Poeppel, 2004; Rauschecker, 2012; Rauschecker and Scott, 2009). Incoming sounds are suggested to be first processed within the pSTL and superior temporal sulcus, which reflect main components of the Wernicke's area. The ventral stream is thought to be involved in speech recognition and lexical concepts and flows through to the anterior temporal lobe (ATL) and middle temporal lobe (MTL; Figure 2) (Chang et al., 2015; Friederici and Gierhan, 2013). The dorsal stream is suggested to be engaged in spatial processing and sensorimotor integration by conflating phonological information and articulatory motor representations, and it involves portions of the IFG, partially overlapping with the Broca's area, the premotor cortex, and the parieto-temporal boundary region (Figure 2) (Chang et al., 2015; Friederici and Gierhan, 2013). While the dorsal stream is thought to be left-dominant, the ventral stream is likely to be represented bilaterally without a clear dominance in favour of one hemisphere (Chang et al., 2015; Damasio, 1992).

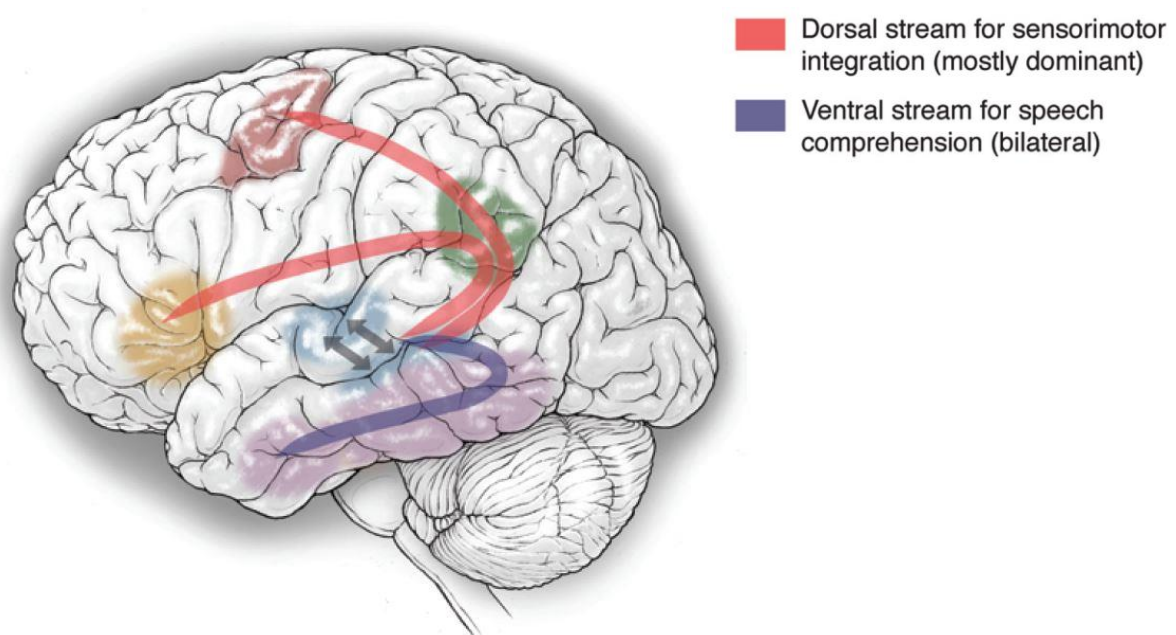


**Figure 2: Contemporary model of language organization**

*Contemporary models are heavily based on the theory of 2 principal streams of language processing, which are the ventral (red) and dorsal (purple) stream (Chang et al., 2015). These streams flow through different brain structures of the frontal (brown & yellow), parietal (green), and temporal (blue & purple) lobe (Chang et al., 2015).*

Furthermore, contemporary views on language organization and representation also aim to include subcortical white matter (WM) pathways as structural correlates for information transmission and processing of the aforementioned tasks implemented in the model of dual streams. Regarding such language-related WM pathways, the arcuate fascicle (AF) and the superior longitudinal fascicle (SLF) are the largest tracts, and they are believed to be part of the dorsal stream (Chang et al., 2015; Friederici and Gierhan, 2013). The AF primarily connects posterior temporal and fronto-opercular cortical sites, partially overlapping with the Broca's and Wernicke's area, but also presents various additional terminations (Figures 1 & 3) (Catani and Thiebaut de Schotten, 2008; Chang et al., 2015). Lesions to the AF can lead to conduction aphasia, which has already been suggested by the early work of Wernicke (Anderson et al., 1999; Wernicke, 1874). The SLF can be subdivided into 4 main components, which are the SLF I, SLF II, SLF III, and SLF-tp, each of which serve different specific functions during language processing except for the SLF I (Figure 3) (Catani and Thiebaut de Schotten, 2008; Chang et al., 2015; Fridriksson et al., 2010; Galantucci et al., 2011; Leclercq et al., 2010; Makris et al., 2005). The inferior fronto-occipital fascicle (FoF) is assumed to be one of the longest WM pathways involved in language processing, belongs to the ventral stream, and is engaged in semantic and syntactic processing (Figure 3) (Catani and Thiebaut de Schotten, 2008; Chang et al., 2011; Leclercq et al., 2010). The uncinate fascicle (UC), which connects the ATL to the IFG, is also said to play an important role in semantic function, but this is still discussed controversially (Figure 3) (Catani and Thiebaut de Schotten, 2008; Chang et al., 2015; Duffau et al., 2009; Papagno et al., 2011). Besides these major and comparatively well-investigated tracts, further WM pathways, such as the inferior longitudinal fasciculus (ILF), corticonuclear tract (CNT), short arcuate fibers (ArF), corticothalamic fibers (CtF), and commissural fibers (CF) are taken into account in contemporary models (Figure 3) (Axer et al., 2013; Bello et al., 2008; Catani et al., 2002; Catani and Thiebaut de Schotten, 2008; Chang et al., 2015; Friederici and Gierhan, 2013; Gierhan, 2013). In conclusion, when considering contemporary models versus the classical model of language organization and representation, language processing seems to exist within a complex network that is composed of both cortical areas and various, but specific subcortical WM pathways subserving different functional aspects.

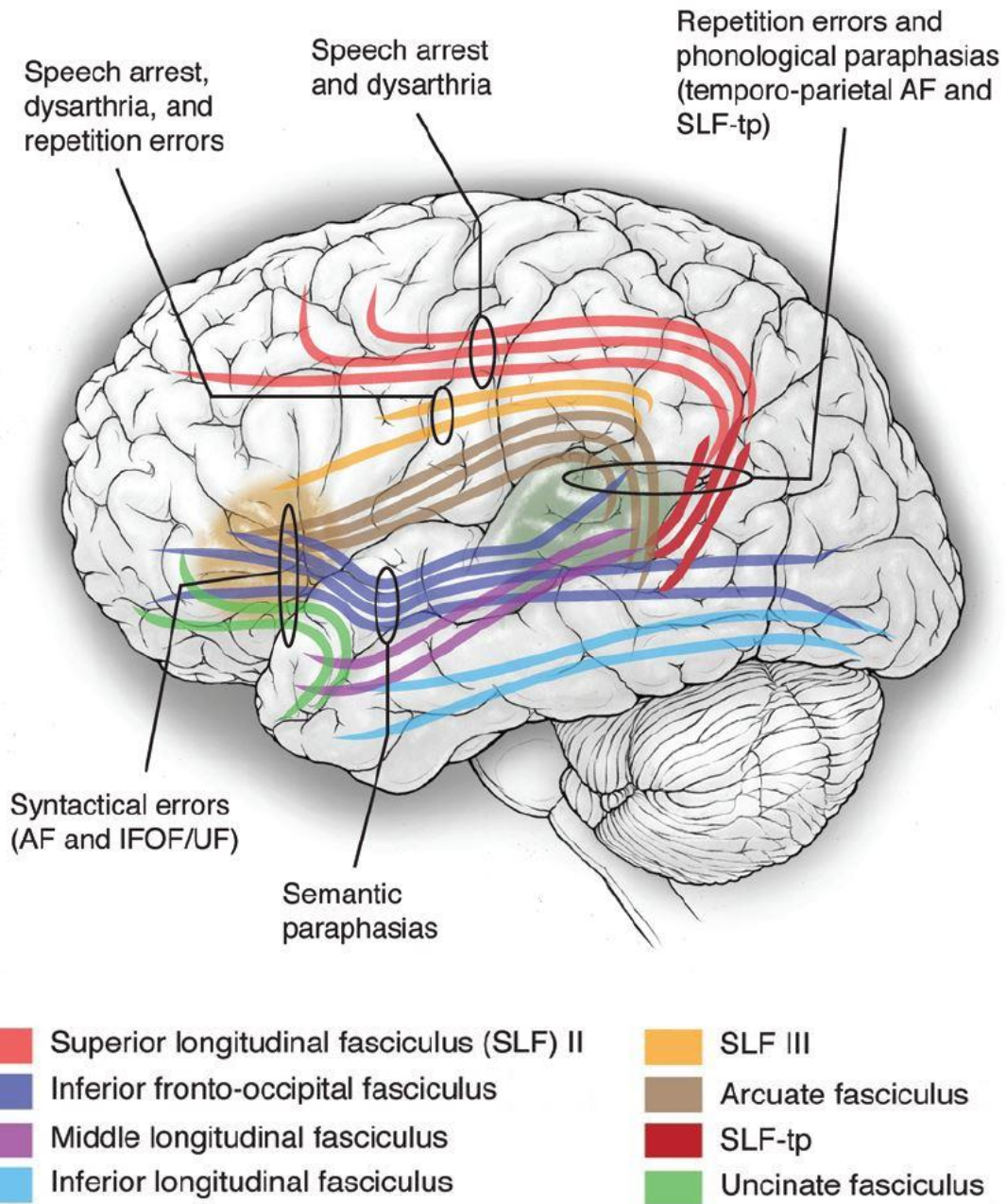


**Figure 3: Subcortical white matter (WM) pathways involved in language processing**

According to contemporary models, language processing is not only mediated by cortical areas (Chang et al., 2015). Instead, it also includes various subcortical WM pathways that are composed of, but not limited to the arcuate fascicle (AF), superior longitudinal fascicle (SLF), inferior longitudinal fascicle (ILF), inferior fronto-occipital fascicle (FoF), and uncinate fascicle (UC) (Chang et al., 2015).

## **1.2. Mapping language function**

### **1.2.1. Direct electrical stimulation**

The current gold standard to test whether a brain structure is involved in language function is reflected by intraoperative direct electrical stimulation (DES) during awake surgery, which was first reported in neurosurgical patients by Wilder Penfield (Feindel, 1982; Penfield and Roberts, 1959). In principle, intraoperative DES is a highly invasive technique that requires opening of the skull and dura in order to allow the neurosurgeon to put a handheld stimulation probe directly on cortical areas or subcortical structures to map either cortex or WM fibers (Chang et al., 2015; Mandonnet et al., 2010; Szelenyi et al., 2010). This is conducted in awake and conscious patients that are advised to perform one or more language-related tasks (e.g., object naming) during stimulation (Talacchi et al., 2013). The induced current can produce language disturbance during task performance, which allows the investigator to parcellate the cortex into language-positive (spots at which an error was elicited) and language-negative (spots at which no error was elicited) sites (Corina et al., 2010; Haglund et al., 1994). Correspondingly, subcortical DES can be used to reveal language-related WM pathways with respect to a similar principle: if subcortical DES produces an error at a specific site, the stimulated area is likely to be involved in language function; at least with respect to the language subfunctions the applied task was able to activate (Duffau, 2015; Sanai and Berger, 2010). A variety of different errors can be elicited during cortical or subcortical DES, which can be categorized and used to further specify the function of certain brain structures (Corina et al., 2010; Ojemann and Mateer, 1979; Ojemann, 1991; Penfield and Roberts, 1959; Sanai et al., 2008).

In specialized neurosurgical centers, cortical and subcortical DES is applied to systematically map the brain for language-positive sites during surgery when resecting tumors presumably located within language-eloquent parts of the brain. This is important as the language network is complex and widespread, thus making it difficult to operate on the brain without continuous information about the spatial relation between the resection area and adjacent language-related sites (Chang et al., 2015; Mandonnet et al., 2010; Szelenyi et al., 2010). Furthermore, the brain harbors a large plastic potential, which becomes evident in the context of tumor-induced reallocation of functional language-related areas and, therefore, can be made responsible for dramatic discrepancies between individual functional anatomy and standard language maps derived from healthy individuals (Duffau, 2014b; Duffau et al., 2002; Robles et al., 2008; Southwell et al., 2016). Accordingly, intraoperative DES is crucial to map individual language-related structures and to preserve language function during resection. This allows the neurosurgeon to operate according to a simple principle (Duffau and Mandonnet, 2013): he or she aims to remove as much tumor-infiltrated brain tissue as

possible whilst trying to preserve as much function as possible, a concept referred to as the so-called “onco-functional balance”. Together with chemo- and radiotherapy, surgical tumor removal including intraoperative DES is an important part of a multimodal treatment approach that aims to extend the overall survival of patients whilst preserving a maximum of quality of life and function (Capelle et al., 2013; De Witt Hamer et al., 2012; Duffau and Mandonnet, 2013; Jakola et al., 2012). In this context, it has repeatedly been shown that a maximum extent of resection is crucial for prolonged survival and can be facilitated by intraoperative DES (Ammirati et al., 1987; Hervey-Jumper and Berger, 2014; Sanai and Berger, 2008; Smith et al., 2008; Stummer et al., 2008).

### **1.2.2. Transcranial magnetic stimulation**

Transcranial magnetic stimulation (TMS) was initially demonstrated to be able to elicit visible motor responses after stimulation of the motor cortex by Anthony Barker (Barker et al., 1985). During TMS, a short-lived magnetic field is induced, which then develops rapidly into a transient electric field capable of modulating nerve cells under a stimulating handheld coil (Barker et al., 1985; Hallett, 2000; Rossini et al., 1994; Rossini et al., 2015). Although initially introduced to stimulate the motor cortex, the technique continuously increased in its applicabilities, thus enabling the stimulation of language-related brain areas and induction of language disturbances (Devlin and Watkins, 2007; Epstein et al., 1999; Michelucci et al., 1994; Pascual-Leone et al., 1991).

Early TMS approaches were performed without neuronavigation, thus making it difficult to determine precisely where the stimulation actually hit the brain. However, the development of combinations of neuronavigation and TMS systems enabled more focused stimulation with control of the stimulation site according to individual brain anatomy (Ettinger et al., 1998; Ruohonen and Karhu, 2010). Thanks to this development, navigated TMS (nTMS) became feasible for presurgical diagnostics where the cortex of patients harboring supratentorial brain tumors is systematically mapped to gain information about the exact location and extent of functional regions, such as motor- or language-related areas (Krieg et al., 2012b; Krieg et al., 2013a; Picht et al., 2013; Picht et al., 2009; Tarapore et al., 2013; Tarapore et al., 2012). Similar to cortical DES for language mapping, nTMS can be used to induce language disturbances during performance of a language-related task, thus allowing the differentiation of language-positive and language-negative sites on the cortical surface (Picht et al., 2013; Tarapore et al., 2013). The resulting language maps can then be used for surgical planning and resection guidance in patients with brain tumors presumably located within language-eloquent parts of the brain (Picht et al., 2013; Tarapore et al., 2013).

In recent years, language mapping by nTMS has shown to be a useful clinical technique that should be applied in addition to intraoperative DES (Picht, 2014). In this context, it may provide several benefits to both the patient and the neurosurgeon. First, nTMS has shown to be more accurate in localizing language function when compared to task-based functional magnetic resonance imaging (fMRI) or magnetoencephalography (MEG) using standard protocols, thus suggesting that it might be superior to these more common modalities in the preoperative neurosurgical setting (Sollmann et al., 2013; Tarapore et al., 2013). Consequently, the use of nTMS facilitates improved detectability of language-related areas preoperatively, thus providing the neurosurgeon with useful data. Second, the availability of nTMS language maps during preoperative planning and resection guidance has shown to result in improved clinical outcomes from the patients' perspectives (Sollmann et al., 2015b). Thus, nTMS may help to achieve a better onco-functional balance, which has already been discussed as a crucial parameter for intraoperative DES and neuro-oncology per se (Duffau and Mandonnet, 2013). Third, in contrast to intraoperative DES, nTMS is a non-invasive technique that can be used preoperatively to prepare the patient for intraoperative DES and to increase awareness about risks and benefits related to tumor resection with respect to visualization of the patients' individual functional anatomy (Picht, 2014; Sollmann et al., 2017a). Fourth, nTMS can be applied preoperatively to detect tumor-induced plastic reallocation of language-related sites similar to intraoperative DES (Krieg et al., 2013b; Krieg et al., 2014b; Rosler et al., 2014). The neurosurgeon can therefore be alerted to altered functional anatomy prior to tumor resection, which can help to adjust surgical approaches and to find more adequate surgical strategies. These benefits are achieved by a technique that is similar to the gold standard of intraoperative DES and has proven to be safe and well tolerated by the individual patient (Rossi et al., 2009; Tarapore et al., 2016).

Although language mapping by nTMS is increasingly being used in neurosurgery and is continuously expanding its application as a powerful preoperative technique, it is limited in a critical aspect when compared to intraoperative DES. Whereas intraoperative DES can be used to map both cortical and subcortical structures, nTMS is mainly restricted to stimulation of cortical areas without providing details about subcortical language-related WM pathways. This important limitation was therefore made the focus of the publications included in this thesis. We hypothesized that subcortical maps of language-related WM pathways can be achieved by combining language mapping by nTMS with diffusion tensor imaging fiber tracking (DTI FT), thus enabling nTMS-based DTI FT.

### **1.3. Objectives of the included publications**

This thesis includes 3 publications on nTMS-based DTI FT of language-related WM pathways (Negwer et al., 2017; Sollmann et al., 2016d; Sollmann et al., 2017b). Since nTMS-based DTI FT of language-related WM pathways represents a novel approach, the objective of the first publication was to assess feasibility in the context of detecting 9 language-related WM pathways known in the literature (Sollmann et al., 2016d). Based on these results, the second publication aims to compare nTMS-based DTI FT of these WM pathways to conventional anatomy-based DTI FT, which reflects the traditional and widely used technique to track subcortical language-related pathways in neurosurgery, in order to evaluate whether our new method can improve tractography results (Negwer et al., 2017). The objective of the third publication was then to expand the applicability of the new method beyond the level of detecting known WM pathways: it aims to explore the perspectives of risk stratification based on tractography of interhemispheric connectivity (IC) by means of nTMS-based DTI FT (Sollmann et al., 2017b).

## **2. MATERIALS AND METHODS**

---

### **2.1. Ethics approval**

The experimental protocols and procedures of the publications included in this thesis were approved by our local ethical committee (Technical University of Munich; registration number: 2793/10) in accordance with the Declaration of Helsinki. All patients provided written informed consent prior to the procedures of these studies (Negwer et al., 2017; Sollmann et al., 2016d; Sollmann et al., 2017b).

### **2.2. Patients**

Patients were eligible for participation if they met the following inclusion criteria:

- age above 18 years,
- written informed consent, and
- diagnosis of a supratentorial brain tumor within perisylvian areas of the LH according to structural magnetic resonance imaging (MRI).

Furthermore, the following exclusion criteria were defined:

- general TMS exclusion criteria for safety reasons (e.g., cochlear implants, presence of a cardiac pacemaker, deep brain stimulation electrodes),
- severe aphasia that would not have allowed for preoperative language mapping by nTMS, and
- other severe neurological diseases.

### **2.3. Setup and procedures**

Prior to surgery for tumor resection, all patients underwent clinical assessments (including evaluation of language function), cranial MRI, and language mapping by nTMS at our hospital according to standardized protocols. If clinically required, positron emission tomography (PET) was performed. Furthermore, tractography of language-related WM pathways was performed based on preoperatively acquired diffusion tensor imaging (DTI) sequences and nTMS data.

All acquired data were then considered during individual patient counseling and during treatment planning by an interdisciplinary tumor board. Tumor resection was performed with these data being available for surgical planning and resection guidance. After surgery, the clinical assessments and cranial MRI were repeated on the first postoperative day and in regular periods until discharge and during follow-up (FU) examinations. All data were available for analyses according to the objectives of the studies included in this thesis (Negwer et al., 2017; Sollmann et al., 2016d; Sollmann et al., 2017b).

## **2.4. Clinical assessment**

Each patient had to undergo a detailed clinical examination according to a standardized internal protocol. This examination included evaluation of sensory function, muscle strength, cranial nerve function, and coordination (Krieg et al., 2016a; Krieg et al., 2015; Sollmann et al., 2015b). Regarding the preoperative language status, we used the Aachen Aphasia Test (AAT) as a tool to evaluate different aspects of language function (Huber et al., 1984). Complementary to the AAT results, we established 4 deficit grades regarding language function (Krieg et al., 2014b; Sollmann et al., 2015b; Sollmann et al., 2016c). These deficit grades were defined as follows:

- no deficit (= grade 0; normal speech comprehension and conversational speech, no impairment of communication ability),
- mild deficit (= grade 1; normal speech comprehension and/or conversational speech with slight amnesic aphasia, adequate communication ability),
- medium deficit (= grade 2; minor disruption of speech comprehension and/or conversational speech, adequate communication ability), and
- severe deficit (= grade 3; major disruption of speech comprehension and/or conversational speech, clear impairment of communication ability).

In addition to the 4 deficit grades, an “A” was added to the respective grade in case of non-fluent aphasia, whereas a “B” was added to indicate fluent aphasia (Krieg et al., 2014b; Sollmann et al., 2015b; Sollmann et al., 2016c). The evaluation of language function according to this grading scheme was repeated during postoperative and FU examinations. In this context, the presence of postoperative aphasia was defined as any grade of language disruption (grades 1 – 3, A/B) at the fifth postoperative day, regardless of the individual preoperative status of language function. Furthermore, surgery-related aphasia was defined as any worsening of language function when comparing the preoperative to the postoperative or FU status of language function, thus paying attention to the development of language function over time.

## **2.5. Magnetic resonance imaging**

Cranial MRI was performed on a 3T scanner (Achieva 3T; Philips Medical Systems, The Netherlands B.V.) using an eight-channel phased-array head coil. Structural imaging consisted of a fluid attenuated inversion recovery (FLAIR) sequence (repetition time [TR] / echo time [TE]: 12,000 / 140 ms, voxel size:  $0.9 \times 0.9 \times 4 \text{ mm}^3$ , acquisition time: 3 min) and three-dimensional (3-D) T1-weighted gradient echo sequences (TR / TE: 9 / 4 ms,  $1 \text{ mm}^3$  isovoxel covering the whole head, acquisition time: 6 min 58 s) with and without application of an intravenous gadolinium-based contrast agent (gadopentetate dimeglumine; Magnograf, Marotrust GmbH, Germany).

Regarding diffusion-weighted imaging (DWI), sequences with 6 (TR / TE: 7,571 / 55 ms, b-values: 0 and 800, spatial resolution:  $2 \times 2 \times 2 \text{ mm}^3$ , acquisition time: 2 min 15 s) or 15 (TR / TE: 10,737 / 55 ms, b-values: 0 and 800, spatial resolution:  $2 \times 2 \times 2 \text{ mm}^3$ , acquisition time: 6 min 26 s) diffusion directions were acquired during the same scanning session. The software of the scanner was used to immediately adjust for motion artifacts in these sequences. Further DWI sequences were added to the scanning protocol during scanning at the first postoperative day to search for surgery-related bleeding or ischemic events.

## **2.6. Navigated transcranial magnetic stimulation**

### **2.6.1. Experimental setup**

For nTMS, we used the Nexstim eXimia NBS system (versions 3.2.2 and 4.3) in combination with a NEXSPEECH® module (version 1.1.0) for presentation of an object-naming task and evaluation of task performance (Nexstim Plc., Finland; Figure 4). For simultaneous electromyography (EMG) recording, a built-in EMG system with a total of 6 channels was used, and neuronavigation was established by the help of an infrared navigation device (Polaris Spectra; Polaris, Ontario, Canada). The application of nTMS pulses by this system is achieved with the help of a focal figure-of-eight stimulation coil that delivers biphasic pulses and induces an electric field (pulse length: 230  $\mu\text{s}$ , maximum electric field strength: 172 V / m  $\pm 2\%$ ). During the whole nTMS procedure, the patients sat in a comfortable chair with armrests in front of a screen used for later task presentation (Figure 4).

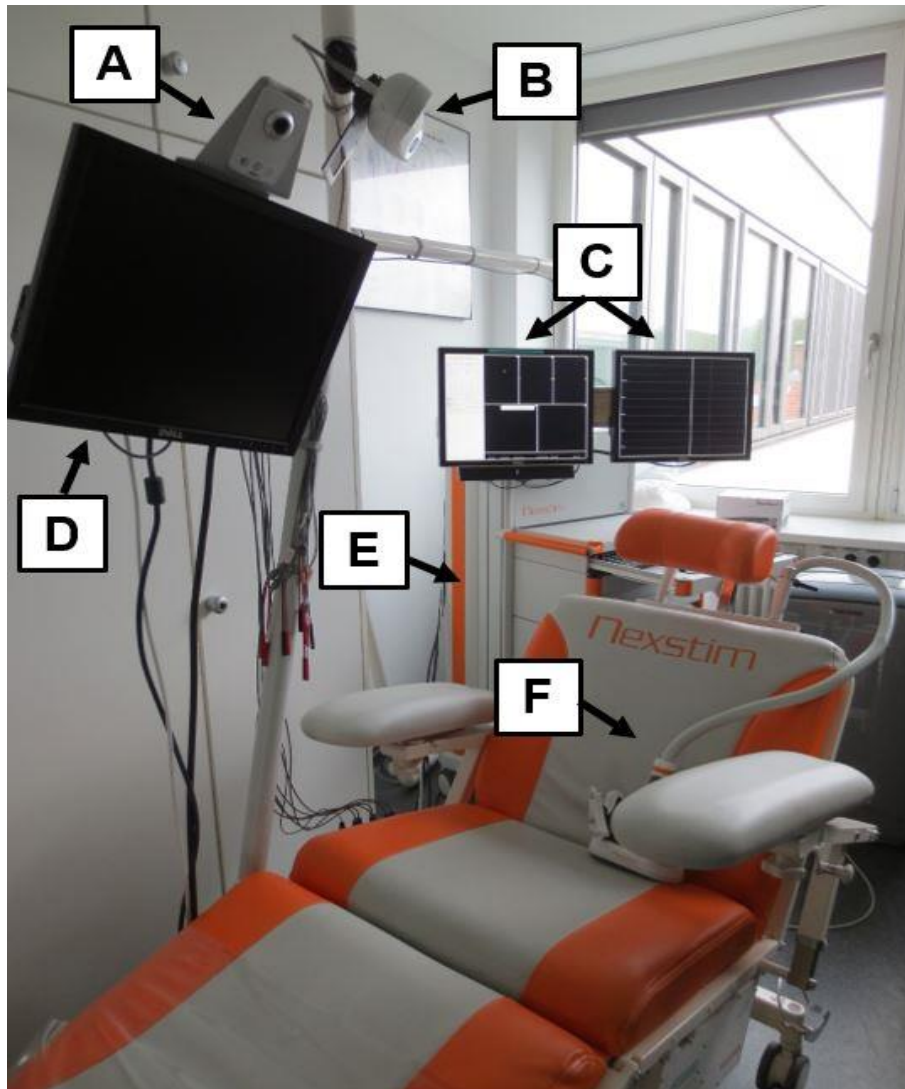


**Figure 4: Setup of navigated transcranial magnetic stimulation (nTMS)**

*The principal components of the nTMS system, which consists of a camera for recording of task performance (A), an infrared tracking device for neuronavigation purposes (B), screens for control of the stimulation including coil positioning (C), a screen for task presentation (D), a stimulator generating nTMS pulses (E), and a figure-of-eight stimulation coil (F) are tagged in this photograph.*

The Nexstim eXimia NBS system represents a neuronavigated device making use of electric-field-navigated transcranial magnetic stimulation (En-TMS). En-TMS is achieved by the calculation of the electric field that is generated by the stimulating coil and its maximum field strength applied, and it considers individual factors that can affect nTMS during estimation of the exact stimulus localization and intensity (e.g., shape and size of the patient's head) (Ruohonen and Ilmoniemi, 1999; Ruohonen and Karhu, 2010; Schmidt et al., 2015; Sollmann et al., 2016a; Tarapore et al., 2013).

First, the individual contrast-enhanced 3-D gradient echo sequences were transferred from the MRI scanner to the nTMS system in Digital Imaging and Communications in Medicine (DICOM) format and taken as an anatomical reference during later stimulation (Ruohonen and Ilmoniemi, 1999; Ruohonen and Karhu, 2010; Sollmann et al., 2016a; Sollmann et al., 2017a). Based on the MRI data set, the nTMS system automatically calculates an individual 3-D head model that is then co-registered to the respective patient's skull (Figure 5). The infrared navigation device is used to track the coil's position in relation to the reconstructed 3-D head model by sensing both reflectors attached to the back side of the coil and reflectors located on a strap tied to the patient's head (Ruohonen and Ilmoniemi, 1999; Ruohonen and Karhu, 2010; Sollmann et al., 2016a).

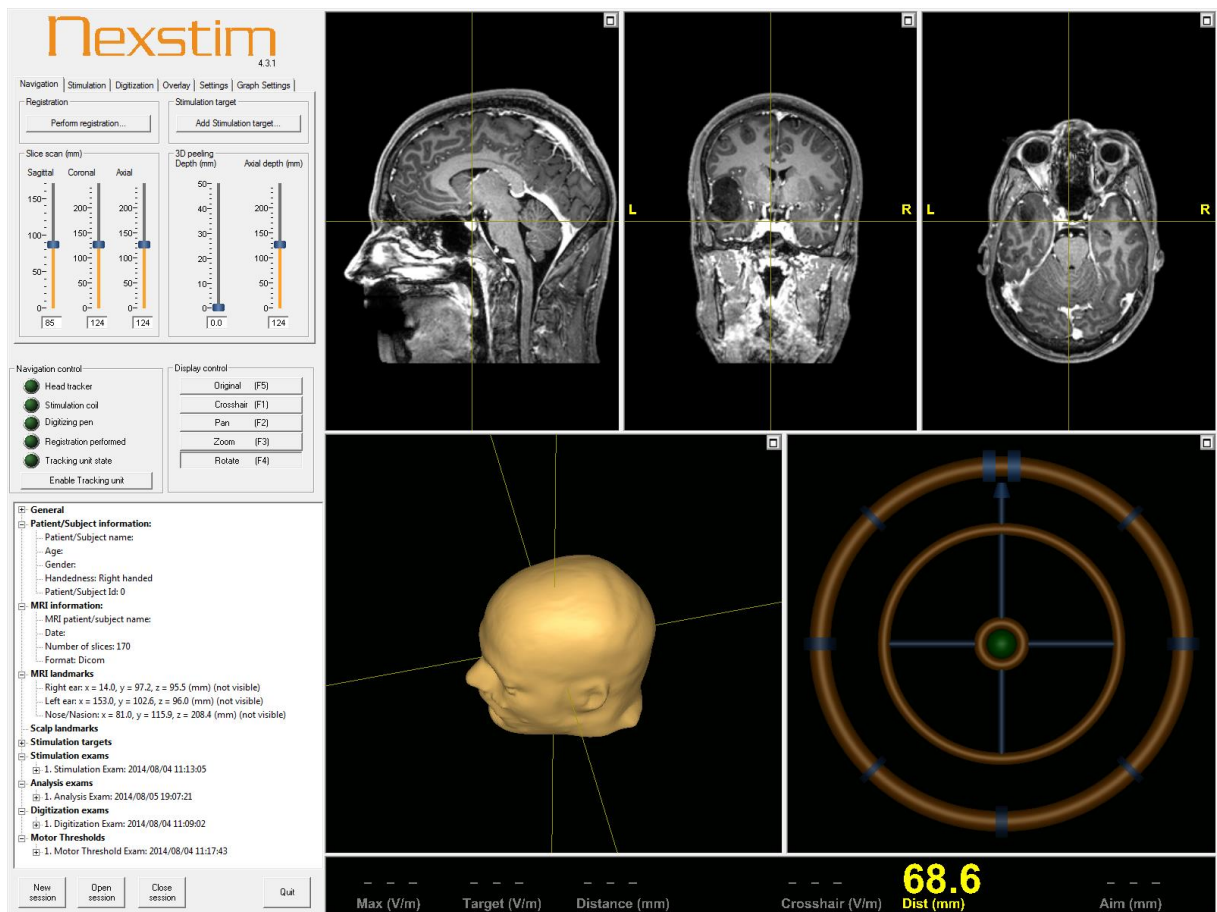


**Figure 5: Three-dimensional (3-D) head model**

Based on individual magnetic resonance imaging (MRI) data sets, the software calculates a 3-D head model that can be used during neuronavigation. This model considers individual anatomical characteristics and allows for visualization of the head and brain in different views, angulations, and peeling depths during stimulation.

### 2.6.2. Determination of the resting motor threshold

To individualize the stimulation intensity for later mapping, the resting motor threshold (rMT) was determined. In order to prepare for mapping of the motor area during rMT determination, pregelled surface electrodes (Neuroline 720; Ambu A/S, Denmark) were attached to the abductor pollicis brevis muscle (APB) of the right hand and used to record motor evoked potentials (MEPs) during stimulation of the LH. A reference electrode was placed at the ipsilateral elbow, and the sitting patient was instructed to relax during the procedure of rMT determination (Figure 6).



**Figure 6: Determination of the resting motor threshold (rMT)**

*The rMT was determined by motor mapping of the cortical representation of the abductor pollicis brevis muscle (APB) within the left hemisphere (LH). Motor evoked potentials (MEPs) were recorded by continuous electromyography (EMG) using electrodes attached to this muscle.*

The rMT is defined as the lowest stimulation intensity that elicits MEPs with amplitudes above 50  $\mu\text{V}$  in at least half of the applied stimulations in a relaxed muscle (Rossini et al., 1994; Rossini et al., 2015; Sollmann et al., 2016e). To determine a patient's individual rMT, the most excitable cortical spot in terms of MEP amplitudes derived from EMG monitoring of the APB was identified and defined as the so-called motor hotspot (Figure 7) (Krieg et al., 2012b; Krieg et al., 2013a; Picht et al., 2012; Sollmann et al., 2016e). Hotspot identification required application of several single nTMS pulses to the cortex, starting at the anatomical hand knob within the precentral gyrus (PrG) as visually identified by its typical inversed omega structure (Niskanen et al., 2010; Park et al., 2007; Yousry et al., 1997). Although stimulation began within the PrG, it was continued in all directions and outside of the PrG to localize the individual motor hotspot.

After careful hotspot identification, at least 10 further single nTMS pulses with the same angulation of the coil and orientation of the electric field were applied to guarantee that the correct spot was defined as the motor hotspot (Sollmann et al., 2016e). To rule out the possibility that other coil angulations or electric field orientations may have led to higher MEP amplitudes, 10 additional stimulation pulses were given with orientations of  $-45^\circ$  and  $+45^\circ$  in relation to the initial stimulus (Sollmann et al., 2016e). At the motor hotspot defined under these premises, the nTMS system's built-in threshold-hunting application, which is based on the maximum likelihood algorithm, was then used to determine the exact rMT value (in % of the nTMS system's maximum output) (Awiszus, 2003; Sollmann et al., 2016e). During threshold hunting, single nTMS pulses were only applied to the motor hotspot with optimal electric field orientation and coil angulation whilst the nTMS system systematically altered the applied stimulation intensity until MEP amplitudes above 50  $\mu\text{V}$  were registered (Awiszus, 2003; Sollmann et al., 2016e). In this context, the nTMS system automatically decreased the intensity when MEPs with amplitudes above 50  $\mu\text{V}$  were elicited, whereas it increased the intensity in case that MEP amplitudes equal or lower than 50  $\mu\text{V}$  were recorded by EMG. Facilitated motor responses (e.g., voluntary muscle contractions of the APB) were excluded manually to guarantee accurate rMT determination (Sollmann et al., 2016e).

For all stimulation pulses delivered for identification of the motor hotspot and rMT determination, the inter-stimulus interval (ISI; time interval between 2 consecutive stimulation pulses) was at least 2 s. Furthermore, the stimulating coil was angulated perpendicular to the patient's skull during pulse application, with the induced electric field being oriented perpendicular to the stimulated gyrus (Figure 7) (Krieg et al., 2012b; Krieg et al., 2013a; Picht et al., 2012; Sollmann et al., 2016e). The coil angulation and electric field orientation were tracked online during nTMS pulse application by the help of the infrared navigation device (Ruohonen and Ilmoniemi, 1999; Ruohonen and Karhu, 2010; Sollmann et al., 2016a).

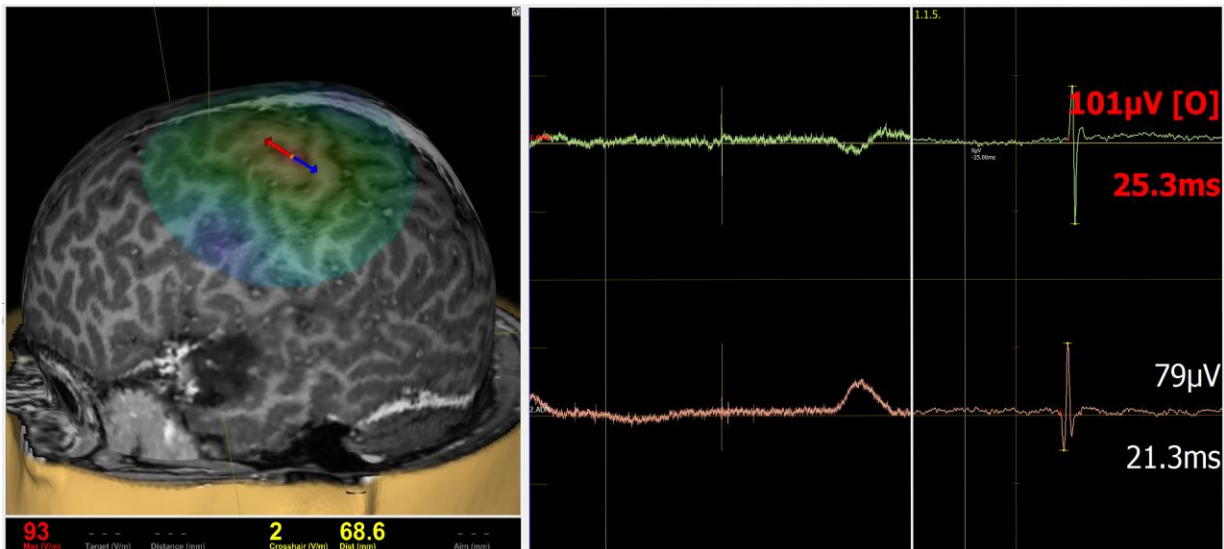


**Figure 7: Identification of the motor hotspot**

During determination of the resting motor threshold (rMT), the motor hotspot had to be identified. This spot is defined as the most excitable cortical spot in terms of motor evoked potential (MEP) amplitudes recorded by electromyography (EMG; in this case: amplitude of 101  $\mu\text{V}$  with a latency of 25.3 ms for stimulation of the abductor pollicis brevis muscle [APB]). The orange point marks the site of the hotspot, and the colored arrow depicts the direction of the induced electric field, which should be oriented perpendicular to the stimulated gyrus to elicit optimal MEPs.

### 2.6.3. Object-naming task and baseline

To map the cortex for language-related areas, a task is required. We applied an object-naming task consisting of a total of 131 colored photographs of living and non-living, common objects depicted on white background (Figure 8). (Hernandez-Pavon et al., 2014; Krieg et al., 2016b; Picht et al., 2013; Sollmann et al., 2016c; Sollmann et al., 2014). All objects are present in everyday life (e.g., hammer, orange, ball, ship) and were shown on a computer screen that was positioned in front of the sitting patient. No abstract or fictional objects were included in the selection of photographs, which was similar to the Snodgrass and Vanderwart picture set (Snodgrass and Vanderwart, 1980; Snodgrass, 1996). Such a visual object-naming task is known to engage all main language production functions (form, articulation, and meaning), which are processed partly simultaneously and chronologically stepwise during task performance (Indefrey, 2011; Indefrey and Levelt, 2004; Sollmann et al., 2016b).



**Figure 8: Examples of pictures used in the object-naming task**

*During task performance, a set of various colored photographs depicting common objects, such as a hammer, orange, ball, or ship, was used. These objects were shown on a screen that was placed in front of the patient, and he or she was requested to name the presented objects.*

Before nTMS for language mapping was conducted, the set of objects was shown to each patient in the context of at least 2 consecutive rounds of picture presentation without stimulation. This was done to adapt the set of objects according to the skills of the respective patient and to train the patient for the subsequent mapping procedure (Hernandez-Pavon et al., 2014; Krieg et al., 2016b; Picht et al., 2013; Sollmann et al., 2016c; Sollmann et al., 2014). Furthermore, picture presentation without simultaneous stimulation allows achieving a baseline of objects that the respective patient was able to name correctly and without delays, thus being usable under the condition of later stimulation. The patients were instructed to name the presented objects as precisely and quickly as possible without a preceding article or sentence (Krieg et al., 2016b; Sollmann et al., 2014). In case of any unclear response (e.g., repetition of syllables during naming), misnaming (e.g., incorrect naming of an object), or hesitation during naming performance, the respective object was deleted from the sequence and not used during subsequent language mapping. As a standard reference regarding naming agreement, we used the International Picture Naming Project (IPNP) database (Szekely et al., 2004).

During the 2 rounds of baseline assessment, the objects were displayed on the screen with a fixed inter-picture interval (IPI; time interval between 2 consecutive objects) of 2,500 ms. The display time (DT; time interval during which a single object was shown on the screen) was standardly set at 700 ms. The baseline assessments were video- and audio-recorded and

saved for later analyses (Hernandez-Pavon et al., 2014; Lioumis et al., 2012; Rogic et al., 2014; Tarapore et al., 2013).

#### **2.6.4. Mapping procedure**

Language mapping by nTMS was performed within the same session after the baseline assessments. The objects were presented with the same IPI and DT as during baseline testing. Regarding the picture-to-trigger interval (PTI; time interval between the screening of an object and the onset of the stimulation pulses), we used 300 ms or 0 ms, with the nTMS trains being automatically delivered in a time-locked fashion that was correlated to the PTI (Krieg et al., 2016b; Krieg et al., 2014c; Picht et al., 2013; Sollmann et al., 2016b; Sollmann et al., 2014; Tarapore et al., 2013). The individual set of correctly named baseline objects was used, with the single objects being presented in randomized order. To effectively induce naming disturbances, the stimulation parameters for a repetitive nTMS (rTMS) sequence were first individualized according to the following approach that was applied to the LH (Krieg et al., 2016b; Sollmann et al., 2014). First, nTMS trains with 100% of the individual rMT were delivered to the opIFG, trIFG, and ventral PrG with 5 Hz / 5 pulses, 7 Hz / 5 pulses, and 7 Hz / 7 pulses as an attempt to achieve a high error rate (ER; number of errors divided by the number of delivered stimulation trains). The parameters that led to the highest ER (5 Hz / 5 pulses, 7 Hz / 5 pulses, or 7 Hz / 7 pulses) were then used during mapping of the entire hemisphere. If object naming was not clearly disrupted, the stimulation intensity was increased to 110 – 120% rMT, whereas it was decreased to 80 – 90% rMT if the patient reported considerable discomfort during stimulation (Krieg et al., 2016b; Sollmann et al., 2014). In the case that no clear difference was registered between stimulation with the different parameters in terms of ERs, we chose the most comfortable adjustment to avoid any pain due to stimulation-induced muscle twitching (Krieg et al., 2016b; Sollmann et al., 2014). After the optimal stimulation settings were determined in each patient under these premises, both hemispheres were mapped in consecutive order starting with the LH followed by the right hemisphere (RH) (Figure 9).

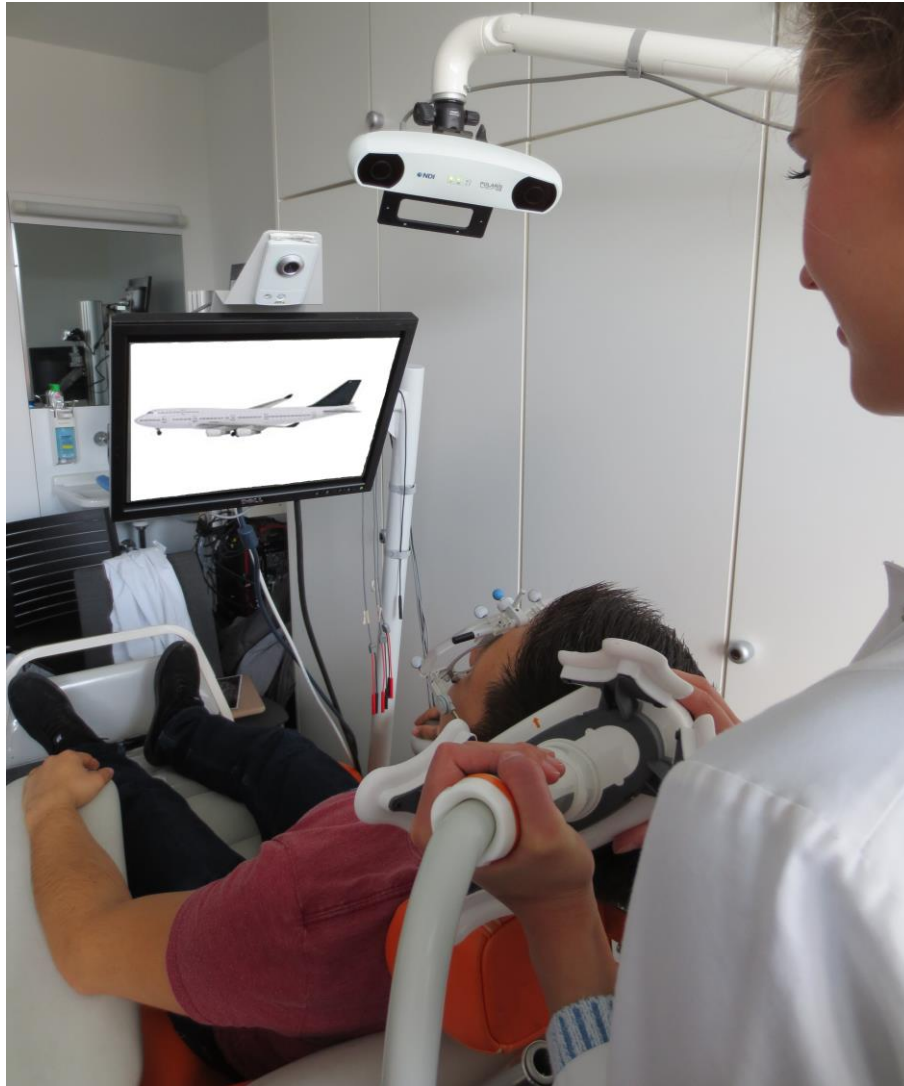


**Figure 9: Language mapping procedure**

*The patient was presented with objects on a screen during language mapping. Stimulation was then carried out on both hemispheres, starting with the left hemisphere (LH). The stimulating coil was placed on the head of the patient, and its position was controlled with the help of the infrared navigation device.*

The coil was randomly moved during the IPI after having stimulated one spot at least 3 times in a row (Krieg et al., 2016b; Sollmann et al., 2014). The distance between the spots was about 10 mm and most of the gyri of the LH and RH were targeted during this stimulation approach (Figure 10). However, the spatial extent of mapping had to be restricted due to clear discomfort in orbital and polar cortical regions and due to comparatively low induced field strengths within the inferior temporal gyrus because of greater skull-cortex distances in this area (Krieg et al., 2016b; Sollmann et al., 2014). To achieve optimal field induction, the coil was placed perpendicular to the patient's skull with anterior-posterior orientation of the

electric field (Figure 10) (Epstein et al., 1996; Lioumis et al., 2012; Sollmann et al., 2015c; Wassermann et al., 1999). As for the previous baseline assessments, the naming performances were video- and audio-recorded for later offline analyses (Hernandez-Pavon et al., 2014; Lioumis et al., 2012; Rogic et al., 2014; Tarapore et al., 2013). The locations of the induced electric field and its shape and direction as well as the coil angulation and the spots of stimulation were saved for post hoc analyses.

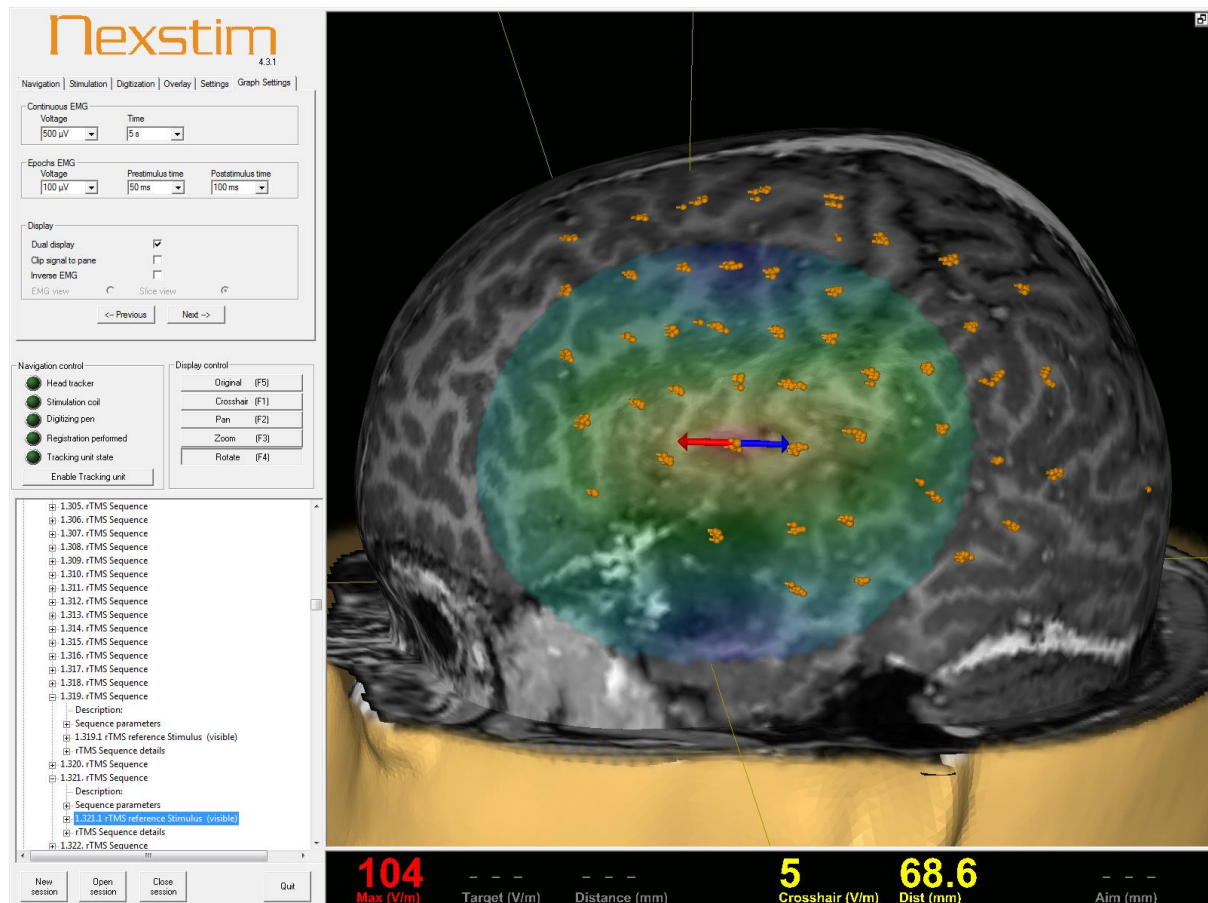


**Figure 10: Cortical points of stimulation**

The points of stimulation are shown as orange spots on the three-dimensional (3-D) reconstruction of the cortex. Each area was stimulated at least 3 times, and the orientation of the electric field, as shown by the colored arrow, was controlled during pulse application so that it was oriented anterior-posteriorly. The induced field strength is calculated by the system and displayed for each stimulation spot (in this case: 104 V/m).

### 2.6.5. Mapping analysis

The recordings during baseline assessments and language mappings were analyzed post hoc to identify and categorize any naming errors induced by the nTMS trains during task performance. The video and audio recordings were played and any suspected disturbances during object naming were compared with the corresponding baseline performance regarding the respective object (Figure 11) (Hernandez-Pavon et al., 2014; Krieg et al., 2016b; Lioumis et al., 2012; Picht et al., 2013; Sollmann et al., 2016c; Sollmann et al., 2014; Tarapore et al., 2013).

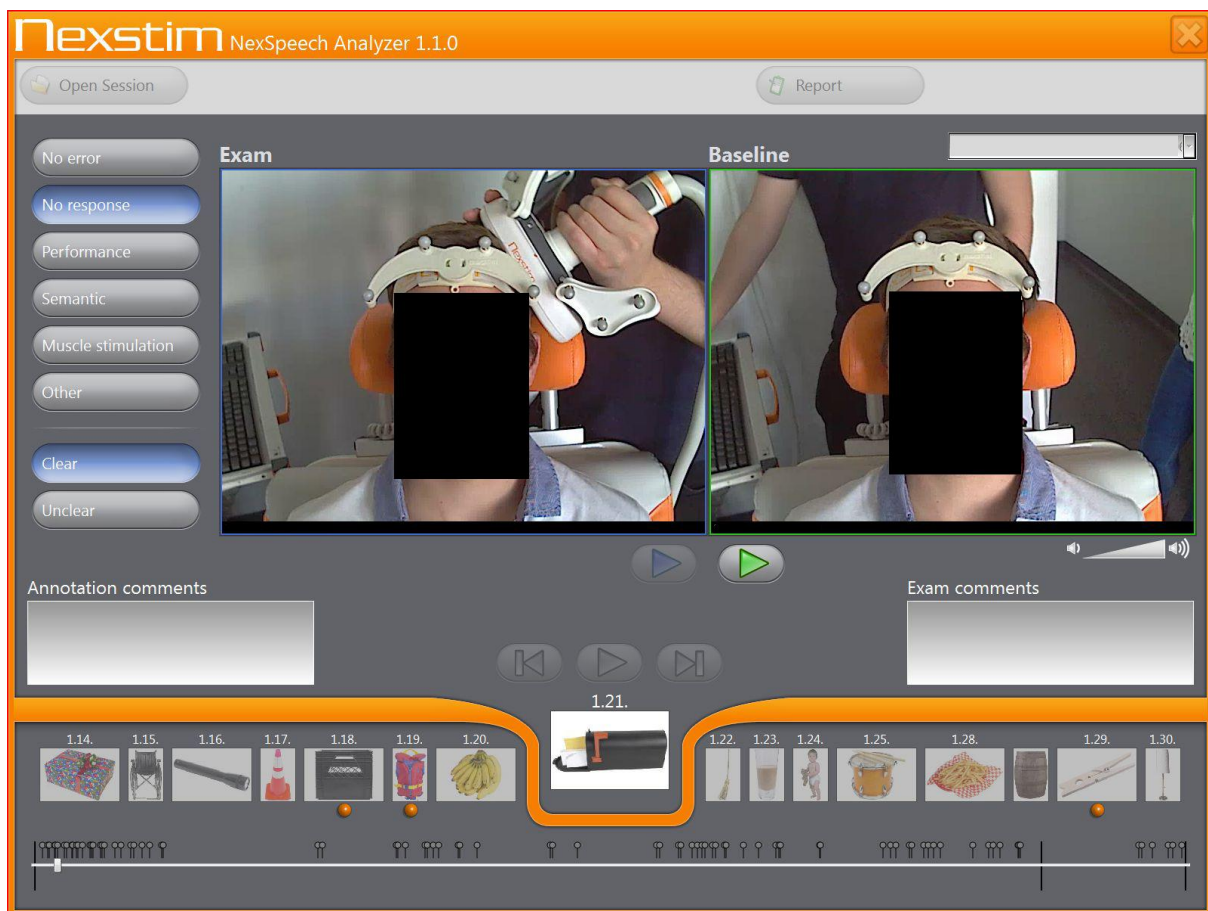


**Figure 11: Comparison of mapping recordings to baseline assessments**

The analysis software allowed for comparison of the task performance during stimulation to baseline assessment to facilitate detection and categorization of naming errors. The respective object that was screened during the error, together with the identification number of the nTMS pulse (in this case: “letter box” during application of pulse 1.21), was also shown. To tag an error, the respective category had to be chosen from a set of predefined categories (in this case: no response).

All detected naming errors were marked and systematically categorized with respect to the specific error type (Corina et al., 2010; Krieg et al., 2016b; Lioumis et al., 2012; Sollmann et al., 2014). In this context, no responses (no naming at all during stimulation), performance errors (articulatory naming errors during articulation of the target word), neologisms (articulation of a possible but non-existent word instead of the target word), semantic paraphasias (substitution of a semantically related or associated word for the target word), and phonological paraphasias (unintended phonemic modification of the target word) were considered (Corina et al., 2010; Krieg et al., 2016b; Lioumis et al., 2012; Sollmann et al., 2014). The categorization of naming errors was performed blinded to the respective stimulation spots at which the errors were elicited during language mapping. After the categorization was finished, the spots that were prone to errors of the above-mentioned types were tagged and defined as language-positive spots, whereas the remaining stimulation spots were defined as language-negative spots (Figure 12). Only the language-positive spots were then exported in DICOM format, which was achieved separately for the LH and RH (Sollmann et al., 2017a).

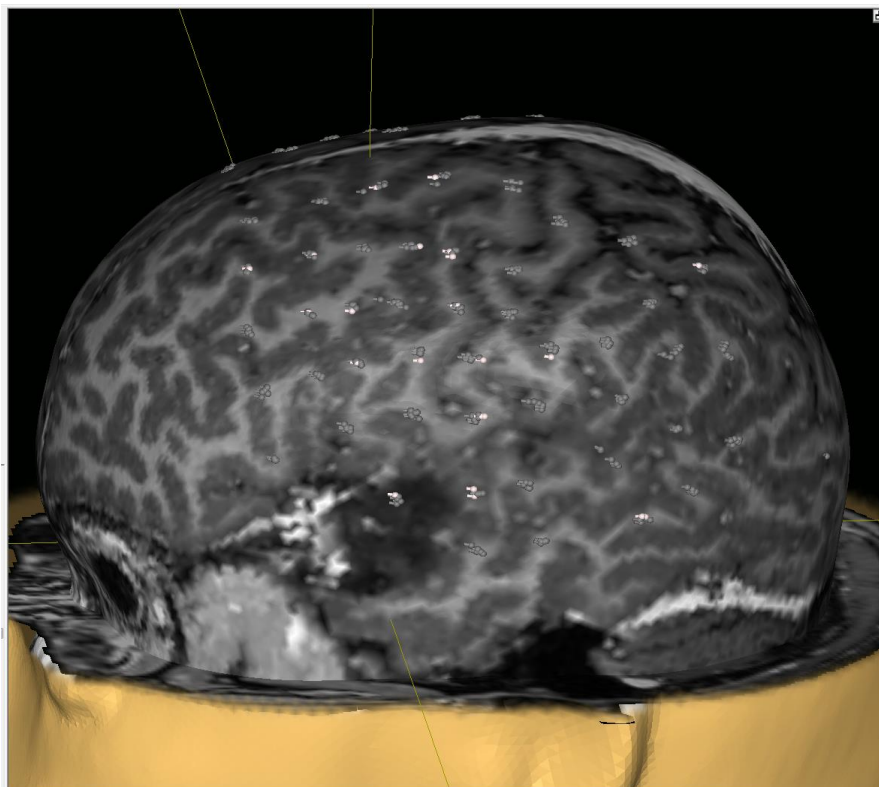


**Figure 12: Cortical language map**

*Cortical points at which a naming error was elicited are depicted in white, whereas language-negative spots are shown in grey. The language-positive spots were exported for later tractography.*

## **2.7. Diffusion tensor imaging fiber tracking**

### **2.7.1. Experimental setup**

For DTI FT based on nTMS language data, we used a deterministic tractography algorithm implemented into a surgical neuronavigation server (BrainLAB iPlan Net, version 3.0.1; BrainLab AG, Germany). This deterministic approach follows the algorithms of the fiber assignment by continuous tracking (FACT) method (Mori and Barker, 1999; Mori and van Zijl, 2002): subcortical fibers are reconstructed stepwise by tracking along the principal diffusion direction from a certain point until preselected stop criteria are met.

First, the individual DTI, FLAIR, and gradient echo sequences of each patient, all acquired during preoperative MRI, were uploaded to the server, which was then followed by fusion and alignment of data sets. Moreover, during upload of the DTI sequences, eddy current correction was applied throughout. In addition, all language-positive stimulation spots were transferred to the server, uploaded, and aligned to the imaging data sets. This was done separately for the language-positive spots of the LH and RH. Consequently, the language-negative stimulation spots, which were not included in the transferred file, were not considered during tractography (Sollmann et al., 2017a). Thus, the final data fusion included both imaging data and nTMS maps within a shared coordinate space (Frey et al., 2012; Krieg et al., 2012a; Sollmann et al., 2017a).

### **2.7.2. Tractography procedure**

For 2 of the studies included in this thesis, only left-hemispheric language-positive spots were further used (Figure 13) (Negwer et al., 2017; Sollmann et al., 2016d). The whole group of these spots reflecting error sites of the LH was defined as one single object in each patient, which is a prerequisite for the definition of a region of interest (ROI) needed for later tractography. Consequently, the object was defined as a ROI during the next step by adding a rim of 5 mm to each language-positive stimulation spot (Figure 13). For the first study, DTI FT was carried out using an individualized tracking approach purely based on these left-hemispheric nTMS data as the only ROI (Frey et al., 2012). The minimum fiber length (MFL) was defined by standard as 110 mm in all patients, whereas the fractional anisotropy (FA) was manually adjusted to individualize this value for tractography (Frey et al., 2012; Sollmann et al., 2016d). It was first increased stepwise until no WM fibers were detected and was then gradually decreased in steps of 0.01 until only a minimum WM fiber course was visualized (Frey et al., 2012; Sollmann et al., 2016d). This individual FA value was defined as the 100% FA threshold (FAT). After definition of the 100% FAT, tractography was conducted

with 75% FAT, 50% FAT, and 25% FAT with the group of left-hemispheric language-positive spots as a ROI to detect subcortical language-related pathways.

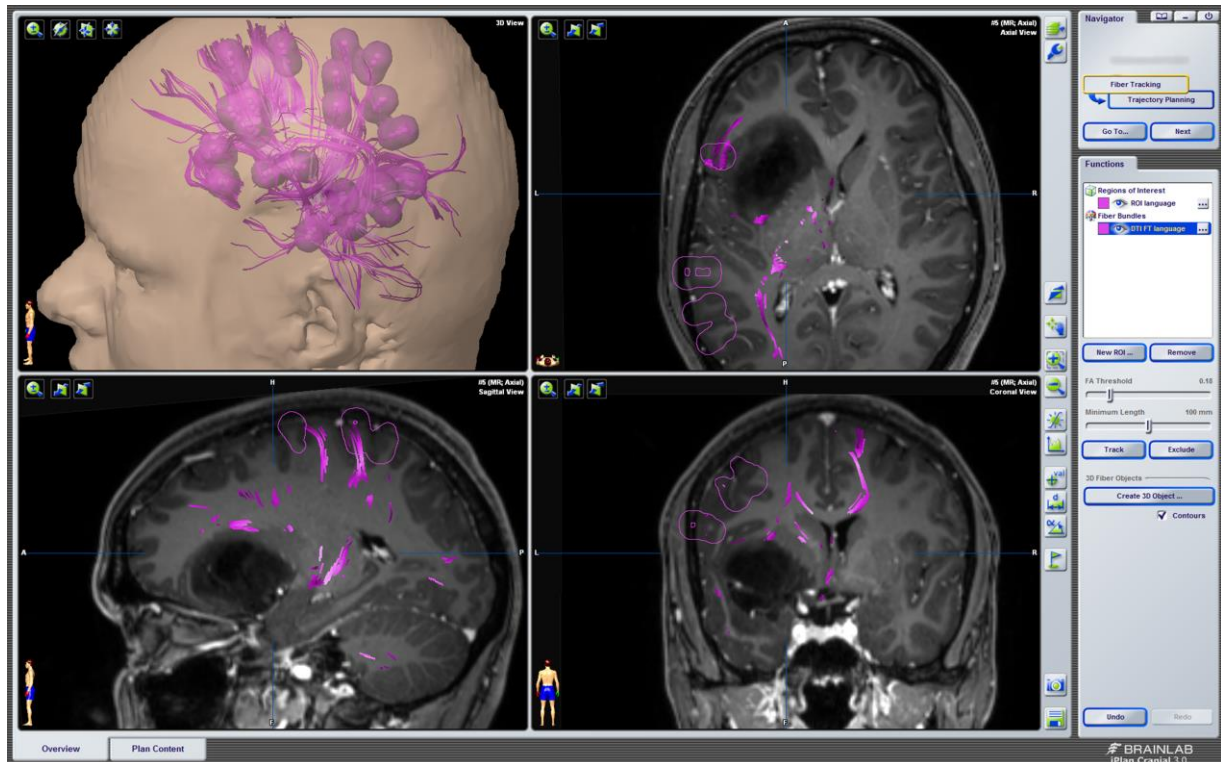


**Figure 13: Tractography based on cortical language maps**

Diffusion tensor imaging fiber tracking (DTI FT) was performed with language-positive spots, enlarged by a rim of 5 mm, as a region of interest (ROI). The language-positive spots and the tracked subcortical language-related pathways are shown in purple, projected onto a contrast-enhanced gradient echo sequence.

For the second study using only language-positive spots of the LH as a ROI, DTI FT was performed using different predefined values for MFL and FA pairs, which were MFL 70 mm / FA 0.2, MFL 80 mm / FA 0.15, MFL 90 mm / FA 0.15, MFL 100 mm / FA 0.1, and MFL 100 mm / FA 0.15 (Negwer et al., 2017). Additionally, classical anatomy-based tractography was carried out according to a cubic ROI-based protocol by placing 3 independent cubic boxes along anatomically suspected courses of subcortical fiber tracts (Henning Stieglitz et al., 2012; Negwer et al., 2017). One cubic ROI was placed within the opIFG and the inferior part of the PrG, another ROI was put within posterior areas of the medial and superior temporal gyri, and the third ROI included the supramarginal gyrus with extensions into medial parts of the lateral ventricles (Henning Stieglitz et al., 2012; Negwer et al., 2017). During tractography

using these cubic boxes, the ROI derived from language-positive stimulation spots was not considered.

Regarding the last study included in this thesis, the right-hemispheric language-positive spots were used in addition to the nTMS data of the LH (Sollmann et al., 2017b). Analogously to the procedure considering left-hemispheric spots, these spots were defined as another single object and subsequently transformed into a ROI by adding a 5-mm margin to each language-positive spot. Tractography was then carried out with the MFL set at 40 mm and the FA value set at 0.01 and 0.2 in order to detect WM fibers connecting the left-hemispheric with the right-hemispheric ROI and vice versa (Sollmann et al., 2017b).

### **2.7.3. Tractography analysis**

The tractography results of the first 2 studies were visually evaluated for 9 major WM fiber bundles known to be involved in different aspects of language function (Ayer et al., 2013; Bello et al., 2008; Catani et al., 2002; Catani and Thiebaut de Schotten, 2008; Gierhan, 2013; Henning Stieglitz et al., 2012). These fiber tracts were the AF, SLF, ILF, FoF, UC, CNT, ArF, CtF, and CF (Negwer et al., 2017; Sollmann et al., 2016d). We then documented which tracts were reconstructed by tractography in each patient depending on the different MFL and FA values applied according to the protocol (Negwer et al., 2017; Sollmann et al., 2016d). Furthermore, the overall numbers of detected WM fibers for each DTI FT setting were extracted (Negwer et al., 2017; Sollmann et al., 2016d).

Concerning tractography performed for the third study, which was conducted using both a left-hemispheric and a right-hemispheric nTMS-based ROI at the same time, we first documented whether any fibers connecting these 2 ROIs were present (Sollmann et al., 2017b). If interhemispheric WM fibers were reconstructed, the condition was defined as IC+ (interhemispheric connectivity detectable; visualization of at least 1 interhemispheric WM fiber bundle), whereas no reconstruction of interhemispheric WM fibers was defined as IC- (interhemispheric connectivity not detectable; no interhemispheric WM fibers visualized) (Sollmann et al., 2017b). We then extracted the overall numbers of reconstructed WM fibers for each DTI FT setting used in this study (Sollmann et al., 2017b).

## 2.8. Surgical procedure

The patients underwent surgery for tumor removal at our department, which was either achieved under general anesthesia or during awake surgery, depending on individual decisions made by an interdisciplinary tumor board in agreement with the respective patient's condition and treatment requirements (Ille et al., 2016; Picht et al., 2006; Picht et al., 2013; Sacko et al., 2011; Szelenyi et al., 2010). The data sets consisting of preoperative MRI sequences including DTI, language-positive nTMS spots of the tumor-affected hemisphere, and nTMS-based tractography of the tumor-affected hemisphere were available for surgical planning and during surgery for resection guidance on the intraoperative navigational screen (BrainLAB Curve; BrainLab AG, Germany) (Sollmann et al., 2017a).

For awake surgery, local anesthesia of the galea and dura was performed using bupivacaine and epinephrine, while remifentanyl and propofol were used to achieve an adequate level of sedation. During surgery, the head of the patient was positioned in a Mayfield clamp. After opening of the skull and dura, sedation was stopped to allow for intraoperative language mapping by cortical and subcortical DES. To gain an adequate level of wakefulness, the surgery was paused until a Ramsay sedation score of 2 (awake patient, cooperative and calm) was achieved. Surface recording by electroencephalography (EEG) was used to identify any epileptic seizures during surgery.

Cortical DES was conducted by a bipolar stimulation electrode, whereas subcortical DES was performed with a monopolar probe (Inomed Medizintechnik GmbH, Germany) (Chang et al., 2015; Mandonnet et al., 2010; Szelenyi et al., 2010). The same object-naming task as applied during preoperative language mapping by nTMS was presented to the patient on a laptop screen brought into the patient's field of view. However, in contrast to the preoperative setup, the patient was advised to add the preceding matrix "This is a ..." to each object during naming performance. The areas that gave rise to naming errors during cortical DES were marked with small tags (Figure 14). Subsequent to intraoperative DES, surgery was continued under conscious sedation or general anesthesia.

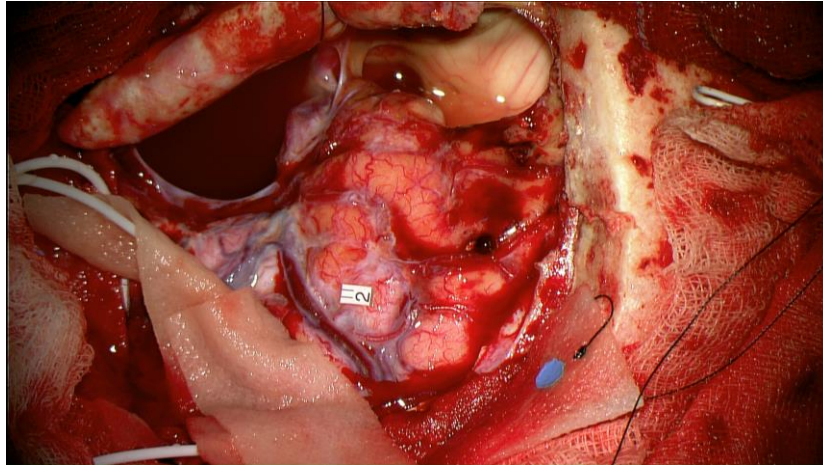


**Figure 14: Intraoperative language mapping**

Cortical and subcortical direct electrical stimulation (DES) is used for intraoperative mapping of language function. A tag (white) was placed on language-positive sites for documentation. During surgery, these sites are spared from resection to prevent surgery-related deterioration of language.

## 2.9. Statistical analysis

For statistical data analyses and creation of graphs, GraphPad Prism was used (version 6.04; GraphPad Software Inc., CA, USA). For patient-related and mapping-related characteristics as well as tractography characteristics, descriptive statistics including means  $\pm$  standard deviation (SD), medians, and the minimum and maximum values were calculated. For all statistical tests, the level of statistical significance was set at  $p < 0.05$ .

Concerning the tractography results of the first 2 studies, we calculated the fraction of visualized WM fibers per number of visualized tracts (fibers / tracts) based on the extracted fiber numbers (Negwer et al., 2017; Sollmann et al., 2016d). This ratio can serve as a measure of fiber density and reflects the tractography's visual portrayal and specificity. Furthermore, the percentage of visualized tracts out of all patients for each of the 9 included subcortical language-related pathways was evaluated (Negwer et al., 2017; Sollmann et al., 2016d). This percentage indicates the visualization sensitivity of the different language-related tracts. Regarding the second study, tractography results of the nTMS-based DTI FT approach were systematically compared to the anatomy-based tractography approach (Negwer et al., 2017). The one-way analysis of variance (ANOVA), Chi-squared tests, or Fisher's exact tests were applied to assess statistical significance.

Concerning the third study, contingency tables were created derived from the number of patients being diagnosed with or without aphasia preoperatively, postoperatively, and during FU examinations in relation to the status regarding visualized IC (IC- or IC+) (Sollmann et al.,

2017b). Chi-squared tests revealed whether differences in these characteristics were statistically significant. In this context, the odds ratio (OR) and the corresponding 95% confidence intervals (CIs) were calculated to specifically evaluate whether nTMS-based IC could serve as a parameter for the prediction of language worsening. Additionally, we calculated the sensitivity, specificity, positive predictive value (PPV), and negative predictive value (NPV) with language deficits representing the ground truth. In this context, the following conditions were defined (Sollmann et al., 2017b):

- True positive (TP): IC+ AND presence of language deficits,
- True negative (TN): IC- AND no presence of language deficits,
- False positive (FP): IC+ AND no presence of language deficits, and
- False negative (FN): IC- AND presence of language deficits.

## 3. RESULTS

---

### 3.1. Feasibility of nTMS-based DTI fiber tracking of language pathways in neurosurgical patients using a fractional anisotropy threshold

#### 3.1.1. Key findings

Tractography of subcortical language-related pathways by the use of newly established nTMS-based DTI FT was technically feasible in all patients suffering from different entities of brain tumors (Sollmann et al., 2016d). Depending on the individual FAT, maps of language-related WM fiber tracts were created (Figure 15) (Sollmann et al., 2016d). In each patient, 9 different fiber tracts were evaluated, which were present at different percentages and with various fiber numbers (Figure 16) (Sollmann et al., 2016d).

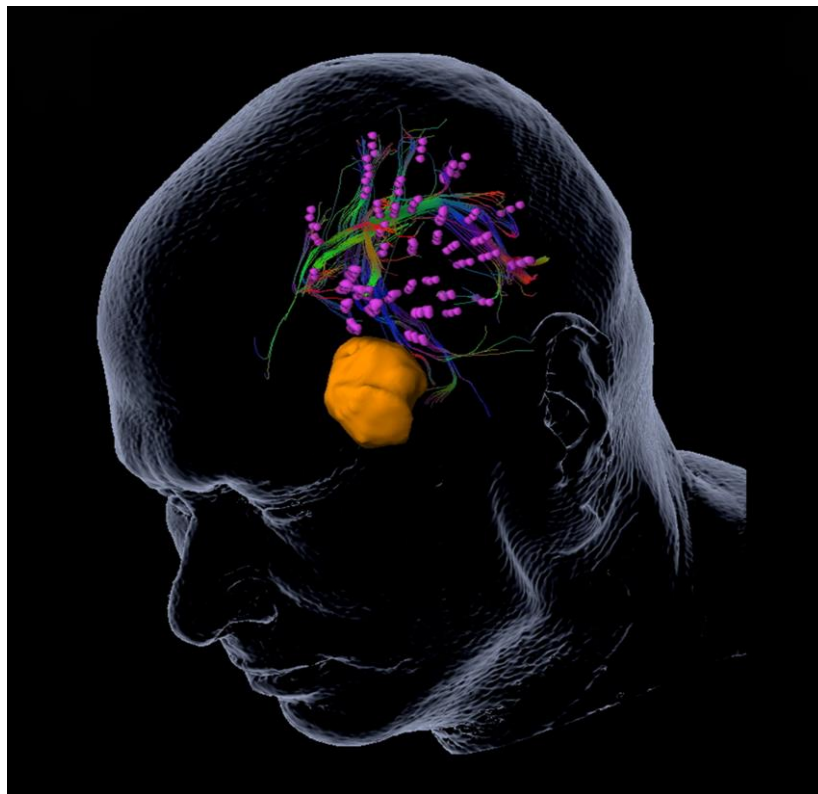


**Figure 15: Feasibility of tractography based on cortical language maps**

*In this illustrative case, diffusion tensor imaging fiber tracking (DTI FT) was conducted purely based on left-hemispheric language-positive spots (purple) (Sollmann et al., 2016d). The tumor volume is depicted in orange, and the subcortical language-related pathways appear in different colors as streamlines originating from or terminating in the language-positive spots (Sollmann et al., 2016d).*

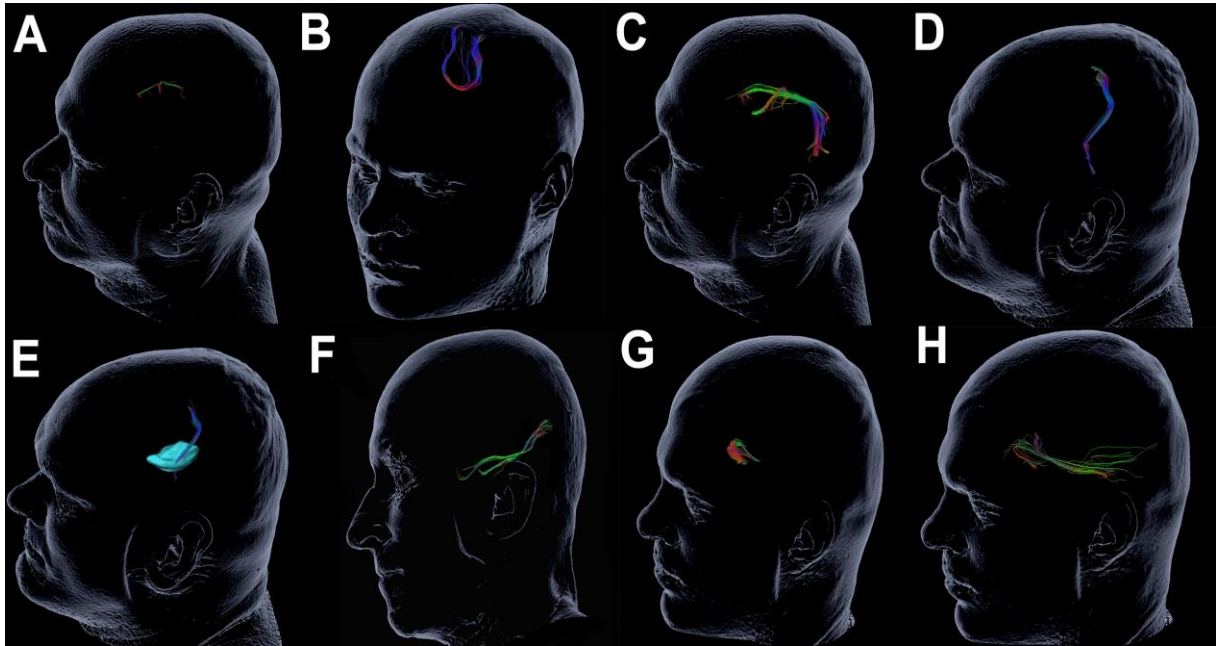


**Figure 16: Tractography of 9 subcortical language-related pathways**

Based on language-positive spots, diffusion tensor imaging fiber tracking (DTI FT) of different subcortical language-related pathways can be achieved, including arcuate fibers (ArF; A), commissural fibers (CF; B), the arcuate fascicle (AF; C) and superior longitudinal fascicle (SLF; C), the corticonuclear tract (CNT; D), corticothalamic fibers (CtF; E, with the thalamus depicted in blue), the inferior longitudinal fascicle (ILF; F), the uncinata fascicle (UC; G), and the inferior fronto-occipital fascicle (FoF; H) (Sollmann et al., 2016d).

According to our tractography protocol, the FA value used for tractography was individualized in each patient with respect to 25%, 50%, 75%, and 100% FAT (Frey et al., 2012). The average FA values  $\pm$  SD were  $0.08 \pm 0.02$  (25% FAT),  $0.16 \pm 0.04$  (50% FAT),  $0.24 \pm 0.06$  (75% FAT), and  $0.32 \pm 0.09$  (100% FAT) (Sollmann et al., 2016d). There was a statistically significant difference in FA values between these adjustments ( $p < 0.0001$ ) (Sollmann et al., 2016d). For tractography applying 25% FAT, the highest fraction of visualized WM fibers per tract was detected (Figure 17) (Sollmann et al., 2016d).

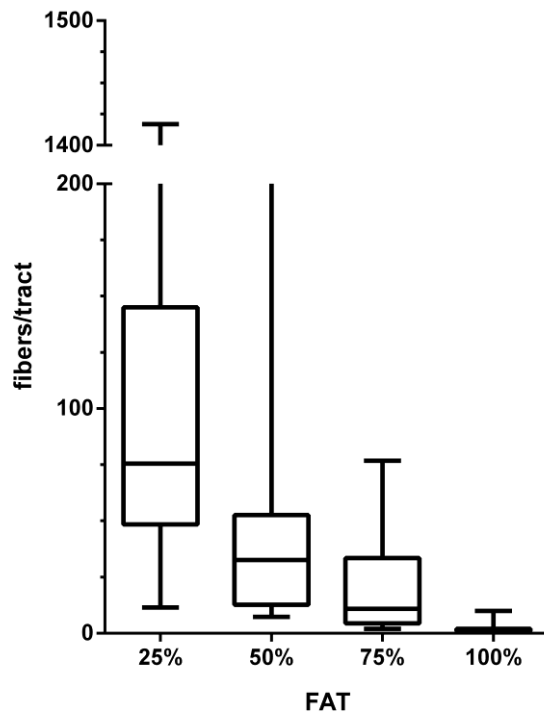


**Figure 17: Fibers per tract**

This box plot depicts the fractional anisotropy thresholds (25% FAT, 50% FAT, 75% FAT, and 100% FAT) used for tractography on the x-axis and the ratio of the fibers per tract on the y-axis (Sollmann et al., 2016d).

The ratio significantly decreased with an increase of FA values ( $p < 0.0001$ ), and a similar result was observed for the percentages of WM fibers of the 9 included language-related WM pathways ( $p < 0.0001$ ; Figure 18) (Sollmann et al., 2016d).

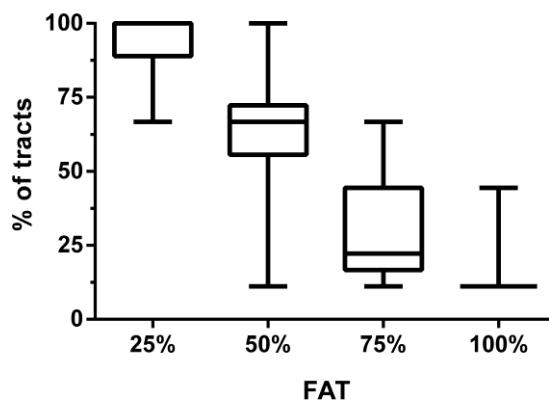


**Figure 18: Percentage of visualized tracts**

This box plot shows the fractional anisotropy thresholds (25% FAT, 50% FAT, 75% FAT, and 100% FAT) on the x-axis and the percentage of visualized tracts on the y-axis (Sollmann et al., 2016d).

The change in FA values used for tractography altered the detectability of the 9 predefined language-related WM pathways, with nTMS-based DTI FT using 25% FAT resulting in visibility of most of these tracts (Figure 19) (Sollmann et al., 2016d).

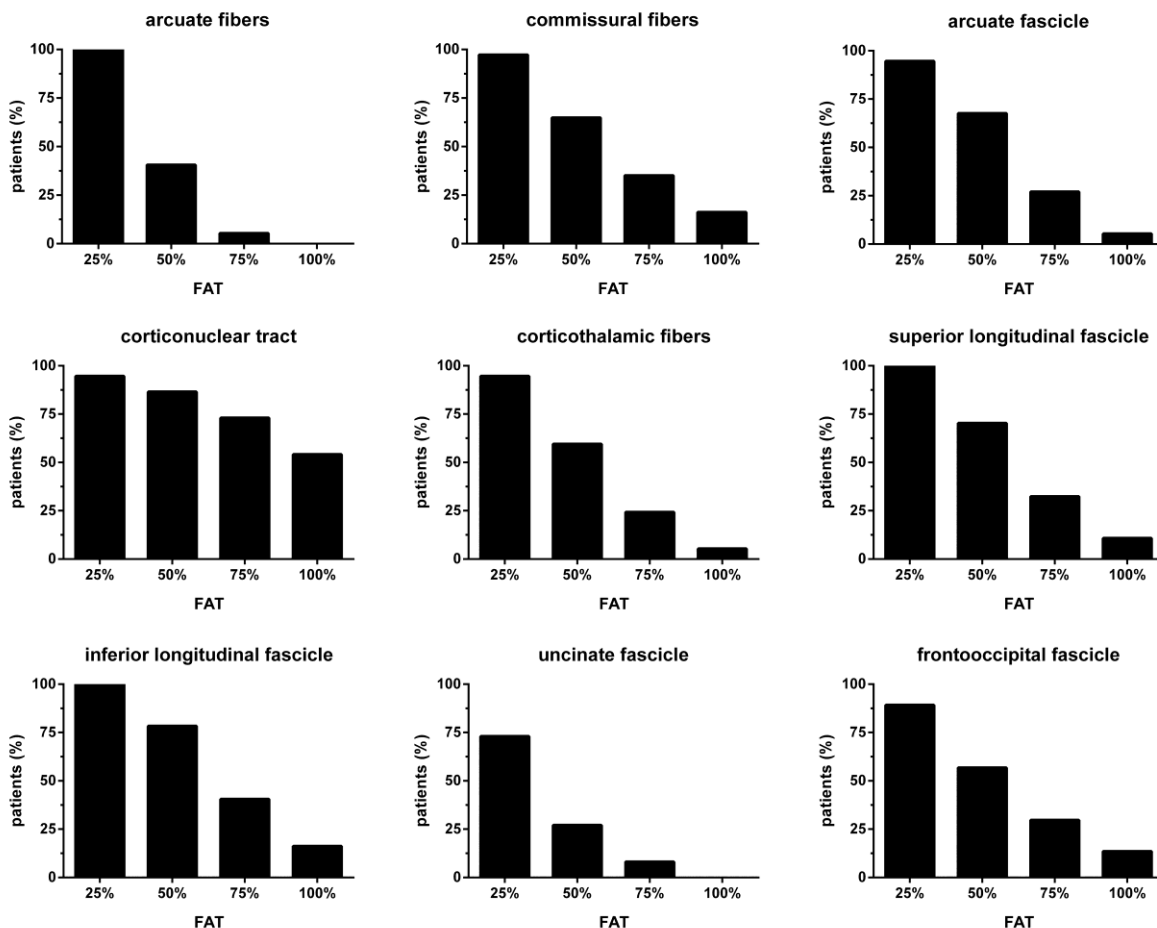


**Figure 19: Percentages of patients showing different subcortical language-related pathways I**

The bar graphs show the percentages of patients in which a certain subcortical language-related pathway was visualized, depending on the tractography adjustments using a fractional anisotropy threshold (25% FAT, 50% FAT, 75% FAT, and 100% FAT) (Sollmann et al., 2016d).

### 3.1.2. Own contribution

For this publication, I recruited patients, performed some of the clinical examinations, and partially organized their appointments for the different preoperative procedures. Furthermore, I performed language mappings by nTMS in these patients, and evaluated the acquired mapping data including video and audio recordings. This also involved categorization of naming errors elicited by nTMS into the different error categories as outlined in the methods

section. I furthermore extracted the mapping data for later nTMS-based tractography. I conducted tractography in close collaboration with C. Negwer (co-author on the publication). After tractography maps were generated, I conducted analysis of these maps, including subsequent statistics. I wrote the manuscript, performed literature research, and revised the manuscript according to the reviewers' comments during the review process carried out by the Journal of Neuroscience Methods. This was performed under close supervision of Dr. Krieg (senior author on the publication).

## 3.2. Language pathway tracking: comparing nTMS-based DTI fiber tracking with a cubic ROIs-based protocol

### 3.2.1. Key findings

Both tractography using nTMS data for ROI generation and tractography using anatomical landmarks for ROI creation were possible in all enrolled patients, leading to subcortical maps consisting of language-related WM pathways (Figures 20 & 21) (Negwer et al., 2017).

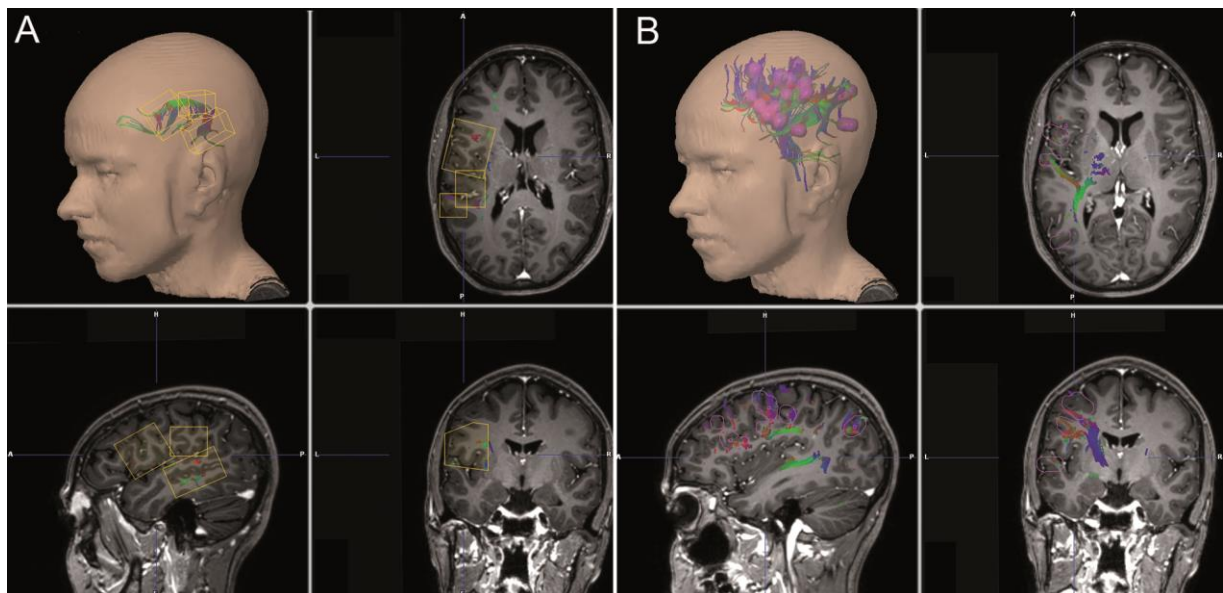


**Figure 20: Comparing anatomy-based tractography to tractography using language maps**

For anatomy-based tractography, 3 cubic regions of interest (ROIs; yellow) were created according to structural landmarks (A) (Negwer et al., 2017). Regarding tractography based on individual language maps, language-positive spots (purple) constituted one ROI (B) (Negwer et al., 2017). The respective results of diffusion tensor imaging fiber tracking (DTI FT) are shown as colored streamlines in the brain (Negwer et al., 2017).

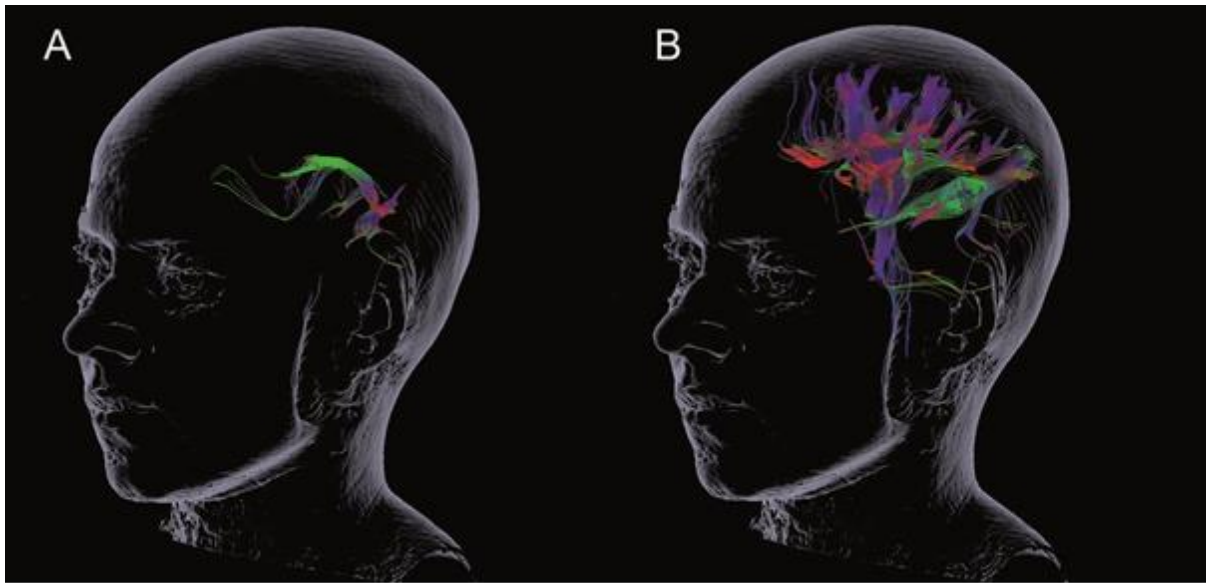


**Figure 21: Superiority of tractography based on language maps**

*When applying tractography based on cubic regions of interest (ROIs), clearly less subcortical language-related pathways are detected (A) when compared to tractography based on language-positive spots (B) in this illustrative case (Negwer et al., 2017).*

Regarding nTMS-based DTI FT with various predefined combinations of the MFL and FA (MFL 70 mm / FA 0.2, MFL 80 mm / FA 0.15, MFL 90 mm / FA 0.15, MFL 100 mm / FA 0.1, and MFL 100 mm / FA 0.15), nTMS-based DTI FT led to favorable results in terms of 7 out of 9 tracts (77.7%), whereas the approach using cubic ROI placement according to anatomical landmarks without consideration of nTMS data led to a significantly higher percentage of visualization regarding the AF (Figure 22) (Negwer et al., 2017). Furthermore, the shorter respective language-related WM tracts are (e.g., ArF), the better the visualization when applying nTMS-based DTI FT instead of cubic ROI placement (Figure 22) (Negwer et al., 2017). The UF, which is one of the short tracts involved in language function, was not depicted at all when using cubic ROI placement, whereas it was routinely visualized when applying nTMS-based DTI FT with different settings (Figure 22) (Negwer et al., 2017). The fraction of visualized WM fibers per number of visualized tracts was similar when comparing the cubic ROIs-based and nTMS-based approach ( $286 \pm 9$  vs.  $236 \pm 73$ ) (Negwer et al., 2017).

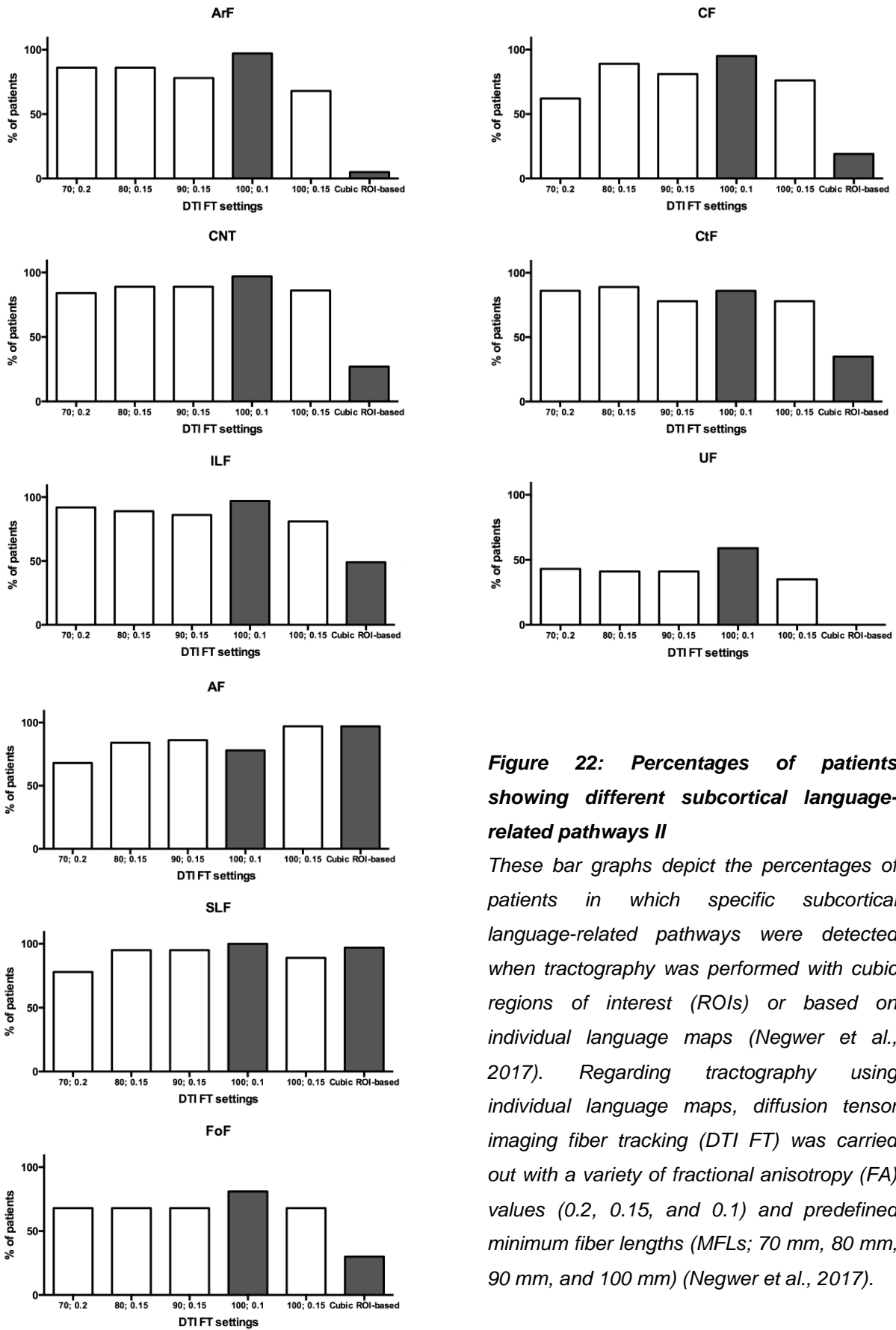


**Figure 22: Percentages of patients showing different subcortical language-related pathways II**

These bar graphs depict the percentages of patients in which specific subcortical language-related pathways were detected when tractography was performed with cubic regions of interest (ROIs) or based on individual language maps (Negwer et al., 2017). Regarding tractography using individual language maps, diffusion tensor imaging fiber tracking (DTI FT) was carried out with a variety of fractional anisotropy (FA) values (0.2, 0.15, and 0.1) and predefined minimum fiber lengths (MFLs; 70 mm, 80 mm, 90 mm, and 100 mm) (Negwer et al., 2017).

### 3.2.2. Own contribution

In cooperation with C. Negwer (first author on this publication), I recruited patients and partially organized their appointments for preoperative clinical examinations, MRI, and language mapping by nTMS. I then conducted mappings and analyzed the acquired mapping data including video and audio recordings. The categorization of naming errors that occurred due to nTMS was performed by myself, and I exported and transferred the analyzed data to the tractography workstation. I assisted during tractography, analysis of the DTI FT results, and statistical testing. I furthermore conducted literature research and revised the final version of the manuscript.

### 3.3. Interhemispheric connectivity revealed by diffusion tensor imaging fiber tracking derived from navigated transcranial magnetic stimulation maps as a sign of language function at risk in patients with brain tumors

#### 3.3.1. Key findings

Overall, IC+ was present in 42.1% (tractography with FA = 0.01) and 26.3% (tractography with FA = 0.2) of patients (Figure 23) (Sollmann et al., 2017b). The average number of visualized IC fibers  $\pm$  SD was  $260.5 \pm 394.7$  (tractography with FA=0.01) and  $111.0 \pm 118.2$  (tractography with FA=0.2) (Sollmann et al., 2017b).

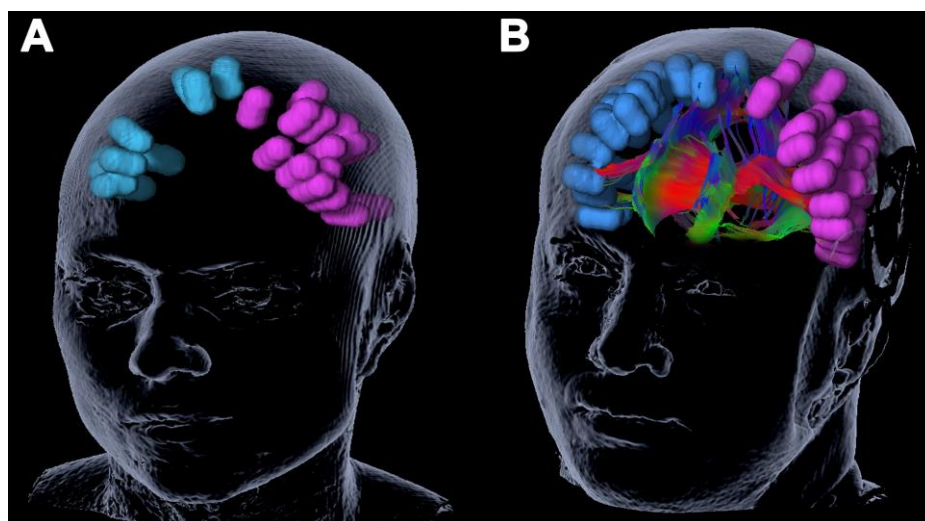


**Figure 23: Detection of interhemispheric connectivity (IC) by tractography**

No IC was found in illustrative case (A), whereas IC was present in case (B) (Sollmann et al., 2017b).

When comparing the number of patients suffering from language deficits to the number of patients without deficits depending on the presence or absence of IC (FA = 0.01), there were statistically significant differences observed for both postoperative ( $p=0.0161$ , OR 0.1429, 95% CI: 0.0261 – 0.7831) and surgery-related aphasia ( $p=0.0111$ , OR 0.1705, 95% CI: 0.0415 – 0.7008; Table 1). (Sollmann et al., 2017b). The specificity / sensitivity for the postoperative status was 85% / 56% and 76% / 65% for surgery-related aphasia (Table 2; Figure 24) (Sollmann et al., 2017b).

FA = 0.01				
Aphasia		Interhemispheric connectivity		p
		IC +	IC -	
Preoperative	no	9	14	0.6456
	yes	7	8	
Postoperative	no	2	11	0.0161
	yes	14	11	
Follow-up	no	9	17	0.1687
	yes	7	5	
Surgery-related	no	5	16	0.0111
	yes	11	6	

**Table 1: Interhemispheric connectivity (IC) and aphasia I**

This table compares the number of patients suffering from aphasia and the number of patients in which no aphasia was found correlated to the presence of IC (interhemispheric connectivity detected: IC+; no interhemispheric connectivity detected: IC-) for tractography with a predefined fractional anisotropy (FA) of 0.01 (Sollmann et al., 2017b).

FA = 0.01		
	postoperative aphasia	surgery-related aphasia
PPV	88%	69%
NPV	50%	73%
Sensitivity	56%	65%
Specificity	85%	76%

**Table 2: Sensitivity, specificity, positive predictive value (PPV), and negative predictive value (NPV) I**

This table shows the sensitivity, specificity, PPV, and NPV for tractography with a predefined fractional anisotropy (FA) of 0.01 to predict postoperative and surgery-related aphasia (Sollmann et al., 2017b).

Regarding tractography with 0.2 as the predefined FA value, similar results were obtained again for postoperative ( $p=0.0404$ , OR 0.1282, 95% CI: 0.0143 – 1.1520) and surgery-related aphasia ( $p=0.0090$ , OR 0.1184, 95% CI: 0.0208 – 0.6754; Table 3) (Sollmann et al., 2017b). The specificity / sensitivity for the postoperative status was 93% / 38% and 90% / 47% for surgery-related aphasia (Table 4; Figure 24) (Sollmann et al., 2017b).

FA = 0.2				
Aphasia		Interhemispheric connectivity		p
		IC +	IC -	
Preoperative	no	7	16	0.4752
	yes	3	12	
Postoperative	no	1	13	0.0404
	yes	9	15	
Follow-up	no	6	20	0.5045
	yes	4	8	
Surgery-related	no	2	19	0.0090
	yes	8	9	

**Table 3: Interhemispheric connectivity (IC) and aphasia II**

This table compares the number of patients suffering from aphasia and the number of patients in which no aphasia was found correlated to the presence of IC (interhemispheric connectivity detected: IC+; no interhemispheric connectivity detected: IC-) for tractography with a predefined fractional anisotropy (FA) of 0.2 (Sollmann et al., 2017b).

FA = 0.2		
	postoperative aphasia	surgery-related aphasia
PPV	90%	80%
NPV	46%	68%
Sensitivity	38%	47%
Specificity	93%	90%

**Table 4: Sensitivity, specificity, positive predictive value (PPV), and negative predictive value (NPV) II**

This table shows the sensitivity, specificity, PPV, and NPV for tractography with a predefined fractional anisotropy (FA) of 0.2 to predict postoperative and surgery-related aphasia (Sollmann et al., 2017b).

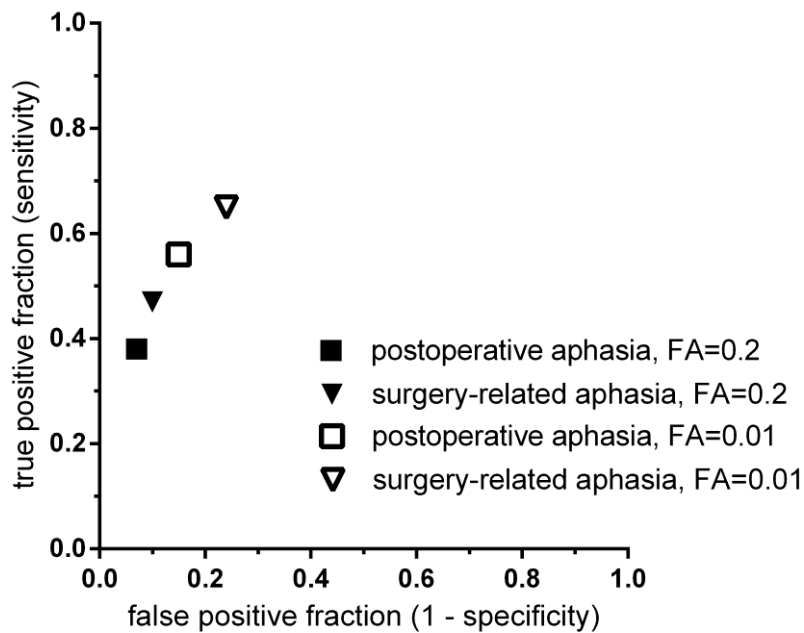


**Figure 24: False-positive versus true-positive fraction**

The results for 1 – specificity (x-axis) are plotted against the sensitivity (y-axis) for tractography of interhemispheric connectivity (IC) in relation to postoperative and surgery-related aphasia (Sollmann et al., 2017b). Regarding the fractional anisotropy (FA) values used for tractography, both 0.01 and 0.2 were applied (Sollmann et al., 2017b).

### 3.3.2. Own contribution

For this publication, I recruited patients, partially organized their appointments for the different preoperative procedures, and conducted some of the clinical examinations. Furthermore, I performed language mappings of both hemispheres by nTMS, and I evaluated the mapping sessions and video and audio recordings to identify and categorize any elicited naming errors during task performance. I furthermore extracted and transferred the data of both hemispheres separately for subsequent nTMS-based tractography, which was performed by myself to assess IC. After DTI FT was completed, tractography maps were successfully created, and I continued with the data analysis and statistics as described in the methods section. I wrote the manuscript, was responsible for literature research, and finally revised the manuscript according to the reviewers' comments during the review process by the Journal of Neurosurgery. These steps were performed under close supervision of Dr. Krieg (senior author on the publication).

## 4. DISCUSSION

---

### 4.1. Tractography based on nTMS data

The combination of nTMS data with DTI FT is a novel approach that has recently been used for reconstruction of the corticospinal tract (CST) in a limited amount of studies (Conti et al., 2014; Forster et al., 2015; Frey et al., 2012; Krieg et al., 2012a; Weiss et al., 2015). First work on nTMS-based DTI FT of the CST was able to demonstrate technical feasibility of using cortical stimulation spots at which MEPs above a certain amplitude were elicited for generation of ROIs in neurosurgical patients (Frey et al., 2012; Krieg et al., 2012a). Using either a manually adjusted FA value of less than or equal to 0.2 or a FAT-based approach, visualization of the CST was achieved successfully using a deterministic tractography algorithm (Frey et al., 2012; Krieg et al., 2012a). These early studies were followed up by methodological attempts to improve the reconstruction results of the CST by adding further anatomically-defined ROIs during tractography (e.g., at the level of the anterior inferior pontine region and/or the posterior limb of the internal capsule) or by using subdivisions of the cortical nTMS motor map as 3 or more single ROIs to perform somatotopic CST reconstruction with respect to specific cortical muscle representations (Conti et al., 2014; Weiss et al., 2015). Even more important, comparisons of nTMS-based DTI FT to conventional tractography of the CST (manual delineation of the suspected motor cortex according to anatomical landmarks) yielded favorable results regarding the nTMS-based approach, thus providing first hints for its potential clinical usefulness (Conti et al., 2014; Forster et al., 2015). Furthermore, subcortical DES was able to confirm the CST location and its somatotopic organization according to nTMS data in all enrolled patients that underwent surgery for resection of motor-eloquent brain tumors in one of these studies (Conti et al., 2014). This confirmation of reconstruction results by the gold standard method of intraoperative DES further suggests that the combination of nTMS and DTI FT may serve as a valuable clinical tool.

However, nTMS data have only been used for reconstruction of the CST in these studies, and the practicability of applying data derived from nTMS language mapping to reconstruct different subcortical language-related pathways has only been suggested in a single case report including one patient prior to publication of the articles included in this thesis (Sollmann et al., 2015a). Regarding the human motor system, the CST represents the main pathway of motor function with a comparatively unambiguous course of WM fibers from the PrG to the spinal cord (Nathan et al., 1990). Still, tractography of the CST can be improved by innovative approaches like the consideration of nTMS for ROI seeding especially in

patients with altered cortical anatomy, but the situation is obviously more complex for a widespread network that is composed of a variety of cortical and subcortical structures, such as the human language network (Chang et al., 2015; Friederici and Gierhan, 2013). The multiplicity of subcortical language-related pathways has largely hampered consensus on standardized approaches to reconstruct language-related WM fibers so far, whereas in contrast, most studies on CST tractography consider manual delineation of the motor cortex, sometimes combined with further additional ROIs, as a standard and agreed-upon procedure for ROI definition (Conturo et al., 1999; Kunimatsu et al., 2004). The urgent need for approaches that enable reliable tractography of language-related WM pathways, starting with best-possible ROI seeding as a prerequisite for subsequent fiber reconstructions, is tackled by the implementation of nTMS language data in DTI FT as presented in the articles included in this thesis (Negwer et al., 2017; Sollmann et al., 2016d; Sollmann et al., 2017b).

Against this background, nTMS-based DTI FT has to be set in relation to already existing approaches for the purpose of tracking language-related WM pathways. So far, this has been achieved based on one of 2 main setups, which are anatomical seeding (manual delineation of suspected language-related areas as a ROI) or functional seeding (ROI definition with respect to information on the functional involvement of brain regions to delineate language-related areas). For anatomical seeding, imaging data derived from previous MRI scanning is commonly used, whereas functional seeding primarily derives from information acquired by fMRI, with nTMS mapping reflecting a new functional seeding approach. Whereas both setups are frequently applied to date, functional-based seeding is increasingly being favored, which is mainly due to 3 shortcomings of the anatomy-based method. First, ROI seeding based on structural landmarks of the brain depends on the individual anatomic knowledge of the investigator, and, thus, can vary between different investigators to a certain extent (Catani and Thiebaut de Schotten, 2008; Wakana et al., 2004). Second, the investigator may have difficulties during unequivocal identification of structural landmarks that should be enclosed during ROI placement when it comes to patients with changed intracranial anatomy (e.g., due to brain tumors) (Lehericy et al., 2000; Nimsky et al., 2006). Third, especially slowly developing brain pathologies (e.g., low-grade gliomas) have proven to harbor the potential to trigger spatial reallocation of brain functions, thus possibly resulting in shifting of functions away from characteristic brain structures towards adjacent or remote areas (Duffau, 2014b; Robles et al., 2008; Southwell et al., 2016). When function is no longer represented within the traditional area where the investigator would assume it according to anatomy, anatomy-based ROI placement may not include the function that should be targeted for subsequent tractography. These 3 aspects can heavily contribute to poor reproducibility or even incorrect tractography in patients suffering from brain tumors.

Although these factors should not be present during functional ROI seeding, other shortcomings that are primarily linked to the limitations of the underlying modality used to acquire functional data are well known. Concerning task-based fMRI, it has been shown that the applied blood oxygenation level dependent (BOLD) contrast lacks accuracy in patients with altered intracranial oxygen levels, which are regularly present in the vicinity of gliomas due to their glucose and oxygen consumption from adjacent brain tissue (Fraga de Abreu et al., 2016; Holodny et al., 2000; Schreiber et al., 2000). Other modalities with sufficient temporal and spatial resolution that allow for acquisition of data for identification of language-related areas such as MEG, for example, reflect more expensive alternatives and are not widely available. Thus, nTMS-based DTI FT of subcortical language-related pathways offers the opportunity to use functional data for tractography without the limitations shown for fMRI.

## **4.2. Feasibility and superiority of nTMS-based DTI FT of language-related pathways**

As a first step to establish nTMS-based DTI FT for delineation of subcortical language-related pathways, technical feasibility had to be shown (Sollmann et al., 2016d). In this context, our approach of defining language-positive stimulation spots as a ROI and using this nTMS-based ROI during tractography allowed for reconstruction of different WM fiber tracts in all included patients (Sollmann et al., 2016d). This was achieved without any methodological problems, and we used a FAT-based approach in the first included study since tractography applying FATs has shown to enable smooth DTI FT whilst being standardized and well established (Frey et al., 2012; Sollmann et al., 2016d).

While application of 100% FAT or 75% FAT during DTI FT did not lead to regular detection of the 9 predefined tracts (e.g., UF not detected in any case for 100% FAT and in less than 10% for 75% FAT) and, moreover, led to low fractions of visualized WM fibers per number of visualized tracts, better results in terms of visualized tracts were achieved for 50% FAT and 25% FAT (Sollmann et al., 2016d). In this context, tractography with 50% FAT or 25% FAT enabled DTI FT of most of the 9 predefined tracts within a clear majority of patients, with subcortical language-related pathways being constituted of a considerable number of fibers as reflected by the fibers-per-tract ratios (Sollmann et al., 2016d). However, tractography using 25% FAT might have most likely resulted in an overrepresentation of WM fibers, making it hard to identify tracts whilst simultaneously leading to delineation of aberrant fibers, as already shown for nTMS-based DTI FT when used for CST reconstructions (Frey et al., 2012; Sollmann et al., 2016d).

Founded on these initial experience and demonstrated feasibility, comparison of tractography results based on nTMS to anatomical ROI seeding had to be investigated (Negwer et al., 2017). Overall, the applied nTMS-based DTI FT protocols showed superior results when compared to anatomy-based seeding considering one of the few available standardized approaches to tractography of language-related WM pathways (Henning Stieglitz et al., 2012; Negwer et al., 2017). While only the AF was visualized in a significantly larger fraction of patients when using the anatomy-based approach, other tracts were not constantly visualized, with the UF not being detectable in any of the patients (Negwer et al., 2017). Thus, improved visualization of different subcortical language-related pathways can be achieved by incorporating nTMS data, whereas the anatomy-based setup proved to be a good option only for a subselection of tracts (Negwer et al., 2017). As a consequence, nTMS-based DTI FT instead of conventional anatomical ROI seeding should be standardly used in the future to optimize tractography.

### **4.3. Risk stratification by nTMS-based DTI FT of language-related pathways**

Furthermore, we evaluated whether the status of visualized IC detected by nTMS-based DTI-FT can be used for risk assessment in terms of language deficits at different time points (Sollmann et al., 2017b). In this context, IC+ was present to a variable degree but less frequently in patients without postoperative language deficits, and similar results were also found in terms of surgery-related language impairment (Sollmann et al., 2017b). The presence or absence of detectable IC might be related to plastic reshaping of language-related brain areas, which can be found partially shifted to the non-affected hemisphere as an expression of interhemispheric reorganization to compensate for potential loss of function due to a tumor (Briganti et al., 2012; Krieg et al., 2013b; Rosler et al., 2014; Wang et al., 2013). Hence, detectability of IC by means of nTMS-based DTI FT could express an early form of compensatory mechanism for recovery of language function via an interhemispheric functional shift when language function is already at risk (Sollmann et al., 2017b). Taken together, our results suggest that IC detected by nTMS-based DTI FT could be regarded as a risk factor for the occurrence of postoperative and, more specifically, surgery-related language deficits with a high specificity of up to 93% (Sollmann et al., 2017b).

#### 4.4. Significance and implications

In general, nTMS-based DTI FT of subcortical language-related pathways has not been reported prior to publication of the articles included in this thesis except for one case report (Sollmann et al., 2015a). Thus, it reflects a novel approach for visualization of WM tracts related to language function, which leads to tractography maps that can be used during consultation of patients based on individual functional data and for case discussions during interdisciplinary tumor boards to determine the best treatment options for the respective patient considering both individual anatomical and functional data (Figure 25).

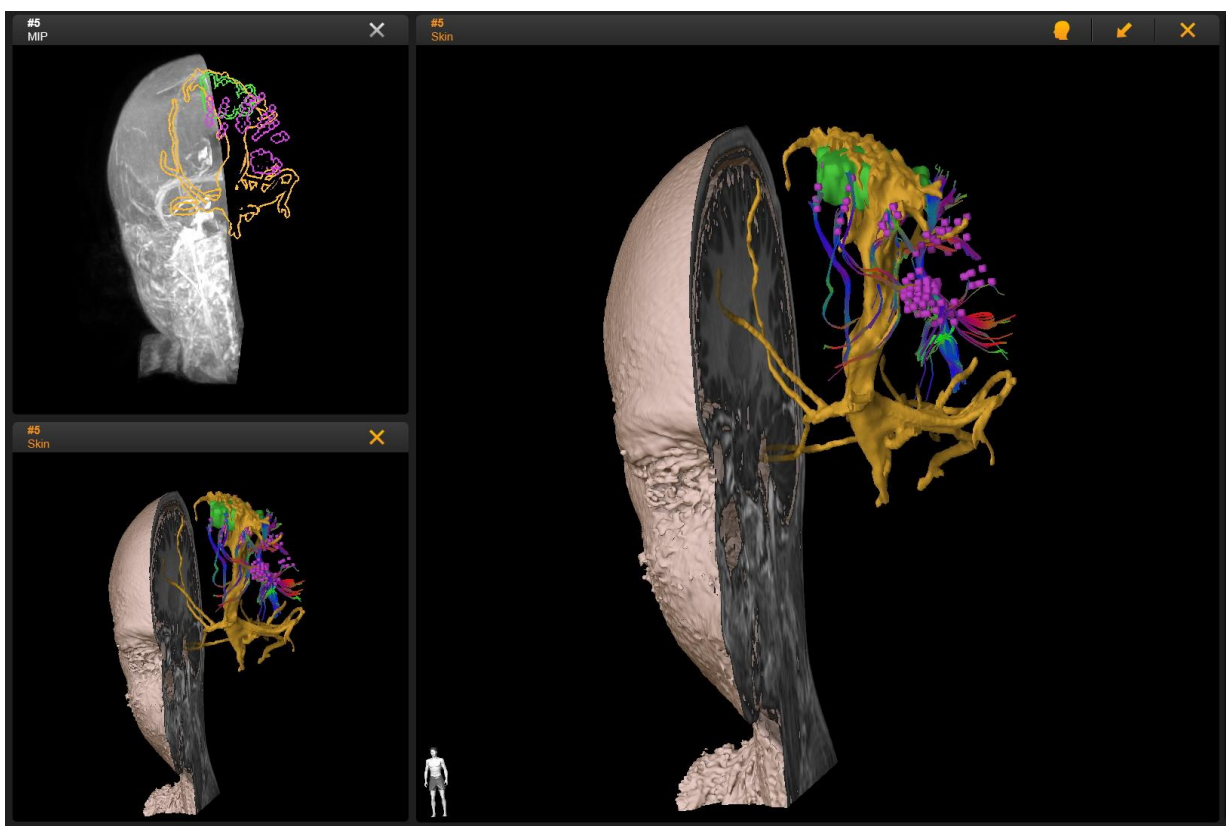


**Figure 25: Combined anatomical and functional data for patient consultation**

Cortical and subcortical maps of language-related pathways derived from individual language maps can support visualization of functional anatomy that can be illustrated to the patient to facilitate the risks and chances of surgery for tumor resection. In this illustrative case, cortical language-positive spots (purple), subcortical language-related pathways (mixed colors), cortical motor-positive spots (green), and fibers belonging to the corticospinal tract (CST; yellow), all derived from preoperative mapping by navigated transcranial magnetic stimulation (nTMS), are visualized together with anatomical magnetic resonance imaging (MRI).

Furthermore, such data can be used for preoperative resection planning and intraoperative resection guidance during tumor removal. Visualization of cortical and subcortical language structures derived from nTMS language mapping and nTMS-based DTI FT of subcortical language pathways can then guide the surgeon's hands with the DES electrode. Furthermore, it has already been shown that the reconstructed tracts can reflect reality since intraoperative stimulation of WM fibers belonging to the SLF led to stimulation-induced language disturbances (Figure 26) (Sollmann et al., 2015a). While intraoperative comparisons have only been reported in one patient due to the novelty of the technique, direct clinical usefulness for neurosurgeons already seems evident (Sollmann et al., 2015a).

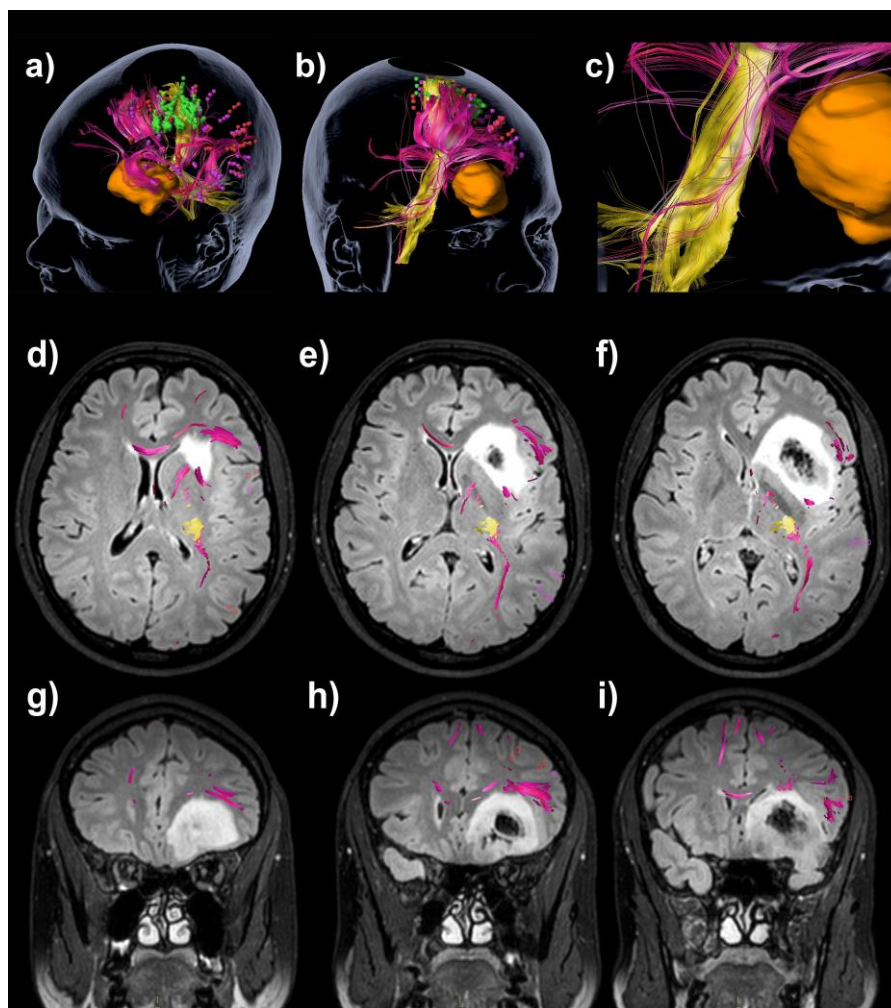


**Figure 26: Tractography based on language maps as used during surgery**

Language maps combined with tractography based on navigated transcranial magnetic stimulation (nTMS) can visualize motor-positive spots (green) and language-positive spots (red & pink), the corticospinal tract (CST; yellow), and subcortical language-related pathways (red & pink) during tumor removal (tumor depicted in orange), with good accordance between subcortical direct electrical stimulation (DES) and reconstructions of the superior longitudinal fascicle (SLF) (Sollmann et al., 2015a).

Regarding the parameters that should be used during nTMS-based DTI FT of subcortical language-related pathways, recommendations are already possible and were evaluated simultaneously to assessments of feasibility and comparisons to anatomy-based tractography (Negwer et al., 2017; Sollmann et al., 2016d). This is important since most of the tractography software used in neurosurgery are based on deterministic algorithms and require manual definitions of at least the FA value. In this context, this parameter reflects the direction dependence in a diffusion process, and it has a major impact on the final tractography results (Basser et al., 1994; Basser et al., 2000). Because of its strong influence, the FA value should not be set arbitrarily. Instead, a certain standardized approach should be established that either applies optimal settings or uses individualized FA values, such as FAT-based tractography (Frey et al., 2012). Otherwise, an arbitrary FA value is used for all subjects without considering inter-subject variations in tractography or the FA value is simply altered according to the investigator's expectation about what the tractography should look like. These rather insufficient approaches might probably fail to show optimal DTI FT results, whereas the adjustments evaluated in our studies including initial recommendations (e.g., 50% or 25% FAT) could overcome the above-mentioned issues (Negwer et al., 2017; Sollmann et al., 2016d). Further research has even provided more extensive protocol comparisons for nTMS-based DTI FT of language pathways, which should be considered in the clinical routine among patients with brain tumors (Negwer et al., 2016).

Regarding risk stratification derived from nTMS-based DTI FT of language pathways, we are not aware of any other publication distinctly investigating IC as a potential risk factor in terms of language deficits (Sollmann et al., 2017b). Thus, nTMS-based DTI FT might already be expanded to further clinical applications beyond its role for pre- and intraoperative visualization of WM fiber tracts. Such risk stratification may implicate benefits for both the treating neurosurgeon as well as the patient. For the neurosurgeon, presence of nTMS-based IC as a risk factor for language deterioration could increase awareness of language function at risk even in patients where imaging might not suggest that, whereas the patient could already be informed preoperatively about the individual risk concerning language deterioration due to surgery (Sollmann et al., 2017b). On both sides, the process of decision-making for or against surgery for tumor removal or a specific surgical approach should be facilitated (Sollmann et al., 2017b).

Importantly, the time required to generate nTMS-based DTI FT of language pathways according to the approach presented in this thesis ranges between 10 and 15 min on average, thus supporting direct clinical use (Sollmann et al., 2016d). Therefore, only limited additional efforts are needed to generate data that have shown to be superior to conventional anatomy-based tractography and that can assist during risk stratification and decision-making. Clinical applicability is further enhanced by the universal data format of nTMS maps

and tractography, which can be smoothly implemented in the hospital's preexisting environment, including the picture archiving and communication system (PACS) and the hospital information system (Sollmann et al., 2017a). This facilitates availability of cortical and subcortical functional data based on nTMS during the inpatient stay of a respective patient and during FU visits, and allows other departments to access such information that might be beneficial for further treatment approaches such as radiosurgery (Conti et al., 2013; Picht et al., 2014; Sollmann et al., 2017a).

#### **4.5. Limitations**

Although the feasibility of nTMS-based DTI FT for detection of language-related subcortical pathways was successfully demonstrated with superiority when compared to anatomy-based ROI seeding and data derived from this approach furthermore allows for risk stratification, some limitations have to be discussed (Negwer et al., 2017; Sollmann et al., 2016d; Sollmann et al., 2017b). One main limitation is related to the nature of tractography based on DTI sequences as it has been shown that correct WM fiber reconstructions can be hampered by crossing or kissing fiber courses because these situations have an impact on reliable identification of a primary eigenvector of a voxel (Berman et al., 2007; Le Bihan et al., 2006). Furthermore, WM fibers adjacent or within brain tumors, the brain's ventricular system, or edema are likely to be not reconstructed properly during DTI FT due to low anisotropy (Assaf and Pasternak, 2008; Berman et al., 2007). Due to these considerable shortcomings, efforts are being made to both develop better diffusion sequences and more advanced analysis algorithms. These include, but are not limited to the multiple tensor approach in which more than one tensor is allowed to exist in each voxel or high angular resolution diffusion imaging that enables the visualization of multiple fiber orientations (Assaf and Pasternak, 2008; Bucci et al., 2013; Kuhnt et al., 2013; Tuch et al., 2002). These approaches which are currently under development commonly struggle with partial volume effects, and are still far away from being routinely implemented in standard clinical software (Assaf and Pasternak, 2008). Nevertheless, it is obvious that further developments of DTI FT are highly needed to overcome various limitations in the clinical setting, and testing of the described advances should not be restricted a priori due to potentially more complex data implementation (Abhinav et al., 2014; Bucci et al., 2013; Kuhnt et al., 2013).

Furthermore, cortical language mapping by nTMS still suffers from a comparatively low specificity and PPV, whereas the opposite is true for the sensitivity and NPV (Ille et al., 2015; Picht et al., 2013; Tarapore et al., 2013). This implies that not all language-positive stimulation spots that survive post hoc analysis of mapping data can be considered language-eloquent and, therefore, as indispensable locations of the language network.

Instead, these spots should be regarded as language-involved, thus implying that the distinct function and necessity of some of these spots in terms of language function are not completely clear. Due to this high sensitivity, an overrepresentation of spots might have occurred for later nTMS-based DTI FT in some patients, thus probably leading to a certain fraction of spurious fibers in addition to the reconstructed language-related WM pathways. This should not limit our results per se, but attempts should be made to further improve the specificity of language mapping by nTMS. In this context, advances have already been made by trying to optimize stimulation parameters and by focusing on specific error categories instead of incorporating all types during definition of ROIs, which has led to promising results in initial investigations (Ille et al., 2015; Sollmann et al., 2015c; Sollmann et al., 2016c). Nevertheless, more studies are needed to determine optimal settings leading to favorable cortical language maps and, in the next step, to optimized DTI FT results when carried out based on nTMS data with higher specificity.

As another limitation, the articles included in this thesis did not compare tractography results based on nTMS data to intraoperative subcortical DES in order to validate the correct localization and extent of the reconstructed WM fiber tracts. However, since intraoperative DES represents the current gold standard for detection of language-eloquent structures, this comparison is required in the near future to judge whether results derived from nTMS-based DTI FT for language pathways are actually valid with last certainty. This need for validation is based both on the high sensitivity of cortical nTMS mapping as well as the limitations of the DTI technique, with the latter even leading to the question if DTI is ready to be used in the clinical routine (Duffau, 2014a; Nimsky, 2010). Although the debate is still ongoing, many centers already implemented the DTI technique without the newly developed supplementation by nTMS data in their surgical approaches to treat brain tumors (Bello et al., 2008; Kuhnt et al., 2012; Leclercq et al., 2010). In this context, subcortical DES for the detection of language-related WM pathways without using nTMS data actually showed that intraoperative DES can principally be in good accordance with tractography, which is reflected by an overall sensitivity of up to 97% (Bello et al., 2008). For nTMS-based DTI FT, only one case report compared tractography and subcortical DES for language-related pathways, whereas another study performed an analogous comparison for reconstruction of the CST, with encouraging results being reported in both publications (Conti et al., 2014; Sollmann et al., 2015a). However, a study validating tractography of subcortical language-related pathways by nTMS-based DTI FT in a representative cohort of patients is still missing.

## 4.6. Outlook

Concerning future perspectives based on our results on nTMS-based tractography of language-related WM pathways, a systematic comparison to fMRI used for functional seeding should be established. Comparison of nTMS-based DTI FT to anatomy-based seeding has already shown superiority of the nTMS-based approach, but it is not yet clear whether the same is actually true for comparison against other function-based seeding methods as well (Negwer et al., 2017). As previously mentioned, fMRI for language mapping has regularly shown to lack sufficient accuracy, but this was primarily shown for cortical mapping without taking fMRI activation maps as starting points for tractography into account (Fraga de Abreu et al., 2016; Holodny et al., 2000; Schreiber et al., 2000). Hence, upcoming studies should also incorporate fMRI-based seeding and compare it to nTMS-based DTI FT for tracking of subcortical language-related pathways to further evaluate this novel approach in comparison to its potential alternatives.

Moreover, intra- and inter-observer reliability should be assessed next for nTMS-based DTI FT. Regarding seeding of ROIs, no difference is expected between investigators since it is exclusively performed based on functional data that are not further modified during ROI generation. However, the tracking itself using a FAT-based approach and the evaluation concerning different subcortical language-related pathways can lead to differences between investigators, which might especially hold true for patients with large brain tumors and altered intracranial anatomy where identification of specific tracts might be difficult. As nTMS-based DTI FT is a new technique, assessment of reliability seems to be mandatory to further strengthen its usefulness in clinical routine where different investigators are likely to perform tractography.

To make use of further opportunities the new approach might provide, distances between language-related fibers tracked by preoperative nTMS-based DTI FT and the brain lesion should be assessed and set in relation to postoperative language deficits. Such measurements may allow a minimum lesion-to-fiber distance to be determined which should be maintained during surgery to prevent language deterioration. Similar approaches already exist for nTMS-based tractography of the CST, showing that patients with preoperatively measured lesion-to-CST distances of at least 8 to 12 mm did not suffer from postoperative worsening of motor function (Figure 27) (Rosenstock et al., 2017; Sollmann et al., 2017c). It has to be proven whether the same range of distances holds true for tractography based on nTMS language maps.

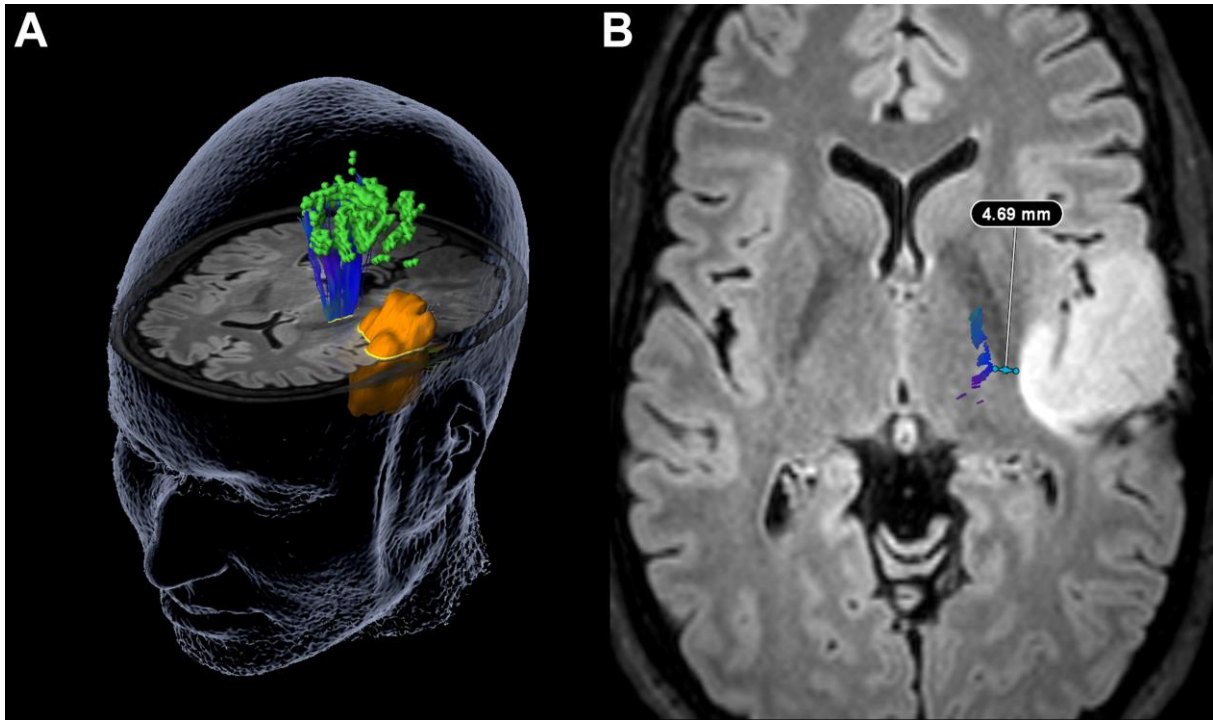


**Figure 27: Distance measurements between reconstructed fibers and the brain tumor**

*Regarding diffusion tensor imaging fiber tracking (DTI FT) of the corticospinal tract (CST) based on navigated transcranial magnetic stimulation (nTMS), measurements of lesion-to-CST distances, set in relation to the motor status of the patient, allow for definition of a minimum distance that should be considered during surgery to prevent new functional impairment (Sollmann et al., 2017c). A similar approach should be followed in terms of nTMS-based tractography of subcortical language-related pathways.*

When nTMS data derived from cortical language or motor mapping are incorporated in clinical routine and are used during surgical planning and intraoperative resection guidance, improved outcome can be achieved in terms of several perioperative characteristics. This has been demonstrated in several studies comparing the clinical course of patients that underwent nTMS mapping to those of historic control groups without nTMS mapping (Frey et al., 2014; Krieg et al., 2016a; Krieg et al., 2014a; Krieg et al., 2015; Sollmann et al., 2015b). Among other factors, patients that underwent preoperative nTMS language mapping showed postoperative language deficits significantly less frequently and had smaller craniotomies, whereas trends towards fewer tumor residuals, shorter durations of surgery, and shorter inpatient stays were observed when compared to a non-nTMS group (Sollmann et al., 2015b). Although these results are already encouraging and beneficial for the individual patient, they have been achieved based on cortical nTMS maps without consideration of nTMS-based DTI FT (Sollmann et al., 2015b). Thus, they might be improved when

incorporating nTMS-based DTI FT of language-related WM pathways as well, which should be ideally assessed within the scope of a randomized controlled trial.

Regarding risk stratification based on the evaluation of IC as detected by nTMS-based tractography, we used a comparatively rough grading scheme that might not necessarily detect minor changes in the patients' language status although it is regarded as sufficiently accurate for application in most neurosurgical patients (Krieg et al., 2014b; Sollmann et al., 2015b; Sollmann et al., 2017b). However, from a more linguistic point of view, this scheme is unlikely to cover all possible aspects of language function, which implicates that a subgroup of enrolled patients were not diagnosed with language impairment although there might have been subclinical or slight deficits (Sollmann et al., 2017b). Although our approach evaluating IC revealed by nTMS-based DTI FT as a parameter for risk stratification was successful, more sensitive assessment tools for language evaluation might further improve the specificity and should replace the comparatively rough grading within the scope of FU studies on the matter.

## 5. SUMMARY

---

Navigated transcranial magnetic stimulation (nTMS) is a non-invasive neurostimulation technique that elicits a transient electric field and enables systematic mapping of the human cortex to localize and spatially enclose specific functions. In the recent years, nTMS is being increasingly used in neurosurgery to conduct motor or language mapping in patients suffering from brain tumors. The resulting cortical motor or language maps can then be used during surgical planning and resection guidance with the aim to preserve function while facilitating a more extensive tumor resection leading to increased survival and quality of life.

In general, nTMS mapping is primarily restricted to the cortical surface, thus mainly providing information about the cortical organization and representation of motor or language function. However, especially the human language network is complex and widespread, and new models incorporate a variety of subcortical fiber pathways besides specific superficial cortical areas. To be able to identify subcortical language-related pathways, we combined diffusion tensor imaging fiber tracking (DTI FT) with cortical nTMS-based language maps, which reflects a novel approach. After feasibility was shown for a set of 9 predefined language-related fiber tracts in patients with brain tumors, we compared our novel approach to anatomy-based DTI FT, which is commonly used to delineate subcortical fiber anatomy related to language. Our novel approach yielded better results than the classic anatomy-based tractography algorithm since we were able to detect 76.0% of the included subcortical language-related pathways (nTMS-based DTI FT) compared to 39.9% (anatomy-based DTI FT). Furthermore, extending beyond the level of detecting specific fiber tracts by nTMS-based DTI FT, we applied our approach to individual risk stratification regarding aphasia. In this context, interhemispheric connectivity (IC) tracked by nTMS-based DTI FT was present more frequently in patients that showed postoperative or surgery-related language deficits, which might be related to the plastic reshaping of language-related areas which may partially shift to the non-affected hemisphere due to the tumor volume, mediated by detectable IC. Thus, IC revealed by preoperative nTMS-based DTI FT can be regarded as a risk factor for aphasia with a specificity of up to 93% in patients with brain tumors.

Taken together, the studies incorporated in this thesis showed that nTMS language maps are feasible for DTI FT of subcortical language-related pathways. The novel approach of nTMS-based DTI FT proved to be superior to classic anatomy-based tractography. Furthermore, it might serve as a beneficial tool for individual risk assessment concerning surgery-related language deterioration in patients with brain tumors, thus improving the clinical management and consultation of our patients.

## 6. REFERENCES

---

Abhinav, K., Yeh, F.C., Pathak, S., Suski, V., Lacomis, D., Friedlander, R.M., Fernandez-Miranda, J.C., 2014. Advanced diffusion MRI fiber tracking in neurosurgical and neurodegenerative disorders and neuroanatomical studies: A review. *Biochim Biophys Acta* 1842, 2286-2297.

Ammirati, M., Vick, N., Liao, Y.L., Ciric, I., Mikhael, M., 1987. Effect of the extent of surgical resection on survival and quality of life in patients with supratentorial glioblastomas and anaplastic astrocytomas. *Neurosurgery* 21, 201-206.

Anderson, J.M., Gilmore, R., Roper, S., Crosson, B., Bauer, R.M., Nadeau, S., Beversdorf, D.Q., Cibula, J., Rogish, M., 3rd, Kortencamp, S., Hughes, J.D., Gonzalez Rothi, L.J., Heilman, K.M., 1999. Conduction aphasia and the arcuate fasciculus: A reexamination of the Wernicke-Geschwind model. *Brain Lang* 70, 1-12.

Assaf, Y., Pasternak, O., 2008. Diffusion tensor imaging (DTI)-based white matter mapping in brain research: a review. *J Mol Neurosci* 34, 51-61.

Awiszus, F., 2003. TMS and threshold hunting. *Suppl Clin Neurophysiol* 56, 13-23.

Axer, H., Klingner, C.M., Prescher, A., 2013. Fiber anatomy of dorsal and ventral language streams. *Brain Lang* 127, 192-204.

Barker, A.T., Jalinous, R., Freeston, I.L., 1985. Non-invasive magnetic stimulation of human motor cortex. *Lancet* 1, 1106-1107.

Basser, P.J., Mattiello, J., LeBihan, D., 1994. MR diffusion tensor spectroscopy and imaging. *Biophys J* 66, 259-267.

Basser, P.J., Pajevic, S., Pierpaoli, C., Duda, J., Aldroubi, A., 2000. In vivo fiber tractography using DT-MRI data. *Magn Reson Med* 44, 625-632.

Bello, L., Gambini, A., Castellano, A., Carrabba, G., Acerbi, F., Fava, E., Giussani, C., Cadioli, M., Blasi, V., Casarotti, A., Papagno, C., Gupta, A.K., Gaini, S., Scotti, G., Falini, A.,

2008. Motor and language DTI Fiber Tracking combined with intraoperative subcortical mapping for surgical removal of gliomas. *Neuroimage* 39, 369-382.

Berker, E.A., Berker, A.H., Smith, A., 1986. Translation of Broca's 1865 report. Localization of speech in the third left frontal convolution. *Arch Neurol* 43, 1065-1072.

Berman, J.I., Berger, M.S., Chung, S.W., Nagarajan, S.S., Henry, R.G., 2007. Accuracy of diffusion tensor magnetic resonance imaging tractography assessed using intraoperative subcortical stimulation mapping and magnetic source imaging. *J Neurosurg* 107, 488-494.

Bogen, J.E., Bogen, G.M., 1976. Wernicke's region--Where is it? *Ann N Y Acad Sci* 280, 834-843.

Briganti, C., Sestieri, C., Mattei, P.A., Esposito, R., Galzio, R.J., Tartaro, A., Romani, G.L., Caulo, M., 2012. Reorganization of functional connectivity of the language network in patients with brain gliomas. *AJNR Am J Neuroradiol* 33, 1983-1990.

Broca, P., 1861. Remarques sur le siège de la faculté du langage articulé, suivies d'une observation d'aphémie (perte de la parole). *Bull Soc Anat* 36, 330-357.

Bucci, M., Mandelli, M.L., Berman, J.I., Amirbekian, B., Nguyen, C., Berger, M.S., Henry, R.G., 2013. Quantifying diffusion MRI tractography of the corticospinal tract in brain tumors with deterministic and probabilistic methods. *Neuroimage Clin* 3, 361-368.

Capelle, L., Fontaine, D., Mandonnet, E., Taillandier, L., Golmard, J.L., Bauchet, L., Pallud, J., Peruzzi, P., Baron, M.H., Kujas, M., Guyotat, J., Guillevin, R., Frenay, M., Taillibert, S., Colin, P., Rigau, V., Vandebos, F., Pinelli, C., Duffau, H., French Réseau d'Etude des, G., 2013. Spontaneous and therapeutic prognostic factors in adult hemispheric World Health Organization Grade II gliomas: a series of 1097 cases: clinical article. *J Neurosurg* 118, 1157-1168.

Catani, M., Howard, R.J., Pajevic, S., Jones, D.K., 2002. Virtual in vivo interactive dissection of white matter fasciculi in the human brain. *Neuroimage* 17, 77-94.

Catani, M., Thiebaut de Schotten, M., 2008. A diffusion tensor imaging tractography atlas for virtual in vivo dissections. *Cortex* 44, 1105-1132.

Chang, E.F., Raygor, K.P., Berger, M.S., 2015. Contemporary model of language organization: an overview for neurosurgeons. *J Neurosurg* 122, 250-261.

Chang, E.F., Wang, D.D., Perry, D.W., Barbaro, N.M., Berger, M.S., 2011. Homotopic organization of essential language sites in right and bilateral cerebral hemispheric dominance. *J Neurosurg* 114, 893-902.

Conti, A., Pontoriero, A., Ricciardi, G.K., Granata, F., Vinci, S., Angileri, F.F., Pergolizzi, S., Alafaci, C., Rizzo, V., Quartarone, A., Germano, A., Foroni, R.I., De Renzi, C., Tomasello, F., 2013. Integration of functional neuroimaging in CyberKnife radiosurgery: feasibility and dosimetric results. *Neurosurg Focus* 34, E5.

Conti, A., Raffa, G., Granata, F., Rizzo, V., Germano, A., Tomasello, F., 2014. Navigated transcranial magnetic stimulation for "somatotopic" tractography of the corticospinal tract. *Neurosurgery* 10 Suppl 4, 542-554; discussion 554.

Conturo, T.E., Lori, N.F., Cull, T.S., Akbudak, E., Snyder, A.Z., Shimony, J.S., McKinstry, R.C., Burton, H., Raichle, M.E., 1999. Tracking neuronal fiber pathways in the living human brain. *Proc Natl Acad Sci U S A* 96, 10422-10427.

Corina, D.P., Loudermilk, B.C., Detwiler, L., Martin, R.F., Brinkley, J.F., Ojemann, G., 2010. Analysis of naming errors during cortical stimulation mapping: implications for models of language representation. *Brain Lang* 115, 101-112.

Damasio, A.R., 1992. Aphasia. *N Engl J Med* 326, 531-539.

De Witt Hamer, P.C., Robles, S.G., Zwinderman, A.H., Duffau, H., Berger, M.S., 2012. Impact of intraoperative stimulation brain mapping on glioma surgery outcome: a meta-analysis. *J Clin Oncol* 30, 2559-2565.

Devlin, J.T., Watkins, K.E., 2007. Stimulating language: insights from TMS. *Brain* 130, 610-622.

Duffau, H., 2014a. Diffusion tensor imaging is a research and educational tool, but not yet a clinical tool. *World Neurosurg* 82, e43-45.

Duffau, H., 2014b. The huge plastic potential of adult brain and the role of connectomics: new insights provided by serial mappings in glioma surgery. *Cortex* 58, 325-337.

Duffau, H., 2015. Stimulation mapping of white matter tracts to study brain functional connectivity. *Nat Rev Neurol* 11, 255-265.

Duffau, H., Denvil, D., Capelle, L., 2002. Long term reshaping of language, sensory, and motor maps after glioma resection: a new parameter to integrate in the surgical strategy. *J Neurol Neurosurg Psychiatry* 72, 511-516.

Duffau, H., Gatignol, P., Moritz-Gasser, S., Mandonnet, E., 2009. Is the left uncinate fasciculus essential for language? A cerebral stimulation study. *J Neurol* 256, 382-389.

Duffau, H., Mandonnet, E., 2013. The "onco-functional balance" in surgery for diffuse low-grade glioma: integrating the extent of resection with quality of life. *Acta Neurochir (Wien)* 155, 951-957.

Epstein, C.M., Lah, J.J., Meador, K., Weissman, J.D., Gaitan, L.E., Dihenia, B., 1996. Optimum stimulus parameters for lateralized suppression of speech with magnetic brain stimulation. *Neurology* 47, 1590-1593.

Epstein, C.M., Meador, K.J., Loring, D.W., Wright, R.J., Weissman, J.D., Sheppard, S., Lah, J.J., Puhlovich, F., Gaitan, L., Davey, K.R., 1999. Localization and characterization of speech arrest during transcranial magnetic stimulation. *Clin Neurophysiol* 110, 1073-1079.

Ettinger, G.J., Leventon, M.E., Grimson, W.E., Kikinis, R., Gugino, L., Cote, W., Sprung, L., Aglio, L., Shenton, M.E., Potts, G., Hernandez, V.L., Alexander, E., 1998. Experimentation with a transcranial magnetic stimulation system for functional brain mapping. *Med Image Anal* 2, 133-142.

Feindel, W., 1982. The contributions of Wilder Penfield to the functional anatomy of the human brain. *Hum Neurobiol* 1, 231-234.

Forster, M.T., Hoecker, A.C., Kang, J.S., Quick, J., Seifert, V., Hattingen, E., Hilker, R., Weise, L.M., 2015. Does navigated transcranial stimulation increase the accuracy of tractography? A prospective clinical trial based on intraoperative motor evoked potential monitoring during deep brain stimulation. *Neurosurgery* 76, 766-775; discussion 775-766.

Fraga de Abreu, V.H., Peck, K.K., Petrovich-Brennan, N.M., Woo, K.M., Holodny, A.I., 2016. Brain Tumors: The Influence of Tumor Type and Routine MR Imaging Characteristics at BOLD Functional MR Imaging in the Primary Motor Gyrus. *Radiology*, 151951.

Frey, D., Schilt, S., Strack, V., Zdunczyk, A., Rosler, J., Niraula, B., Vajkoczy, P., Picht, T., 2014. Navigated transcranial magnetic stimulation improves the treatment outcome in patients with brain tumors in motor eloquent locations. *Neuro Oncol* 16, 1365-1372.

Frey, D., Strack, V., Wiener, E., Jussen, D., Vajkoczy, P., Picht, T., 2012. A new approach for corticospinal tract reconstruction based on navigated transcranial stimulation and standardized fractional anisotropy values. *Neuroimage* 62, 1600-1609.

Fridriksson, J., Kjartansson, O., Morgan, P.S., Hjaltason, H., Magnúsdóttir, S., Bonilha, L., Rorden, C., 2010. Impaired speech repetition and left parietal lobe damage. *J Neurosci* 30, 11057-11061.

Friederici, A.D., Gierhan, S.M., 2013. The language network. *Curr Opin Neurobiol* 23, 250-254.

Galantucci, S., Tartaglia, M.C., Wilson, S.M., Henry, M.L., Filippi, M., Agosta, F., Dronkers, N.F., Henry, R.G., Ogar, J.M., Miller, B.L., Gorno-Tempini, M.L., 2011. White matter damage in primary progressive aphasia: a diffusion tensor tractography study. *Brain* 134, 3011-3029.

Gierhan, S.M., 2013. Connections for auditory language in the human brain. *Brain Lang* 127, 205-221.

Haglund, M.M., Berger, M.S., Shamseldin, M., Lettich, E., Ojemann, G.A., 1994. Cortical localization of temporal lobe language sites in patients with gliomas. *Neurosurgery* 34, 567-576; discussion 576.

Hallett, M., 2000. Transcranial magnetic stimulation and the human brain. *Nature* 406, 147-150.

Henning Stieglitz, L., Seidel, K., Wiest, R., Beck, J., Raabe, A., 2012. Localization of primary language areas by arcuate fascicle fiber tracking. *Neurosurgery* 70, 56-64; discussion 64-55.

Hernandez-Pavon, J.C., Makela, N., Lehtinen, H., Lioumis, P., Makela, J.P., 2014. Effects of navigated TMS on object and action naming. *Front Hum Neurosci* 8, 660.

Hervey-Jumper, S.L., Berger, M.S., 2014. Role of surgical resection in low- and high-grade gliomas. *Curr Treat Options Neurol* 16, 284.

Hickok, G., Poeppel, D., 2004. Dorsal and ventral streams: a framework for understanding aspects of the functional anatomy of language. *Cognition* 92, 67-99.

Holodny, A.I., Schulder, M., Liu, W.C., Wolko, J., Maldjian, J.A., Kalnin, A.J., 2000. The effect of brain tumors on BOLD functional MR imaging activation in the adjacent motor cortex: implications for image-guided neurosurgery. *AJNR Am J Neuroradiol* 21, 1415-1422.

Huber, W., Poeck, K., Willmes, K., 1984. The Aachen Aphasia Test. *Adv Neurol* 42, 291-303.

Ille, S., Sollmann, N., Butenschoen, V.M., Meyer, B., Ringel, F., Krieg, S.M., 2016. Resection of highly language-eloquent brain lesions based purely on rTMS language mapping without awake surgery. *Acta Neurochir (Wien)* 158, 2265-2275.

Ille, S., Sollmann, N., Hauck, T., Maurer, S., Tanigawa, N., Obermueller, T., Negwer, C., Droese, D., Zimmer, C., Meyer, B., Ringel, F., Krieg, S.M., 2015. Combined noninvasive language mapping by navigated transcranial magnetic stimulation and functional MRI and its comparison with direct cortical stimulation. *J Neurosurg* 123, 212-225.

Indefrey, P., 2011. The spatial and temporal signatures of word production components: a critical update. *Front Psychol* 2, 255.

Indefrey, P., Levelt, W.J., 2004. The spatial and temporal signatures of word production components. *Cognition* 92, 101-144.

Jakola, A.S., Myrmet, K.S., Kloster, R., Torp, S.H., Lindal, S., Unsgard, G., Solheim, O., 2012. Comparison of a strategy favoring early surgical resection vs a strategy favoring watchful waiting in low-grade gliomas. *JAMA* 308, 1881-1888.

Krieg, S.M., Buchmann, N.H., Gempt, J., Shiban, E., Meyer, B., Ringel, F., 2012a. Diffusion tensor imaging fiber tracking using navigated brain stimulation--a feasibility study. *Acta Neurochir (Wien)* 154, 555-563.

Krieg, S.M., Picht, T., Sollmann, N., Bahrend, I., Ringel, F., Nagarajan, S.S., Meyer, B., Tarapore, P.E., 2016a. Resection of Motor Eloquent Metastases Aided by Preoperative nTMS-Based Motor Maps-Comparison of Two Observational Cohorts. *Front Oncol* 6, 261.

Krieg, S.M., Sabih, J., Bulubasova, L., Obermueller, T., Negwer, C., Janssen, I., Shiban, E., Meyer, B., Ringel, F., 2014a. Preoperative motor mapping by navigated transcranial

magnetic brain stimulation improves outcome for motor eloquent lesions. *Neuro Oncol* 16, 1274-1282.

Krieg, S.M., Shiban, E., Buchmann, N., Gempt, J., Foerschler, A., Meyer, B., Ringel, F., 2012b. Utility of presurgical navigated transcranial magnetic brain stimulation for the resection of tumors in eloquent motor areas. *J Neurosurg* 116, 994-1001.

Krieg, S.M., Shiban, E., Buchmann, N., Meyer, B., Ringel, F., 2013a. Presurgical navigated transcranial magnetic brain stimulation for recurrent gliomas in motor eloquent areas. *Clin Neurophysiol* 124, 522-527.

Krieg, S.M., Sollmann, N., Hauck, T., Ille, S., Foerschler, A., Meyer, B., Ringel, F., 2013b. Functional language shift to the right hemisphere in patients with language-eloquent brain tumors. *PLoS One* 8, e75403.

Krieg, S.M., Sollmann, N., Hauck, T., Ille, S., Meyer, B., Ringel, F., 2014b. Repeated mapping of cortical language sites by preoperative navigated transcranial magnetic stimulation compared to repeated intraoperative DCS mapping in awake craniotomy. *BMC Neurosci* 15, 20.

Krieg, S.M., Sollmann, N., Obermueller, T., Sabih, J., Bulubas, L., Negwer, C., Moser, T., Droese, D., Boeckh-Behrens, T., Ringel, F., Meyer, B., 2015. Changing the clinical course of glioma patients by preoperative motor mapping with navigated transcranial magnetic brain stimulation. *BMC Cancer* 15, 231.

Krieg, S.M., Sollmann, N., Tanigawa, N., Foerschler, A., Meyer, B., Ringel, F., 2016b. Cortical distribution of speech and language errors investigated by visual object naming and navigated transcranial magnetic stimulation. *Brain Struct Funct* 221, 2259-2286.

Krieg, S.M., Tarapore, P.E., Picht, T., Tanigawa, N., Houde, J., Sollmann, N., Meyer, B., Vajkoczy, P., Berger, M.S., Ringel, F., Nagarajan, S., 2014c. Optimal timing of pulse onset for language mapping with navigated repetitive transcranial magnetic stimulation. *Neuroimage* 100, 219-236.

Kuhnt, D., Bauer, M.H., Becker, A., Merhof, D., Zolal, A., Richter, M., Grummich, P., Ganslandt, O., Buchfelder, M., Nimsky, C., 2012. Intraoperative visualization of fiber tracking based reconstruction of language pathways in glioma surgery. *Neurosurgery* 70, 911-919; discussion 919-920.

Kuhnt, D., Bauer, M.H., Egger, J., Richter, M., Kapur, T., Sommer, J., Merhof, D., Nimsky, C., 2013. Fiber tractography based on diffusion tensor imaging compared with high-angular-resolution diffusion imaging with compressed sensing: initial experience. *Neurosurgery* 72 Suppl 1, 165-175.

Kunimatsu, A., Aoki, S., Masutani, Y., Abe, O., Hayashi, N., Mori, H., Masumoto, T., Ohtomo, K., 2004. The optimal trackability threshold of fractional anisotropy for diffusion tensor tractography of the corticospinal tract. *Magn Reson Med Sci* 3, 11-17.

Le Bihan, D., Poupon, C., Amadon, A., Lethimonnier, F., 2006. Artifacts and pitfalls in diffusion MRI. *J Magn Reson Imaging* 24, 478-488.

Leclercq, D., Duffau, H., Delmaire, C., Capelle, L., Gatignol, P., Ducros, M., Chiras, J., Lehericy, S., 2010. Comparison of diffusion tensor imaging tractography of language tracts and intraoperative subcortical stimulations. *J Neurosurg* 112, 503-511.

Lehericy, S., Duffau, H., Cornu, P., Capelle, L., Pidoux, B., Carpentier, A., Auliac, S., Clemenceau, S., Sichez, J.P., Bitar, A., Valery, C.A., Van Effenterre, R., Faillot, T., Srour, A., Fohanno, D., Philippon, J., Le Bihan, D., Marsault, C., 2000. Correspondence between functional magnetic resonance imaging somatotopy and individual brain anatomy of the central region: comparison with intraoperative stimulation in patients with brain tumors. *J Neurosurg* 92, 589-598.

Lioumis, P., Zhdanov, A., Makela, N., Lehtinen, H., Wilenius, J., Neuvonen, T., Hannula, H., Deletis, V., Picht, T., Makela, J.P., 2012. A novel approach for documenting naming errors induced by navigated transcranial magnetic stimulation. *J Neurosci Methods* 204, 349-354.

Makris, N., Kennedy, D.N., McInerney, S., Sorensen, A.G., Wang, R., Caviness, V.S., Jr., Pandya, D.N., 2005. Segmentation of subcomponents within the superior longitudinal fascicle in humans: a quantitative, in vivo, DT-MRI study. *Cereb Cortex* 15, 854-869.

Mandonnet, E., Winkler, P.A., Duffau, H., 2010. Direct electrical stimulation as an input gate into brain functional networks: principles, advantages and limitations. *Acta Neurochir (Wien)* 152, 185-193.

Michelucci, R., Valzania, F., Passarelli, D., Santangelo, M., Rizzi, R., Buzzi, A.M., Tempestini, A., Tassinari, C.A., 1994. Rapid-rate transcranial magnetic stimulation and

hemispheric language dominance: usefulness and safety in epilepsy. *Neurology* 44, 1697-1700.

Mohr, J.P., Pessin, M.S., Finkelstein, S., Funkenstein, H.H., Duncan, G.W., Davis, K.R., 1978. Broca aphasia: pathologic and clinical. *Neurology* 28, 311-324.

Mori, S., Barker, P.B., 1999. Diffusion magnetic resonance imaging: its principle and applications. *Anat Rec* 257, 102-109.

Mori, S., van Zijl, P.C., 2002. Fiber tracking: principles and strategies - a technical review. *NMR Biomed* 15, 468-480.

Nathan, P.W., Smith, M.C., Deacon, P., 1990. The corticospinal tracts in man. Course and location of fibres at different segmental levels. *Brain* 113 ( Pt 2), 303-324.

Negwer, C., Ille, S., Hauck, T., Sollmann, N., Maurer, S., Kirschke, J.S., Ringel, F., Meyer, B., Krieg, S.M., 2016. Visualization of subcortical language pathways by diffusion tensor imaging fiber tracking based on rTMS language mapping. *Brain Imaging Behav*.

Negwer, C., Sollmann, N., Ille, S., Hauck, T., Maurer, S., Kirschke, J.S., Ringel, F., Meyer, B., Krieg, S.M., 2017. Language pathway tracking: comparing nTMS-based DTI fiber tracking with a cubic ROIs-based protocol. *J Neurosurg* 126, 1006-1014.

Nimsky, C., 2010. Fiber tracking--a reliable tool for neurosurgery? *World Neurosurg* 74, 105-106.

Nimsky, C., Ganslandt, O., Merhof, D., Sorensen, A.G., Fahlbusch, R., 2006. Intraoperative visualization of the pyramidal tract by diffusion-tensor-imaging-based fiber tracking. *Neuroimage* 30, 1219-1229.

Niskanen, E., Julkunen, P., Saisanen, L., Vanninen, R., Karjalainen, P., Kononen, M., 2010. Group-level variations in motor representation areas of thenar and anterior tibial muscles: Navigated Transcranial Magnetic Stimulation Study. *Hum Brain Mapp* 31, 1272-1280.

Ojemann, G., Mateer, C., 1979. Human language cortex: localization of memory, syntax, and sequential motor-phoneme identification systems. *Science* 205, 1401-1403.

Ojemann, G.A., 1991. Cortical organization of language. *J Neurosci* 11, 2281-2287.

Papagno, C., Miracapillo, C., Casarotti, A., Romero Lauro, L.J., Castellano, A., Falini, A., Casaceli, G., Fava, E., Bello, L., 2011. What is the role of the uncinat fasciculus? Surgical removal and proper name retrieval. *Brain* 134, 405-414.

Park, M.C., Goldman, M.A., Park, M.J., Friehs, G.M., 2007. Neuroanatomical localization of the 'precentral knob' with computed tomography imaging. *Stereotact Funct Neurosurg* 85, 158-161.

Pascual-Leone, A., Gates, J.R., Dhuna, A., 1991. Induction of speech arrest and counting errors with rapid-rate transcranial magnetic stimulation. *Neurology* 41, 697-702.

Penfield, W., Roberts, L., 1959. *Speech and Brain-Mechanisms*. Princeton University Press, Princeton, NJ.

Picht, T., 2014. Current and potential utility of transcranial magnetic stimulation in the diagnostics before brain tumor surgery. *CNS Oncol* 3, 299-310.

Picht, T., Kombos, T., Gramm, H.J., Brock, M., Suess, O., 2006. Multimodal protocol for awake craniotomy in language cortex tumour surgery. *Acta Neurochir (Wien)* 148, 127-137; discussion 137-128.

Picht, T., Krieg, S.M., Sollmann, N., Rosler, J., Niraula, B., Neuvonen, T., Savolainen, P., Lioumis, P., Makela, J.P., Deletis, V., Meyer, B., Vajkoczy, P., Ringel, F., 2013. A comparison of language mapping by preoperative navigated transcranial magnetic stimulation and direct cortical stimulation during awake surgery. *Neurosurgery* 72, 808-819.

Picht, T., Mularski, S., Kuehn, B., Vajkoczy, P., Kombos, T., Suess, O., 2009. Navigated transcranial magnetic stimulation for preoperative functional diagnostics in brain tumor surgery. *Neurosurgery* 65, 93-98; discussion 98-99.

Picht, T., Schilt, S., Frey, D., Vajkoczy, P., Kufeld, M., 2014. Integration of navigated brain stimulation data into radiosurgical planning: potential benefits and dangers. *Acta Neurochir (Wien)* 156, 1125-1133.

Picht, T., Strack, V., Schulz, J., Zdunczyk, A., Frey, D., Schmidt, S., Vajkoczy, P., 2012. Assessing the functional status of the motor system in brain tumor patients using transcranial magnetic stimulation. *Acta Neurochir (Wien)* 154, 2075-2081.

Poeppel, D., Hickok, G., 2004. Towards a new functional anatomy of language. *Cognition* 92, 1-12.

Rauschecker, J.P., 2012. Ventral and dorsal streams in the evolution of speech and language. *Front Evol Neurosci* 4, 7.

Rauschecker, J.P., Scott, S.K., 2009. Maps and streams in the auditory cortex: nonhuman primates illuminate human speech processing. *Nat Neurosci* 12, 718-724.

Robles, S.G., Gatignol, P., Lehericy, S., Duffau, H., 2008. Long-term brain plasticity allowing a multistage surgical approach to World Health Organization Grade II gliomas in eloquent areas. *J Neurosurg* 109, 615-624.

Rogic, M., Deletis, V., Fernandez-Conejero, I., 2014. Inducing transient language disruptions by mapping of Broca's area with modified patterned repetitive transcranial magnetic stimulation protocol. *J Neurosurg* 120, 1033-1041.

Rosenstock, T., Grittner, U., Acker, G., Schwarzer, V., Kulchytska, N., Vajkoczy, P., Picht, T., 2017. Risk stratification in motor area-related glioma surgery based on navigated transcranial magnetic stimulation data. *J Neurosurg* 126, 1227-1237.

Rosler, J., Niraula, B., Strack, V., Zdunczyk, A., Schilt, S., Savolainen, P., Lioumis, P., Makela, J., Vajkoczy, P., Frey, D., Picht, T., 2014. Language mapping in healthy volunteers and brain tumor patients with a novel navigated TMS system: evidence of tumor-induced plasticity. *Clin Neurophysiol* 125, 526-536.

Rossi, S., Hallett, M., Rossini, P.M., Pascual-Leone, A., Safety of, T.M.S.C.G., 2009. Safety, ethical considerations, and application guidelines for the use of transcranial magnetic stimulation in clinical practice and research. *Clin Neurophysiol* 120, 2008-2039.

Rossini, P.M., Barker, A.T., Berardelli, A., Caramia, M.D., Caruso, G., Cracco, R.Q., Dimitrijevic, M.R., Hallett, M., Katayama, Y., Lucking, C.H., et al., 1994. Non-invasive electrical and magnetic stimulation of the brain, spinal cord and roots: basic principles and procedures for routine clinical application. Report of an IFCN committee. *Electroencephalogr Clin Neurophysiol* 91, 79-92.

Rossini, P.M., Burke, D., Chen, R., Cohen, L.G., Daskalakis, Z., Di Iorio, R., Di Lazzaro, V., Ferreri, F., Fitzgerald, P.B., George, M.S., Hallett, M., Lefaucheur, J.P., Langguth, B.,

Matsumoto, H., Miniussi, C., Nitsche, M.A., Pascual-Leone, A., Paulus, W., Rossi, S., Rothwell, J.C., Siebner, H.R., Ugawa, Y., Walsh, V., Ziemann, U., 2015. Non-invasive electrical and magnetic stimulation of the brain, spinal cord, roots and peripheral nerves: Basic principles and procedures for routine clinical and research application. An updated report from an I.F.C.N. Committee. *Clin Neurophysiol* 126, 1071-1107.

Ruohonen, J., Ilmoniemi, R.J., 1999. Modeling of the stimulating field generation in TMS. *Electroencephalogr Clin Neurophysiol Suppl* 51, 30-40.

Ruohonen, J., Karhu, J., 2010. Navigated transcranial magnetic stimulation. *Neurophysiol Clin* 40, 7-17.

Sacko, O., Lauwers-Cances, V., Brauge, D., Sesay, M., Brenner, A., Roux, F.E., 2011. Awake craniotomy vs surgery under general anesthesia for resection of supratentorial lesions. *Neurosurgery* 68, 1192-1198; discussion 1198-1199.

Sanai, N., Berger, M.S., 2008. Glioma extent of resection and its impact on patient outcome. *Neurosurgery* 62, 753-764; discussion 264-756.

Sanai, N., Berger, M.S., 2010. Intraoperative stimulation techniques for functional pathway preservation and glioma resection. *Neurosurg Focus* 28, E1.

Sanai, N., Mirzadeh, Z., Berger, M.S., 2008. Functional outcome after language mapping for glioma resection. *N Engl J Med* 358, 18-27.

Schmidt, S., Bathe-Peters, R., Fleischmann, R., Ronnefarth, M., Scholz, M., Brandt, S.A., 2015. Nonphysiological factors in navigated TMS studies; confounding covariates and valid intracortical estimates. *Hum Brain Mapp* 36, 40-49.

Schreiber, A., Hubbe, U., Ziyeh, S., Hennig, J., 2000. The influence of gliomas and nonglial space-occupying lesions on blood-oxygen-level-dependent contrast enhancement. *AJNR Am J Neuroradiol* 21, 1055-1063.

Smith, J.S., Chang, E.F., Lamborn, K.R., Chang, S.M., Prados, M.D., Cha, S., Tihan, T., Vandenberg, S., McDermott, M.W., Berger, M.S., 2008. Role of extent of resection in the long-term outcome of low-grade hemispheric gliomas. *J Clin Oncol* 26, 1338-1345.

Snodgrass, J.G., Vanderwart, M., 1980. A standardized set of 260 pictures: norms for name agreement, image agreement, familiarity, and visual complexity. *J Exp Psychol Hum Learn* 6, 174-215.

Snodgrass, J.G., Yuditsky, T., 1996. Naming times for the Snodgrass and Vanderwart pictures. *Behavior Research Methods, Instruments, & Computers* 28 516-536.

Sollmann, N., Giglhuber, K., Tussis, L., Meyer, B., Ringel, F., Krieg, S.M., 2015a. nTMS-based DTI fiber tracking for language pathways correlates with language function and aphasia - A case report. *Clin Neurol Neurosurg* 136, 25-28.

Sollmann, N., Goblirsch-Kolb, M.F., Ille, S., Butenschoen, V.M., Boeckh-Behrens, T., Meyer, B., Ringel, F., Krieg, S.M., 2016a. Comparison between electric-field-navigated and line-navigated TMS for cortical motor mapping in patients with brain tumors. *Acta Neurochir (Wien)* 158, 2277-2289.

Sollmann, N., Ille, S., Hauck, T., Maurer, S., Negwer, C., Zimmer, C., Ringel, F., Meyer, B., Krieg, S.M., 2015b. The impact of preoperative language mapping by repetitive navigated transcranial magnetic stimulation on the clinical course of brain tumor patients. *BMC Cancer* 15, 261.

Sollmann, N., Ille, S., Negwer, C., Boeckh-Behrens, T., Ringel, F., Meyer, B., Krieg, S.M., 2016b. Cortical time course of object naming investigated by repetitive navigated transcranial magnetic stimulation. *Brain Imaging Behav.*

Sollmann, N., Ille, S., Obermueller, T., Negwer, C., Ringel, F., Meyer, B., Krieg, S.M., 2015c. The impact of repetitive navigated transcranial magnetic stimulation coil positioning and stimulation parameters on human language function. *Eur J Med Res* 20, 47.

Sollmann, N., Kubitscheck, A., Maurer, S., Ille, S., Hauck, T., Kirschke, J.S., Ringel, F., Meyer, B., Krieg, S.M., 2016c. Preoperative language mapping by repetitive navigated transcranial magnetic stimulation and diffusion tensor imaging fiber tracking and their comparison to intraoperative stimulation. *Neuroradiology* 58, 807-818.

Sollmann, N., Meyer, B., Krieg, S.M., 2017a. Implementing functional preoperative mapping in the clinical routine of a neurosurgical department: Technical Note. *World Neurosurg.*

Sollmann, N., Negwer, C., Ille, S., Maurer, S., Hauck, T., Kirschke, J.S., Ringel, F., Meyer, B., Krieg, S.M., 2016d. Feasibility of nTMS-based DTI fiber tracking of language pathways in neurosurgical patients using a fractional anisotropy threshold. *J Neurosci Methods* 267, 45-54.

Sollmann, N., Negwer, C., Tussis, L., Hauck, T., Ille, S., Maurer, S., Giglhuber, K., Bauer, J.S., Ringel, F., Meyer, B., Krieg, S.M., 2017b. Interhemispheric connectivity revealed by diffusion tensor imaging fiber tracking derived from navigated transcranial magnetic stimulation maps as a sign of language function at risk in patients with brain tumors. *J Neurosurg* 126, 222-233.

Sollmann, N., Picht, T., Makela, J.P., Meyer, B., Ringel, F., Krieg, S.M., 2013. Navigated transcranial magnetic stimulation for preoperative language mapping in a patient with a left frontoopercular glioblastoma. *J Neurosurg* 118, 175-179.

Sollmann, N., Tanigawa, N., Bulubas, L., Sabih, J., Zimmer, C., Ringel, F., Meyer, B., Krieg, S.M., 2016e. Clinical Factors Underlying the Inter-individual Variability of the Resting Motor Threshold in Navigated Transcranial Magnetic Stimulation Motor Mapping. *Brain Topogr*, 1-24.

Sollmann, N., Tanigawa, N., Ringel, F., Zimmer, C., Meyer, B., Krieg, S.M., 2014. Language and its right-hemispheric distribution in healthy brains: an investigation by repetitive transcranial magnetic stimulation. *Neuroimage* 102 Pt 2, 776-788.

Sollmann, N., Wildschuetz, N., Kelm, A., Conway, N., Moser, T., Bulubas, L., Kirschke, J.S., Meyer, B., Krieg, S.M., 2017c. Associations between clinical outcome and navigated transcranial magnetic stimulation characteristics in patients with motor-eloquent brain lesions: a combined navigated transcranial magnetic stimulation-diffusion tensor imaging fiber tracking approach. *J Neurosurg*, 1-11.

Southwell, D.G., Hervey-Jumper, S.L., Perry, D.W., Berger, M.S., 2016. Intraoperative mapping during repeat awake craniotomy reveals the functional plasticity of adult cortex. *J Neurosurg* 124, 1460-1469.

Stookey, B., 1963. Jean-Baptiste Bouillaud and Ernest AUBURTIN. Early studies on cerebral localization and the speech center. *JAMA* 184, 1024-1029.

Stummer, W., Reulen, H.J., Meinel, T., Pichlmeier, U., Schumacher, W., Tonn, J.C., Rohde, V., Opperl, F., Turowski, B., Woiciechowsky, C., Franz, K., Pietsch, T., Group, A.L.-G.S., 2008. Extent of resection and survival in glioblastoma multiforme: identification of and adjustment for bias. *Neurosurgery* 62, 564-576; discussion 564-576.

Szekely, A., Jacobsen, T., D'Amico, S., Devescovi, A., Andonova, E., Herron, D., Lu, C.C., Pechmann, T., Pleh, C., Wicha, N., Federmeier, K., Gerdjikova, I., Gutierrez, G., Hung, D., Hsu, J., Iyer, G., Kohnert, K., Mehotcheva, T., Orozco-Figueroa, A., Tzeng, A., Tzeng, O., Arevalo, A., Vargha, A., Butler, A.C., Buffington, R., Bates, E., 2004. A new on-line resource for psycholinguistic studies. *J Mem Lang* 51, 247-250.

Szelenyi, A., Bello, L., Duffau, H., Fava, E., Feigl, G.C., Galanda, M., Neuloh, G., Signorelli, F., Sala, F., Workgroup for Intraoperative Management in Low-Grade Glioma Surgery within the European Low-Grade Glioma, N., 2010. Intraoperative electrical stimulation in awake craniotomy: methodological aspects of current practice. *Neurosurg Focus* 28, E7.

Talacchi, A., Santini, B., Casartelli, M., Monti, A., Capasso, R., Miceli, G., 2013. Awake surgery between art and science. Part II: language and cognitive mapping. *Funct Neurol* 28, 223-239.

Tarapore, P.E., Findlay, A.M., Honma, S.M., Mizuiri, D., Houde, J.F., Berger, M.S., Nagarajan, S.S., 2013. Language mapping with navigated repetitive TMS: proof of technique and validation. *Neuroimage* 82, 260-272.

Tarapore, P.E., Picht, T., Bulubas, L., Shin, Y., Kulchytska, N., Meyer, B., Berger, M.S., Nagarajan, S.S., Krieg, S.M., 2016. Safety and tolerability of navigated TMS for preoperative mapping in neurosurgical patients. *Clin Neurophysiol* 127, 1895-1900.

Tarapore, P.E., Tate, M.C., Findlay, A.M., Honma, S.M., Mizuiri, D., Berger, M.S., Nagarajan, S.S., 2012. Preoperative multimodal motor mapping: a comparison of magnetoencephalography imaging, navigated transcranial magnetic stimulation, and direct cortical stimulation. *J Neurosurg* 117, 354-362.

Tuch, D.S., Reese, T.G., Wiegell, M.R., Makris, N., Belliveau, J.W., Wedeen, V.J., 2002. High angular resolution diffusion imaging reveals intravoxel white matter fiber heterogeneity. *Magn Reson Med* 48, 577-582.

Wakana, S., Jiang, H., Nagae-Poetscher, L.M., van Zijl, P.C., Mori, S., 2004. Fiber tract-based atlas of human white matter anatomy. *Radiology* 230, 77-87.

Wang, L., Chen, D., Yang, X., Olson, J.J., Gopinath, K., Fan, T., Mao, H., 2013. Group independent component analysis and functional MRI examination of changes in language areas associated with brain tumors at different locations. *PLoS One* 8, e59657.

Wassermann, E.M., Blaxton, T.A., Hoffman, E.A., Berry, C.D., Oletsky, H., Pascual-Leone, A., Theodore, W.H., 1999. Repetitive transcranial magnetic stimulation of the dominant hemisphere can disrupt visual naming in temporal lobe epilepsy patients. *Neuropsychologia* 37, 537-544.

Weiss, C., Tursunova, I., Neuschmelting, V., Lockau, H., Nettekoven, C., Oros-Peusquens, A.M., Stoffels, G., Rehme, A.K., Faymonville, A.M., Shah, N.J., Langen, K.J., Goldbrunner, R., Grefkes, C., 2015. Improved nTMS- and DTI-derived CST tractography through anatomical ROI seeding on anterior pontine level compared to internal capsule. *Neuroimage Clin* 7, 424-437.

Wernicke, C., 1874. *Der aphasische Symptomencomplex: eine psychologische Studie auf anatomischer Basis*. M. Cohn und Weigert, Breslau.

Yousry, T.A., Schmid, U.D., Alkadhi, H., Schmidt, D., Peraud, A., Buettner, A., Winkler, P., 1997. Localization of the motor hand area to a knob on the precentral gyrus. A new landmark. *Brain* 120 ( Pt 1), 141-157.

## 7. LIST OF ABBREVIATIONS

---

3-D	Three-dimensional
AAT	Aachen Apasia Test
AF	Arcuate fascicle
ANOVA	Analysis of variance
APB	Abductor pollicis brevis muscle
ArF	Arcuate fibers
ATL	Anterior temporal lobe
BOLD	Blood oxygenation level dependent
CF	Commissural fibers
CI	Confidence interval
CNT	Corticonuclear tract
CST	Corticospinal tract
CtF	Corticothalamic fibers
DES	Direct electrical stimulation
DICOM	Digital Imaging and Communications in Medicine
DT	Display time
DTI	Diffusion tensor imaging
DTI FT	Diffusion tensor imaging fiber tracking
DWI	Diffusion-weighted imaging
EEG	Electroencephalography
EMG	Electromyography
En-TMS	Electric-field-navigated transcranial magnetic stimulation
ER	Error rate
FA	Fractional anisotropy
FACT	Fiber assignment by continuous tracking
FAT	Fractional anisotropy threshold
FLAIR	Fluid attenuated inversion recovery
fMRI	Functional magnetic resonance imaging
FN	False negative
FoF	Fronto-occipital fascicle
FP	False positive
FU	Follow-up

IC	Interhemispheric connectivity
IFG	Inferior frontal gyrus
ILF	Inferior frontal gyrus
IPI	Inter-picture interval
IPNP	International Picture Naming Project
ISI	Inter-stimulus interval
LH	Left hemisphere
MEG	Magnetoencephalography
MEP	Motor evoked potential
MFL	Minimum fiber length
MRI	Magnetic resonance imaging
MTL	Middle temporal lobe
NPV	Negative predictive value
nTMS	Navigated transcranial magnetic stimulation
opIFG	Pars opercularis of the inferior frontal gyrus
OR	Odds ratio
PACS	Picture archiving and communication system
PET	Positron emission tomography
PPV	Positive predictive value
PrG	Precentral gyrus
pSTL	Posterior superior temporal lobe
PTI	Picture-to-trigger interval
RH	Right hemisphere
rMT	Resting motor threshold
ROI	Region of interest
rTMS	Repetitive navigated transcranial magnetic stimulation
SD	Standard deviation
SLF	Superior longitudinal fascicle
TE	Echo time
TMS	Transcranial magnetic stimulation
TN	True negative
TP	True positive
TR	Repetition time
triFG	Pars triangularis of the inferior frontal gyrus
UC	Uncinate fascicle
WM	White matter

## 8. LIST OF FIGURES AND TABLES

---

### 8.1. Figures

Figure 1	Classical model of language organization (Chang et al., 2015)
Figure 2	Contemporary model of language organization (Chang et al., 2015)
Figure 3	Subcortical white matter (WM) pathways involved in language processing (Chang et al., 2015)
Figure 4	Setup of navigated transcranial magnetic stimulation (nTMS)
Figure 5	Three-dimensional (3-D) head model
Figure 6	Determination of the resting motor threshold (rMT)
Figure 7	Identification of the motor hotspot
Figure 8	Examples of pictures used in the object-naming task
Figure 9	Language mapping procedure
Figure 10	Cortical points of stimulation
Figure 11	Comparison of mapping recordings to baseline assessments
Figure 12	Cortical language map
Figure 13	Tractography based on cortical language maps
Figure 14	Intraoperative language mapping
Figure 15	Feasibility of tractography based on cortical language maps (Sollmann et al., 2016d)
Figure 16	Tractography of 9 subcortical language-related pathways (Sollmann et al., 2016d)
Figure 17	Fibers per tract (Sollmann et al., 2016d)
Figure 18	Percentage of visualized tracts (Sollmann et al., 2016d)
Figure 19	Percentages of patients showing different subcortical language-related pathways I (Sollmann et al., 2016d)
Figure 20	Comparing anatomy-based tractography to tractography using language maps (Negwer et al., 2017)
Figure 21	Superiority of tractography based on language maps (Negwer et al., 2017)
Figure 22	Percentages of patients showing different subcortical language-related pathways II (Negwer et al., 2017)
Figure 23	Detection of interhemispheric connectivity (IC) by tractography (Sollmann et al., 2017b)
Figure 24	False-positive versus true-positive fraction (Sollmann et al., 2017b)

Figure 25	Combined anatomical and functional data for patient consultation
Figure 26	Tractography based on language maps as used during surgery (Sollmann et al., 2015a)
Figure 27	Distance measurements between reconstructed fibers and the brain tumor (Sollmann et al., 2017c)

## 8.2. Tables

Table 1	Interhemispheric connectivity (IC) and aphasia I (Sollmann et al., 2017b)
Table 2	Sensitivity, specificity, positive predictive value (PPV), and negative predictive value (NPV) I (Sollmann et al., 2017b)
Table 3	Interhemispheric connectivity (IC) and aphasia II (Sollmann et al., 2017b)
Table 4	Sensitivity, specificity, positive predictive value (PPV), and negative predictive value (NPV) II (Sollmann et al., 2017b)

## 9. ACKNOWLEDGEMENTS

---

First, I would like to thank PD Dr. Sandro M. Krieg for his encouraging and close supervision, which was the fundament for the publications included in this thesis and my progress during my time as a PhD student. He further shaped my enthusiasm for both neuroscience and neurosurgery and strongly supported me during my work in his group. I also want to thank him for making my time as a PhD student as efficient as possible by enabling me to work on several projects simultaneously.

I would further like to express my gratitude to Prof. Dr. Claus Zimmer, whose support during my time as a medical student strengthened my decision to apply for the PhD program. Furthermore, I want to thank him for our regular meetings and discussions, which were always both fruitful and helpful to me. It is because of him that I also developed a profound interest for neuroradiology, both clinically and scientifically.

I am also very grateful to Prof. Dr. Bernhard Meyer and his former vice chairman, Prof. Dr. Florian Ringel, without whom this thesis would not have been feasible. Their support and supervision, although being involved in many projects and stressful daily clinical work, facilitated my progress in research.

Furthermore, I want to express my sincere gratitude to Prof. Dr. Florian Heinen, Prof. Dr. Josef P. Rauschecker, Prof. Dr. Inga K. Koerte, PD Dr. Jan S. Kirschke, PD Dr. Dimitrios Karampinos, and Dr. Christian Sorg for their guidance and help during my life as a PhD student. They also had considerable influence on my development in the scientific world that I would not like to miss.

I also want to thank all present and former members of our research group for their excellent work and team spirit. In particular, I would like to thank Dr. Sebastian Ille, Stefanie Maurer, Chiara Negwer, and Dr. Vicki Butenschön for their contributions as members of the group and residents. Furthermore, I also thank Noriko Tanigawa for their help regarding statistical issues.

Many thanks also go to Kristin E. Lucia, who was kind enough to proofread this thesis despite her full schedule as a neurosurgical resident.

Furthermore, the journals that gave permission to use the published articles in my thesis, which are the Journal of Neurosurgery and the Journal of Neuroscience Methods, have to be acknowledged. I also thank Dr. Edward F. Chang for allowing me to reuse his excellent illustrations on human language organization and representation in the introduction of my thesis.

Last but not least, I want to express my heartfelt gratitude to my wife, my parents, my grandmother, and my friends for substantially supporting me during my work. Without their help, this thesis would not have been possible.

## 10. PUBLICATIONS

---

### 10.1. Original Articles

- 1.) Picht T\*, Krieg SM\*, **Sollmann N**, Rösler J, Niraula B, Neuvonen T, Savolainen P, Lioumis P, Mäkelä JP, Deletis V, Meyer B, Vajkoczy P, Ringel F. A comparison of language mapping by preoperative navigated transcranial magnetic stimulation and direct cortical stimulation during awake surgery. *Neurosurgery*. 2013 May;72(5):808-19.
- 2.) **Sollmann N\***, Hauck T\*, Obermüller T, Hapfelmeier A, Meyer B, Ringel F, Krieg SM. Inter- and intraobserver variability in motor mapping of the hotspot for the abductor pollicis brevis muscle. *BMC Neurosci*. 2013 Sep 5;14:94.
- 3.) Krieg SM, **Sollmann N**, Hauck T, Ille S, Foerschler A, Meyer B, Ringel F. Functional language shift to the right hemisphere in patients with language-eloquent brain tumors. *PLoS One*. 2013 Sep 17;8(9):e75403.
- 4.) **Sollmann N\***, Hauck T\*, Hapfelmeier A, Meyer B, Ringel F, Krieg SM. Intra- and interobserver variability of language mapping by navigated transcranial magnetic brain stimulation. *BMC Neurosci*. 2013 Dec 5;14(1):150.
- 5.) Krieg SM\*, **Sollmann N\***, Hauck T, Ille S, Meyer B, Ringel F. Repeated mapping of cortical language sites by preoperative navigated transcranial magnetic stimulation compared to repeated intraoperative DCS mapping in awake craniotomy. *BMC Neurosci*. 2014 Jan 30;15(1):20.
- 6.) Krieg SM\*, Tarapore PE\*, Picht T, Tanigawa N, Houde J, **Sollmann N**, Meyer B, Vajkoczy P, Berger MS, Ringel F, Nagarajan S. Optimal timing of pulse onset for language mapping with navigated repetitive transcranial magnetic stimulation. *Neuroimage*. 2014 Oct 15;100:219-36.
- 7.) **Sollmann N**, Tanigawa N, Ringel F, Zimmer C, Meyer B, Krieg SM. Language and its right-hemispheric distribution in healthy brains: an investigation by repetitive transcranial magnetic stimulation. *Neuroimage*. 2014 Nov 15;102 Pt 2:776-88.
- 8.) **Sollmann N**, Tanigawa N, Tussis L, Hauck T, Ille S, Maurer S, Negwer C, Zimmer C, Ringel F, Meyer B, Krieg SM. Cortical regions involved in semantic processing investigated by repetitive navigated transcranial magnetic stimulation and object naming. *Neuropsychologia*. 2015 Apr;70:185-95.
- 9.) Ille S, **Sollmann N**, Hauck T, Maurer S, Tanigawa N, Obermueller T, Negwer C, Droese D, Zimmer C, Meyer B, Ringel F, Krieg SM. Combined noninvasive language mapping by navigated transcranial magnetic stimulation and functional MRI and its comparison with direct cortical stimulation. *J Neurosurg*. 2015 Jul;123(1):212-25.

- 10.) Hauck T, Tanigawa N, Probst M, Wohlschlaeger A, Ille S, **Sollmann N**, Maurer S, Zimmer C, Ringel F, Meyer B, Krieg SM. Stimulation frequency determines the distribution of language positive cortical regions during navigated transcranial magnetic brain stimulation.  
BMC Neurosci. 2015 Feb 18;16:5.
- 11.) Ille S, **Sollmann N**, Hauck T, Maurer S, Tanigawa N, Obermueller T, Negwer C, Droese D, Boeckh-Behrens T, Meyer B, Ringel F, Krieg SM. Impairment of preoperative language mapping by lesion location – a fMRI, nTMS and DCS study.  
J Neurosurg. 2015 Aug;123(2):314-24.
- 12.) Krieg SM\*, **Sollmann N\***, Obermueller T, Sabih J, Bulubas L, Negwer C, Moser T, Droese D, Boeckh-Behrens T, Ringel F\*, Meyer B\*. Changing the clinical course of glioma patients by preoperative motor mapping with navigated transcranial magnetic brain stimulation.  
BMC Cancer. 2015 Apr 8;15:231.
- 13.) **Sollmann N**, Ille S, Hauck T, Maurer S, Negwer C, Zimmer C, Ringel F, Meyer B, Krieg SM. The impact of preoperative language mapping by repetitive navigated transcranial magnetic stimulation on the clinical course of brain tumor patients.  
BMC Cancer. 2015 Apr 11;15:261.
- 14.) **Sollmann N**, Ille S, Obermueller T, Negwer C, Ringel F, Meyer B, Krieg SM. The impact of repetitive navigated transcranial magnetic stimulation coil positioning and stimulation parameters on human language function.  
Eur J Med Res. 2015 Apr 1;20:47.
- 15.) Krieg SM, **Sollmann N**, Tanigawa N, Foerschler A, Meyer B, Ringel F. Cortical distribution of speech and language errors investigated by visual object naming and navigated transcranial magnetic stimulation.  
Brain Struct Funct. 2016 May;221(4):2259-86.
- 16.) Hauck T, Tanigawa N, Probst M, Wohlschlaeger A, Ille S, **Sollmann N**, Maurer S, Zimmer C, Ringel F, Meyer B, Krieg SM. Task type affects the location of language-positive cortical regions by repetitive navigated transcranial magnetic stimulation mapping.  
PLoS One. 2015 Apr 30;10(4):e0125298.
- 17.) Maurer S, Tanigawa N, **Sollmann N**, Hauck T, Ille S, Boeckh-Behrens T, Meyer B, Krieg SM. Non-invasive mapping of calculation function by repetitive navigated transcranial magnetic stimulation.  
Brain Struct Funct. 2016 Nov;221(8):3927-3947.
- 18.) **Sollmann N**, Ille S, Tussis L, Maurer S, Hauck T, Negwer C, Bauer JS, Ringel F, Meyer B, Krieg SM. Correlating subcortical interhemispheric connectivity and cortical hemispheric dominance in brain tumor patients: A repetitive navigated transcranial magnetic stimulation study.  
Clin Neurol Neurosurg. 2016 Feb;141:56-64.
- 19.) Tussis L\*, **Sollmann N\***, Boeckh-Behrens T, Meyer B, Krieg SM. Language function distribution in left-handers: A navigated transcranial magnetic stimulation study.  
Neuropsychologia. 2016 Feb;82:65-73.

- 20.) Bulubas L, Sabih J, Wohlschlaeger A, **Sollmann N**, Hauck T, Ille S, Ringel F, Meyer B, Krieg SM. Motor Areas of the Frontal Cortex in Patients with Motor Eloquent Brain Lesions.  
J Neurosurg. 2016 Dec;125(6):1431-1442.
- 21.) **Sollmann N\***, Negwer C\*, Tussis L, Hauck T, Ille S, Maurer S, Giglhuber K, Bauer JS, Ringel F, Meyer B, Krieg SM. Interhemispheric connectivity revealed by diffusion tensor imaging fiber tracking derived from navigated transcranial magnetic stimulation maps as a sign of language function at risk in brain tumor patients.  
J Neurosurg. 2017 Jan;126(1):222-233. doi: 10.3171/2016.1.JNS152053.
- 22.) **Sollmann N\***, Negwer C\*, Ille S, Maurer S, Hauck T, Kirschke JS, Ringel F, Meyer B, Krieg SM. Feasibility of nTMS-based DTI fiber tracking of language pathways in neurosurgical patients using a fractional anisotropy threshold.  
J Neurosci Methods. 2016 Apr 6;267:45-54.
- 23.) **Sollmann N**, Kubitscheck A, Maurer S, Ille S, Hauck T, Kirschke JS, Ringel F, Meyer B, Krieg SM. Preoperative language mapping by repetitive navigated transcranial magnetic stimulation and diffusion tensor imaging fiber tracking and their comparison to intraoperative stimulation.  
Neuroradiology. 2016 Aug;58(8):807-18.
- 24.) **Sollmann N\***, Ille S\*, Boeckh-Behrens T, Ringel F, Meyer B, Krieg SM. Mapping of cortical language function by functional magnetic resonance imaging and repetitive navigated transcranial magnetic stimulation in 40 healthy subjects.  
Acta Neurochir (Wien). 2016 Jul;158(7):1303-16.
- 25.) Krieg SM\*, Sonanini S\*, **Sollmann N**, Focke A, Gerstl L, Heinen F. The Complexity Signature: Developing a Tool to Communicate Biopsychosocial Severity of Disease for Children with Chronic Neurological Complexity.  
Neuropediatrics. 2016 Aug;47(4):238-44.
- 26.) Negwer C, **Sollmann N**, Ille S, Hauck T, Maurer S, Kirschke JS, Ringel F, Meyer B, Krieg SM. Language pathway tracking: comparing nTMS-based DTI fiber tracking with a cubic ROIs-based protocol.  
J Neurosurg. 2017 Mar;126(3):1006-1014. doi: 10.3171/2016.2.JNS152382.
- 27.) Negwer C, Ille S, Hauck T, **Sollmann N**, Maurer S, Kirschke JS, Ringel F, Meyer B, Krieg SM. Visualization of subcortical language pathways by diffusion tensor imaging fiber tracking based on rTMS language mapping.  
Brain Imaging Behav. 2016 Jun 20. [Epub ahead of print]
- 28.) **Sollmann N**, Ille S, Negwer C, Boeckh-Behrens T, Ringel F, Meyer B, Krieg SM. Cortical time course of object naming investigated by repetitive navigated transcranial magnetic stimulation.  
Brain Imaging Behav. 2016 Jul 22. [Epub ahead of print]
- 29.) **Sollmann N\***, Trepte-Freisleder F\*, Albers L, Jung NH, Mall V, Meyer B, Heinen F, Krieg SM\*, Landgraf MN\*. Magnetic stimulation of the upper trapezius muscles in patients with migraine - A pilot study.  
Eur J Paediatr Neurol. 2016 Nov;20(6):888-897.

- 30.) Ille S, **Sollmann N**, Butenschoen VM, Meyer B, Ringel F, Krieg SM. Resection of highly language-eloquent brain lesions based purely on rTMS language mapping without awake surgery. *Acta Neurochir (Wien)*. 2016 Dec;158(12):2265-2275.
- 31.) **Sollmann N\***, Goblirsch-Kolb MF\*, Ille S, Butenschoen VM, Boeckh-Behrens T, Meyer B, Ringel F, Krieg SM. Comparison between electric-field-navigated and line-navigated TMS for cortical motor mapping in patients with brain tumors. *Acta Neurochir (Wien)*. 2016 Dec;158(12):2277-2289.
- 32.) Ille S, Kulchytska N, **Sollmann N**, Wittig R, Beurskens E, Butenschoen VM, Ringel F, Vajkoczy P, Meyer B, Picht T\*, Krieg SM\*. Hemispheric language dominance measured by repetitive navigated transcranial magnetic stimulation and postoperative course of language function in brain tumor patients. *Neuropsychologia*. 2016 Oct;91:50-60.
- 33.) **Sollmann N**, Hauck T, Tussis L, Ille S, Maurer S, Boeckh-Behrens T, Ringel F, Meyer B, Krieg SM. Results on the spatial resolution of repetitive transcranial magnetic stimulation for cortical language mapping during object naming in healthy subjects. *BMC Neurosci*. 2016 Oct 24;17(1):67.
- 34.) **Sollmann N**, Tanigawa N, Bulubas L, Sabih J, Zimmer C, Ringel F, Meyer B, Krieg SM. Clinical Factors Underlying the Inter-individual Variability of the Resting Motor Threshold in Navigated Transcranial Magnetic Stimulation Motor Mapping. *Brain Topogr*. 2017 Jan;30(1):98-121. doi: 10.1007/s10548-016-0536-9.
- 35.) **Sollmann N**, Bulubas L, Tanigawa N, Zimmer C, Meyer B, Krieg SM. The variability of motor evoked potential latencies in neurosurgical motor mapping by preoperative navigated transcranial magnetic stimulation. *BMC Neurosci*. 2017 Jan 3;18(1):5. doi: 10.1186/s12868-016-0321-4.
- 36.) Krieg SM\*, Picht T\*, **Sollmann N**, Bährend I, Ringel F, Nagarajan SS, Meyer B, Tarapore PE. Resection of Motor Eloquent Metastases Aided by Preoperative nTMS-Based Motor Maps-Comparison of Two Observational Cohorts. *Front Oncol*. 2016 Dec 21;6:261. doi: 10.3389/fonc.2016.00261.
- 37.) Conway N, Wildschutz N, Moser T, Bulubas L, **Sollmann N**, Tanigawa N, Meyer B, Krieg SM. Cortical plasticity of motor-eloquent areas measured by navigated transcranial magnetic stimulation in patients with glioma. *J Neurosurg*. 2017 Jan 20:1-11. doi: 10.3171/2016.9.JNS161595. [Epub ahead of print]
- 38.) Maurer S, Giglhuber K, **Sollmann N**, Kelm A, Ille S, Hauck T, Tanigawa N, Ringel F, Boeckh-Behrens T, Meyer B, Krieg SM. Non-invasive Mapping of Face Processing by Navigated Transcranial Magnetic Stimulation. *Front Hum Neurosci*. 2017 Jan 23;11:4. doi: 10.3389/fnhum.2017.00004.
- 39.) Tussis L\*, **Sollmann N\***, Boeckh-Behrens T, Meyer B, Krieg SM. Identifying cortical first and second language sites via navigated transcranial magnetic stimulation of the left hemisphere in bilinguals. *Brain Lang*. 2017 May;168:106-116. doi: 10.1016/j.bandl.2017.01.011.

- 40.) Moser T, Bulubas L, Sabih J, Conway N, Wildschutz N, **Sollmann N**, Meyer B, Ringel F, Krieg SM. Resection of Navigated Transcranial Magnetic Stimulation-Positive Prerolandic Motor Areas Causes Permanent Impairment of Motor Function. *Neurosurgery*. 2017 Feb 24. doi: 10.1093/neuros/nyw169. [Epub ahead of print]
- 41.) **Sollmann N**, Wildschuetz N, Kelm A, Conway N, Moser T, Bulubas L, Kirschke JS, Meyer B, Krieg SM. Associations between clinical outcome and navigated transcranial magnetic stimulation characteristics in patients with motor-eloquent brain lesions: a combined navigated transcranial magnetic stimulation-diffusion tensor imaging fiber tracking approach. *J Neurosurg*. 2017 Mar 31:1-11. doi: 10.3171/2016.11.JNS162322. [Epub ahead of print]
- 42.) **Sollmann N**, Meyer B, Krieg SM. Implementing functional preoperative mapping in the clinical routine of a neurosurgical department: Technical Note. *World Neurosurg*. 2017 Apr 1. pii: S1878-8750(17)30437-0. doi: 10.1016/j.wneu.2017.03.114. [Epub ahead of print]

## 10.2. Case Reports

- 43.) **Sollmann N**, Picht T, Mäkelä JP, Meyer B, Ringel F, Krieg SM. Navigated transcranial magnetic stimulation for preoperative language mapping in a patient with a left frontoopercular glioblastoma.  
J Neurosurg. 2013 Jan;118(1):175-9.
- 44.) **Sollmann N**, Giglhuber K, Tussis L, Meyer B, Ringel F, Krieg SM. nTMS-based DTI fiber tracking for language pathways correlates with language function and aphasia – A case report.  
Clin Neurol Neurosurg. 2015 Sep;136:25-8.

(\*: equal contribution; date prepared: April 2017)

## 11. APPENDIX: ORIGINAL PUBLICATIONS

---

1. Feasibility of nTMS-based DTI fiber tracking of language pathways in neurosurgical patients using a fractional anisotropy threshold.

Sollmann N, Negwer C, Ille S, Maurer S, Hauck T, Kirschke JS, Ringel F, Meyer B, Krieg SM. J Neurosci Methods. 2016 Jul 15;267:45-54. doi: 10.1016/j.jneumeth.2016.04.002. Epub 2016 Apr 6.

2. Language pathway tracking: comparing nTMS-based DTI fiber tracking with a cubic ROIs-based protocol.

Negwer C, Sollmann N, Ille S, Hauck T, Maurer S, Kirschke JS, Ringel F, Meyer B, Krieg SM. J Neurosurg. 2017 Mar;126(3):1006-1014. doi: 10.3171/2016.2.JNS152382. Epub 2016 May 27.

3. Interhemispheric connectivity revealed by diffusion tensor imaging fiber tracking derived from navigated transcranial magnetic stimulation maps as a sign of language function at risk in patients with brain tumors.

Sollmann N, Negwer C, Tussis L, Hauck T, Ille S, Maurer S, Giglhuber K, Bauer JS, Ringel F, Meyer B, Krieg SM. J Neurosurg. 2017 Jan;126(1):222-233. doi: 10.3171/2016.1.JNS152053. Epub 2016 Apr 1.

# 11.1. Feasibility of nTMS-based DTI fiber tracking of language pathways in neurosurgical patients using a fractional anisotropy threshold

Journal of Neuroscience Methods 267 (2016) 45–54



Contents lists available at ScienceDirect

Journal of Neuroscience Methods

journal homepage: [www.elsevier.com/locate/jneumeth](http://www.elsevier.com/locate/jneumeth)



## Feasibility of nTMS-based DTI fiber tracking of language pathways in neurosurgical patients using a fractional anisotropy threshold



Nico Sollmann<sup>a,b,1</sup>, Chiara Negwer<sup>a,1</sup>, Sebastian Ille<sup>a,b</sup>, Stefanie Maurer<sup>a,b</sup>,  
Theresa Hauck<sup>a,b</sup>, Jan S. Kirschke<sup>c</sup>, Florian Ringel<sup>a</sup>, Bernhard Meyer<sup>a</sup>,  
Sandro M. Krieg<sup>a,b,\*</sup>

<sup>a</sup> Department of Neurosurgery, Klinikum rechts der Isar, Technische Universität München, Ismaninger Str. 22, 81675 Munich, Germany

<sup>b</sup> TUM-Neuroimaging Center, Klinikum rechts der Isar, Technische Universität München, Ismaninger Str. 22, 81675 Munich, Germany

<sup>c</sup> Section of Neuroradiology, Department of Radiology, Klinikum rechts der Isar, Technische Universität München, Ismaninger Str. 22, 81675 Munich, Germany

### HIGHLIGHTS

- nTMS maps can be used for DTI FT of subcortical language pathways.
- Language pathways are detectable with nTMS spots as ROI.
- 25% and 50% FAT allow for most favorable DTI FT of language pathways.

### ARTICLE INFO

#### Article history:

Received 3 January 2016

Received in revised form 31 March 2016

Accepted 4 April 2016

Available online 6 April 2016

#### Keywords:

Cortical mapping

Diffusion tensor imaging

Fiber tracking

Language

Transcranial magnetic stimulation

### ABSTRACT

**Background:** Navigated transcranial magnetic stimulation (nTMS) provides language maps in brain tumor patients. Yet, corresponding data on the visualization of language-related subcortical pathways is lacking. Therefore, this study evaluates the feasibility of nTMS-based diffusion tensor imaging fiber tracking (DTI FT) for subcortical language pathways by a fractional anisotropy (FA) protocol.

**New method:** DTI FT was performed in 37 patients suffering from left-sided perisylvian brain lesions based on nTMS data exclusively, using the FA-based protocol originally established for the corticospinal tract (CST) by Frey et al. (2012): minimum fiber length was 110 mm and the highest individual FA value leading to visualization of white matter tracts was determined as the FA threshold (FAT). Then, deterministic DTI FT using an FA value of 100%, 75%, 50%, and 25% of the individual FAT (with 25% as an additional setting to the original protocol) was performed.

**Results:** Our approach visualized 9 language-related subcortical white matter pathways. By using 100% FAT, the mean percentage of visualized tracts was 13.5%, whereas DTI FT performed with 75%, 50%, and 25% FAT detected 30.6%, 61.3%, and 93.7% of language-related fiber tracts, respectively.

**Comparison with existing methods:** nTMS language mapping alone is not able to visualize subcortical language-related pathways.

**Abbreviations:** 3-D, three-dimensional; AAT, Aachen Aphasia Test; ANOVA, analysis of variance; AVM, arteriovenous malformation; CST, corticospinal tract; DT, display time; DTI, diffusion tensor imaging; DTI FT, diffusion tensor imaging fiber tracking; DCS, direct cortical stimulation; FA, fractional anisotropy; FACT, fiber assignment by continuous tracking; FAT, fractional anisotropy threshold; fMRI, functional magnetic resonance imaging; GBM, glioblastoma multiforme; HARDI, high angular resolution diffusion imaging; IPI, inter-picture-interval; MEG, magnetoencephalography; MRI, magnetic resonance imaging; nTMS, navigated transcranial magnetic stimulation; PDD, principal diffusion direction; PTI, picture-to-trigger-interval; RMT, resting motor threshold; ROI, region of interest; rTMS, repetitive navigated transcranial magnetic stimulation; SD, standard deviation.

\* Corresponding author at: Department of Neurosurgery, Klinikum rechts der Isar, Technische Universität München, Ismaninger Str. 22, 81675 Munich, Germany. Fax: +49 89 4140 4889.

E-mail addresses: [Nico.Sollmann@tum.de](mailto:Nico.Sollmann@tum.de) (N. Sollmann), [Chiara.Negwer@tum.de](mailto:Chiara.Negwer@tum.de) (C. Negwer), [Sebastian.Ille@tum.de](mailto:Sebastian.Ille@tum.de) (S. Ille), [S.Maurer@tum.de](mailto:S.Maurer@tum.de) (S. Maurer), [Therhauck@googlemail.com](mailto:Therhauck@googlemail.com) (T. Hauck), [Jan.Kirschke@tum.de](mailto:Jan.Kirschke@tum.de) (J.S. Kirschke), [Florian.Ringel@tum.de](mailto:Florian.Ringel@tum.de) (F. Ringel), [Bernhard.Meyer@tum.de](mailto:Bernhard.Meyer@tum.de) (B. Meyer), [Sandro.Krieg@tum.de](mailto:Sandro.Krieg@tum.de) (S.M. Krieg).

<sup>1</sup> These authors contributed equally.

<http://dx.doi.org/10.1016/j.jneumeth.2016.04.002>  
0165-0270/© 2016 Elsevier B.V. All rights reserved.

**Conclusions:** This study shows that nTMS language maps are feasible for DTI FT of language-related pathways within the scope of a FAT-based protocol. Although this approach is novel and might be helpful during scientific neuroimaging and tumor resection, intraoperative validation is needed to go beyond the level of feasibility.

© 2016 Elsevier B.V. All rights reserved.

## 1. Introduction

The principles of diffusion tensor imaging (DTI) were initially described in the early nineties (Basser et al., 1994; Douek et al., 1991; Moseley et al., 1990). Since then, this magnetic resonance imaging (MRI) method has gained increasing importance for the detection and visualization of subcortical white matter fibers in the living human brain within the scope of DTI fiber tracking (DTI FT). Technically, DTI is based on measuring the diffusivity of water molecules in the brain tissue. Since the main diffusion direction of water molecules is typically oriented parallel to subcortical white matter fiber bundles, the information about diffusion directions allows for fiber reconstruction using a certain tractography algorithm (Catani et al., 2002). Concerning so-called deterministic tractography, only one single diffusion direction per voxel is followed to reconstruct fiber tracts, which can then be integrated into three-dimensional (3-D) anatomic MRI sequences for the simultaneous visualization of subcortical white matter tracts and “conventional” anatomical information.

Roughly all tractography algorithms require the placement (=seeding) of one or more regions of interest (ROIs) into the brain tissue. Conventionally, ROIs are manually created according to anatomical landmarks, but they can also be seeded with respect to individual functional data derived from magnetoencephalography (MEG), functional MRI (fMRI), or navigated transcranial magnetic stimulation (nTMS). So far, a very limited number of studies have used nTMS maps for ROI placement, and the feasibility of this approach has primarily been demonstrated for DTI FT of subcortical motor pathways, such as the corticospinal tract (CST) (Conti et al., 2014; Forster et al., 2015; Frey et al., 2012; Krieg et al., 2012; Weiss et al., 2015). Only one single case report has demonstrated that DTI FT based on nTMS language data could be technically feasible to detect specific language-related tracts in general, and might be furthermore helpful during surgery since it proved to be in good accordance with subcortical stimulation during tumor removal (Sollmann et al., 2015a).

Therefore, the present study investigates the feasibility of nTMS language mapping for ROI seeding and DTI FT of subcortical language pathways in 37 patients with left-sided brain tumors. In this context, a modified fractional anisotropy (FA) based protocol was used to assess feasibility and to evaluate the most suitable parameters for optimal visualization of subcortical language pathways (arcuate fibers, commissural fibers, arcuate fascicle, corticonuclear tract, corticothalamic fibers, superior longitudinal fascicle, inferior longitudinal fascicle, uncinate fascicle, and frontooccipital fascicle).

## 2. Materials and methods

### 2.1. Ethics

Written informed consent was obtained from all patients, and the experimental protocol was approved by our local institutional review board (registration number: 2793/10) in accordance with the Declaration of Helsinki.

### 2.2. Patients

In total, 37 patients who presented with left-sided perisylvian brain lesions in our neurosurgical department were enrolled in the present study. The inclusion criteria were left-sided perisylvian tumor location, age above 18 years, and written informed consent. Exclusion criteria were age under 18 years, other severe neurological diseases, and general nTMS exclusion criteria (e.g., the presence of a cochlear implant, deep brain stimulation electrodes, or cardiac pacemaker).

All patients underwent MRI and repetitive nTMS (rTMS) for the mapping of cortical language-related spots prior to surgery. Furthermore, each patient underwent a thorough clinical examination according to a standardized protocol including coordination, sensory function, muscle strength, and cranial nerve function, which was performed by an experienced medical doctor. The examination protocol was established in 2006 as clinical routine in our department. Furthermore, the individual preoperative language status of each patient was evaluated by a trained neuropsychologist. In this context, the Aachen Aphasia Test (AAT) was used (Huber et al., 1984), and, in addition to the AAT, four previously established deficit grades were reported (Krieg et al., 2014a; Sollmann et al., 2015b):

- 1) No deficit.
- 2) Mild deficit: undisrupted conversational speech and/or speech comprehension, adequate communication ability to slight amnesic aphasia.
- 3) Medium deficit: slight impairment of conversational speech and/or speech comprehension, adequate communication ability.
- 4) Severe deficit: clear impairment of conversational speech and/or speech comprehension, disrupted communication ability.

The aim of the present study was then to evaluate the feasibility of language-related cortical areas mapped by nTMS as ROI for DTI FT in the context of the protocol described by Frey et al. (2012).

### 2.3. Magnetic resonance imaging

All imaging was performed on the same magnetic resonance scanner (Achieva 3T, Philips Medical Systems, The Netherlands B.V.) through the use of an eight-channel phased-array head coil. Our scanning protocol consisted of a T2-weighted FLAIR (TR/TE: 12,000/140 ms, voxel size:  $0.9 \times 0.9 \times 4 \text{ mm}^3$ , acquisition time: 3 min) and a 3-D T1-weighted gradient echo sequence (TR/TE: 9/4 ms,  $1 \text{ mm}^3$  isovoxel covering the whole head, acquisition time: 6 min 58 s) with and without intravenous contrast administration (gadopentetate dimeglumine; Magnograf, Marotrust GmbH). Additionally, DTI sequences (TR/TE 7,571/55 ms) with 6 orthogonal diffusion directions were performed in each patient with *b*-values of 0 and 800. Using parallel imaging (sensitivity encoding factor 2), 2 averages of 73 contiguous 2-mm slices with a matrix of  $112^\circ \times 112 \text{ mm}$  covering the whole brain were acquired within 2 min 15 s. Subsequently, all DTI data were interpolated to a matrix of  $224^\circ \times 224$ , which resulted in a voxel size of  $0.88^\circ \times 0.88^\circ \times 2 \text{ mm}^3$ .

The contrast-enhanced 3-D gradient echo sequences of each patient were then exported to the Nexstim eXimia NBS system

(version 3.2.2 or version 4.3, Nexstim Oy, Helsinki, Finland) for nTMS language mapping, and the DTI data were transferred to a BrainLAB iPlan Net server (version 3.0.1, BrainLab AG, Feldkirchen, Germany) for later DTI FT using the DICOM standard.

#### 2.4. Navigated transcranial magnetic stimulation

Cortical language mapping in the patients' primary language was performed using the Nexstim eXimia NBS system (version 3.2.2 or version 4.3, Nexstim Oy, Helsinki, Finland) with a biphasic figure-of-eight coil in combination with an object-naming task (NexSpeech module, Nexstim Oy, Helsinki, Finland). The principles of this approach have been repeatedly described in recent literature (Hernandez-Pavon et al., 2014; Krieg et al., 2015; Lioumis et al., 2012; Rogic et al., 2014; Sollmann et al., 2014; Tarapore et al., 2013).

In short, the resting motor threshold (RMT), which is important for determining the individual stimulation intensity, was obtained by first mapping the cortical motor representation of the abductor pollicis brevis muscle of the tumor-affected left hemisphere. Subsequently, two consecutive baseline trials (object naming without simultaneous nTMS) were carried out. During the baseline condition, the patient was asked to name 131 pictures of everyday objects in the individual mother tongue. Each picture was displayed for 0.7 s (display time = DT) at an inter-picture interval (IPI) of 2.5 s. Objects that did not elicit quick and fluent responses were discarded from the image stack and, therefore, were not included under the stimulation trials. All objects that did elicit correct and fast responses were video-recorded and used for subsequent language mapping (Krieg et al., 2015; Lioumis et al., 2012; Sollmann et al., 2014).

During the stimulation condition, the nTMS pulses were applied time-locked to the objects, which were presented randomly. The DT and IPI were the same as for the baseline trials during the whole mapping session. Regarding the picture-to-trigger interval (PTI; the time between the presentation of an object on the screen and the onset of the nTMS pulse), it accounted for 0.3 s in the first 15 patients, while stimulation started simultaneously upon object presentation (PTI = 0 s) in the latter 22 patients. Although there is evidence for both PTIs (Indefrey, 2011; Rogic et al., 2014; Salmelin et al., 2000; Wheat et al., 2013), we decided to switch to 0 s according to a recent publication outlining the potential benefits of immediate stimulation onset (Krieg et al., 2014b). Furthermore, the mapping intensity and frequency were individualized for each patient according to a standardized mapping protocol that has been used in previous investigations (Krieg et al., 2015; Sollmann et al., 2014):

- 1) a train of 5–7 nTMS pulses was administered to the ventral precentral gyrus and opercular inferior frontal gyrus:
  - a 5 Hz, 5 pulses, 100% RMT
  - b 7 Hz, 5 pulses, 100% RMT
  - c 7 Hz, 7 pulses, 100% RMT
- 2) the setup (a–c), which caused the highest error rate (number of errors/number of stimulations), was identified by the volunteer's and examiner's impression and, in unclear cases, supported by video analysis;
- 3) if there was no clear difference in the effect on language, the most comfortable frequency was chosen;
- 4) if naming was not interrupted clearly by nTMS, the intensity was increased to 110–120% RMT and step 1 was repeated; and
- 5) if significant pain was reported, the stimulation intensity was decreased to 80–90% RMT to avoid any discomfort interfering with the consecutive response evaluation (Epstein et al., 1996; Krieg et al., 2015; Sollmann et al., 2014).

During mapping, the magnetic coil was placed tangential to the skull and with the electrical field in strict anterior–posterior orientation to achieve maximum field induction (Epstein et al., 1996; Lioumis et al., 2012; Sollmann et al., 2015c; Wassermann et al., 1999). The coil was manually moved between two objects (IPI) in about 10 mm steps covering most of the gyri of the left hemisphere. The spatial extent of nTMS was restricted due to severe pain in the orbital part of the inferior frontal gyrus and very frontopolar and temporopolar regions. Due to the greater distance between the scalp and the cortex, and, therefore, a stimulation intensity that was too low, the inferior temporal gyrus was also not routinely stimulated. The induced electrical field strength was >45 V/m in all patients. Similar to baseline testing, the naming performance during stimulation was video-recorded (Krieg et al., 2015; Lioumis et al., 2012; Sollmann et al., 2014).

For post-hoc analysis, the baseline and the stimulation videos were screened, compared, and systematically searched for naming errors by at least one experienced investigator. In unclear cases, the investigator was supervised by a trained linguist. All naming errors were classified as no-response errors, performance errors, neologisms, phonological paraphasias, or semantic paraphasias (Corina et al., 2010; Krieg et al., 2015; Sollmann et al., 2014). Since hesitations were not objectified by latency recordings, we decided not to take this error type into account. Moreover, naming errors due to direct muscle stimulation, non-compliance, or pain were excluded. Then, we exported all left-sided cortical spots at which naming errors of the described categories were elicited (=language-positive spots) to an external BrainLAB iPlan Net server (version 3.0.1, BrainLab AG, Feldkirchen, Germany) via DICOM standard.

#### 2.5. Diffusion tensor imaging fiber tracking

Since we intended to evaluate the feasibility of nTMS-based maps for DTI FT of subcortical language-related pathways in the context of a standardized protocol described by Frey et al. (2012), we decided to choose a deterministic tracking algorithm (Frey et al., 2012). As one goal of the present study was to provide data for the direct clinical use in brain tumor patients, we used one of the most common and well-distributed deterministic tractography software packages (BrainLAB iPlan Net, version 3.0.1, BrainLab AG, Feldkirchen, Germany). This software makes use of the so-called fiber assignment by continuous tracking (FACT) principle, which was first described by Mori and van Zijl (2002): starting at a certain point, a white matter fiber is reconstructed gradually by following the principal diffusion direction (PDD) until a predefined stop criterion (e.g., fiber angulation) is reached. Subsequently, tracking from the same point is started again along the inverse PDD to detect the second fiber part. Thus, the final tracking result is a parametric display of fibers, which is visualized as streamlines within the white matter volume of the brain.

After eddy current correction, the FLAIR, gradient echo, and DTI sequences of each subject were auto-fused and aligned. As described above, no-response errors, performance errors, neologisms, phonological paraphasias, and semantic paraphasias were considered in the present study, and all cortical stimulation spots at which naming errors of these categories were elicited (=language-positive spots) were imported. Then, all imported language-positive spots were fused with the stack of sequences of the individual patient. Subsequently, the whole group of language-positive spots was defined as one object, which is a prerequisite for ROI generation. In this context, the created object (consisting of all language-positive spots) was defined as one ROI by calculating additional rims of 5 mm for each positive stimulation point (Sollmann et al., 2015a). The minimum fiber length was set to 110 mm, and the FA was adjusted according to the protocol established by Frey et al. (2012): it was increased step by step until no



**Fig. 1.** Exemplary case of diffusion tensor imaging fiber tracking (DTI FT) results based on navigated transcranial magnetic stimulation (nTMS) data. Example of diffusion tensor imaging fiber tracking (DTI FT) based on navigated transcranial magnetic stimulation (nTMS) language mapping data in a patient suffering from a left frontotemporal glioblastoma multiforme (GBM). The tumor volume is shown in orange, whereas the left-hemispheric language-positive nTMS spots, constituting the region of interest (ROI), are depicted in purple. In this exemplary case, DTI FT was performed with 50% of the individual fractional anisotropy threshold (FAT). Most probably due to the location of the tumor volume, nTMS-based DTI FT failed to show the inferior longitudinal fascicle, uncinate fascicle, and frontooccipital fascicle. Fibers oriented from left to right: red, anterior to posterior: green, cranial to caudal: blue. (For interpretation of the references to color in this figure legend, the reader is referred to the web version of this article.)

more fibers were displayed; afterwards, the FA was decreased by 0.01, thus visualizing a minimum fiber course originating from the ROI (Frey et al., 2012). The corresponding FA value was defined as 100% fractional anisotropy threshold (FAT). Further DTI FT was subsequently performed with 75% and 50% FAT (Frey et al., 2012), but also with 25% FAT as an additional adjustment. All tracking was continued until the predefined stop criteria (FA value, fiber angulation  $>30^\circ$ ) were reached. The software automatically created a directionally encoded color map of white matter fibers originating from the cortical language-positive stimulation spots for the individual patient (Fig. 1). The 3-D tracking results were then manually evaluated for the following language-related fiber tracts, which were described in recent DTI FT literature (Axe et al., 2013; Bello et al., 2008; Catani and Thiebaut de Schotten, 2008; Chang et al., 2015; Gierhan, 2013; Kuhnt et al., 2012):

- 1) arcuate fibers,
- 2) commissural fibers,
- 3) arcuate fascicle,
- 4) corticonuclear tract,
- 5) corticothalamic fibers,
- 6) superior longitudinal fascicle,
- 7) inferior longitudinal fascicle,
- 8) uncinate fascicle, and
- 9) frontooccipital fascicle.

Arcuate fibers were considered present when structural connections between adjacent gyri were visualized (Fig. 2A). Commissural fibers were regarded as present when at least one fiber bundle connecting both hemispheres via the corpus callosum was detected (Fig. 2B). Furthermore, the arcuate fascicle, which is composed of fibers that connect the temporal cortex and inferior parietal cortex to various regions of the frontal lobe (Catani and Thiebaut de Schotten, 2008), was considered in the present study (Fig. 2C). The superior longitudinal fascicle, which is composed of four major sub-components, subserves language function with the so-called SLF I, SLF II, and SLF-tp, and was considered present when these sub-components were identified (Fig. 2C) (Chang et al., 2015; Makris et al., 2005). Furthermore, the corticonuclear tract was regarded as present when fiber bundles between the cortex and brainstem were clearly visible (Fig. 2D), and, analogously, corticothalamic fibers were registered when structural connections between the cortex and thalamus were revealed (Fig. 2E). The inferior longitudinal fascicle was considered present when a bundle connecting the occipital and temporal lobe was visualized with respect to the typical landmarks (Fig. 2F) (Catani and Thiebaut de Schotten, 2008). Furthermore, the uncinate fascicle was identified as a fiber bundle connecting the anterior temporal lobe with the medial and lateral orbitofrontal cortex (Fig. 2G), as outlined previously (Catani and Thiebaut de Schotten, 2008). The frontooccipital fascicle, a fiber connection between the ventral occipital lobe and the orbitofrontal cortex, was considered as well (Fig. 2H). For identification of single

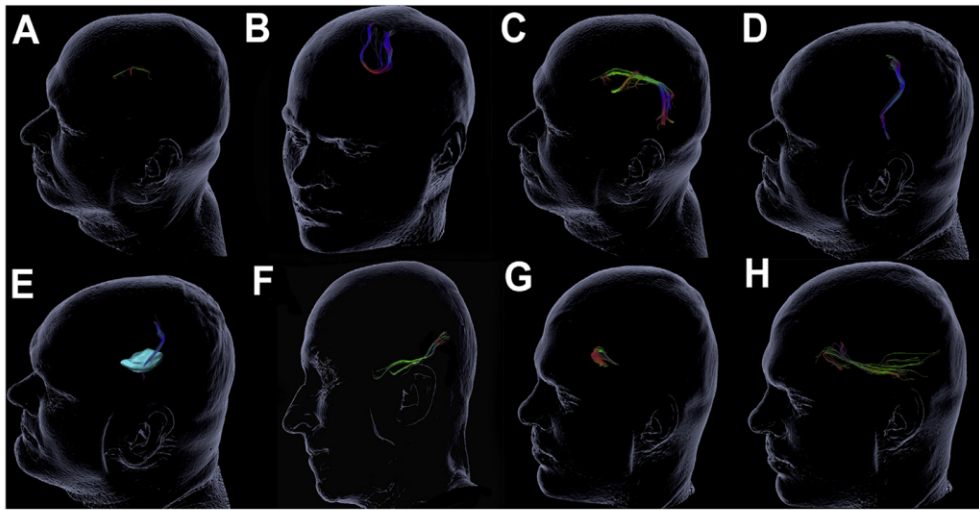


**Fig. 2.** Visualization of language-related tracts generated by diffusion tensor imaging fiber tracking (DTI FT) based on navigated transcranial magnetic stimulation (nTMS) maps.

This figure shows the language-related pathways derived from diffusion tensor imaging fiber tracking (DTI FT) with cortical navigated transcranial magnetic stimulation (nTMS) maps as the region of interest (ROI). Different patients were considered, and each tract was isolated from the overall tractography map for better visualization. (A) arcuate fibers, (B) commissural fibers, (C) arcuate fascicle and superior longitudinal fascicle, (D) corticonuclear tract, (E) corticothalamic fibers (thalamus: blue), (F) inferior longitudinal fascicle, (G) uncinate fascicle, and (H) frontooccipital fascicle. Fibers oriented from left to right: red, anterior to posterior: green, cranial to caudal: blue. (For interpretation of the references to color in this figure legend, the reader is referred to the web version of this article.)

tracts, we thoroughly referred to previous work on human brain connections (Axer et al., 2013; Catani and Thiebaut de Schotten, 2008; Chang et al., 2015).

Furthermore, the overall number of tracked fibers for every setting, the individual FA values of the four FAT adjustments, and the number of tracts that were visible depending on the different FAT adjustments were documented for each patient.

### 2.6. Statistical analysis

The mean values  $\pm$  standard deviation (SD), medians, and the minimum and maximum values were calculated using GraphPad Prism software (GraphPad Prism 6.04, La Jolla, CA, USA). In order to evaluate statistical significance, one-way analysis of variance (ANOVA) or chi-square tests were performed and  $p < 0.05$  was considered significant. Furthermore, we calculated the number of visualized fibers per number of visualized tracts (fibers/tracts) and the percentage of visualized tracts out of all patients for each of the 9 aforementioned subcortical language pathways.

## 3. Results

### 3.1. Patients

Overall, 37 patients with perisylvian brain lesions were included in our study. 14 patients were female (37.8%), and 23 were male (62.2%). The median age was 40 years, and the ages of the total population ranged from 20 to 66 years. Furthermore, 5 patients suffered from an arteriovenous malformation (AVM; 13.5%), 2 from an astrocytoma WHO grade I (5.4%), 9 from astrocytoma WHO grade II (24.3%), 5 from astrocytoma WHO grade III (13.5%), and 16 from glioblastoma WHO grade IV (GBM; 43.3%).

Regarding the preoperative language status, 22 patients were diagnosed with no deficit (59.5%), whereas 8 patients suffered from mild language impairment (21.6%). Moreover, 6 subjects suffered from medium language deficits (16.2%), while the remaining

patient was diagnosed with a severe degree of language impairment (2.7%).

### 3.2. Language mapping parameters

Cortical language mapping by nTMS was possible in all subjects. Language impairment according to our aforementioned grading did not negatively affect the mapping itself among the enrolled subjects; however, the patients with at least medium language deficits tended to recognize less baseline objects when compared to unimpaired subjects, which led to a lower amount of presented objects during mapping. In addition, stimulation was well tolerated in all patients, and no adverse events occurred in the course of stimulation. The mean RMT accounted for  $33.2 \pm 7.9\%$  (range: 21–58%), and the corresponding intensity applied during language mapping was  $103.0 \pm 9.0\%$  RMT (range: 80–120% RMT). According to our protocol, nTMS was carried out with 5 Hz/5 pulses in 22 subjects (59.5%), with 7 Hz/5 pulses in 8 subjects (21.6%), and with 7 Hz/7 pulses in 7 patients (18.9%).

### 3.3. Fiber tracking

In general, DTI FT based on language-positive stimulation spots was technically possible in all cases. Fig. 1 visualizes overall tracking results derived from DTI FT with a cortical nTMS language map as ROI in an exemplary case. Furthermore, Fig. 2 shows all language-related pathways that were considered in the present study. On average, the time needed for DTI FT ranged between 10 and 15 min.

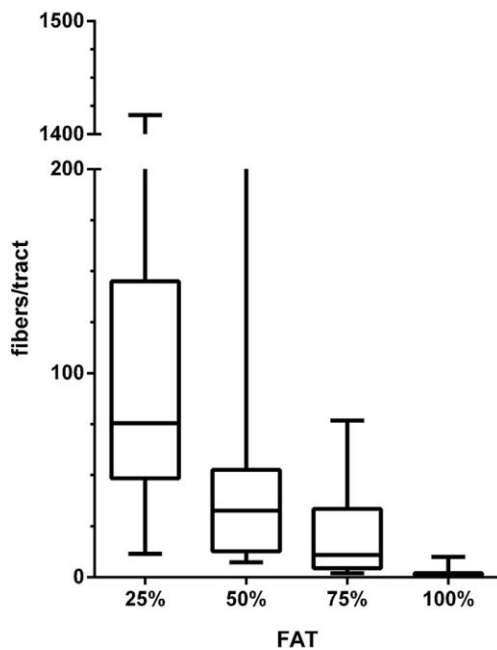
The mean 100% FAT value accounted for  $0.32 \pm 0.09$  (range: 0.14–0.50; median: 0.32), whereas it was  $0.24 \pm 0.06$  for 75% FAT,  $0.16 \pm 0.04$  for 50% FAT, and  $0.08 \pm 0.02$  for 25% FAT respectively ( $p < 0.0001$ ). According to Table 1 and Fig. 3, the highest ratio between the mean number of visualized fibers per tract was observed for DTI FT with 25% FAT, and this value significantly decreased with an increase of the FA ( $p < 0.0001$ ). Moreover, a similar relationship was found for the correlation between the

**Table 1**

Diffusion tensor imaging fiber tracking (DTI FT) results in relation to the used fractional anisotropy (FA) as a percentage of the fractional anisotropy threshold (FAT).

Fractional anisotropy threshold (FAT)	Fibers/tract (mean $\pm$ SD)	Arcuate fibers	Commis-sural fibers	Arcuate fascicle	Cortico-nuclear tract	Cortico-thalamic fibers	Superior longi-tudinal fascicle	Inferior longi-tudinal fascicle	Uncinate fascicle	Fronto-occipital fascicle	Overall visualization of tracts (mean $\pm$ SD)
25% FAT	148.50 $\pm$ 55	100.0%	97.3%	94.6%	94.6%	94.6%	100.0%	100.0%	73.0%	89.2%	93.7 $\pm$ 8.5%
50% FAT	54.06 $\pm$ 23	40.5%	64.9%	67.6%	86.5%	59.5%	70.3%	78.4%	27.0%	56.8%	61.3 $\pm$ 18.3%
75% FAT	22.12 $\pm$ 7	5.4%	35.1%	27.0%	73.0%	24.3%	32.4%	40.5%	8.1%	29.7%	30.6 $\pm$ 19.7%
100% FAT	1.99 $\pm$ 2	0.0%	16.2%	5.4%	54.1%	5.4%	10.8%	16.2%	0.0%	13.5%	13.5 $\pm$ 16.4%

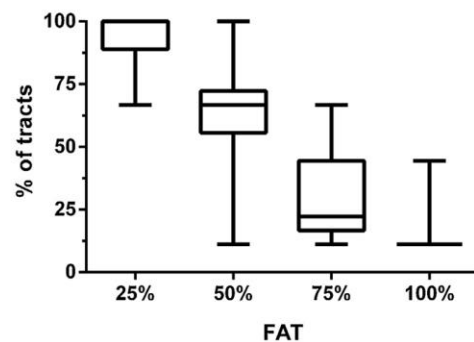
This table provides information about the percentage of patients in which a certain language-related fiber tract was found, depending on the individual fractional anisotropy threshold (FAT). Furthermore, the mean number of visualized fibers/tracts  $\pm$  standard deviation (SD) and the overall visualization of tracts  $\pm$  SD pooled across all subjects are given.

**Fig. 3.** Visualized fibers per tract.

A box plot including median, minimum, and maximum whiskers and quartile boxes to illustrate the correlation between the visualized fibers per visualized tract in relation to the used fractional anisotropy (FA) as a percentage of the fractional anisotropy threshold (FAT) ( $p < 0.0001$ ).

percentages of visualized fibers belonging to the 9 language-related tracts ( $p < 0.0001$ ; Table 1 and Fig. 4).

Regarding the 9 different fiber tracts for which the DTI FT images were searched, the change of the FA value clearly changed their detectability (i.e., an FA decrease principally led to the detection of clearly more fiber tracts; Table 1 and Fig. 5). Correspondingly, DTI FT with 25% FAT allowed for detection of most of the tracts in the patient cohort, whereas DTI FT with 100% FAT only irregularly led to tract identifications (Table 1 and Fig. 5). Concerning missing tracts in tractography resulting from DTI FT with 25% or 50% FAT, the tumor volumes were located within the typical anatomical fiber courses or origins of the respective subcortical pathways. The difference in visible tracts between DTI FT with different FATs was statistically significant for each of the 9 language pathways ( $p < 0.05$ ).

**Fig. 4.** Percentage of visualized tracts.

A box plot including median, minimum, and maximum whiskers and quartile boxes to illustrate the correlation between the percentages of visualized subcortical language-related pathways in relation to the used fractional anisotropy (FA) as a percentage of the fractional anisotropy threshold (FAT) ( $p < 0.0001$ ).

#### 4. Discussion

The intention of our study was to demonstrate the feasibility of nTMS-based DTI FT for detection of language-related subcortical pathways, and to evaluate whether a standardized FAT-based DTI FT protocol developed for the identification of the CST based on nTMS data can also be used for that purpose (Frey et al., 2012). In this context, DTI FT of the CST based on nTMS data has been demonstrated recently (Conti et al., 2014; Forster et al., 2015; Frey et al., 2012; Krieg et al., 2012; Weiss et al., 2015), which seems to underline the general importance of functional data derived from nTMS as a basis for subsequent DTI FT in neurosurgery. However, data on the tractography of specific language-related subcortical pathways is not available yet except for one case report describing a similar approach in a bilingual tumor patient (Sollmann et al., 2015a). The rationale behind using the protocol introduced by Frey et al. (2012) in the present study is based on its easy and fast applicability whilst being standardized and tested during nTMS-based DTI FT (Frey et al., 2012).

As aforementioned, ROI seeding can either be done with respect to anatomical or functional data. Regarding anatomical ROI placement, necessary information is provided by MRI, while ROI generation based on functional information can be achieved by using MEG, fMRI, or nTMS results. Functional-based seeding is usually favored because of two main disadvantages of the anatomy-based approach: First, the seeding of ROIs according to mere anatomical landmarks depends on the individual anatomic knowledge of the examiner and is, therefore, likely to vary from one operator to another (Catani and Thiebaut de Schotten, 2008; Wakana et al., 2004), which limits the validity and reproducibil-

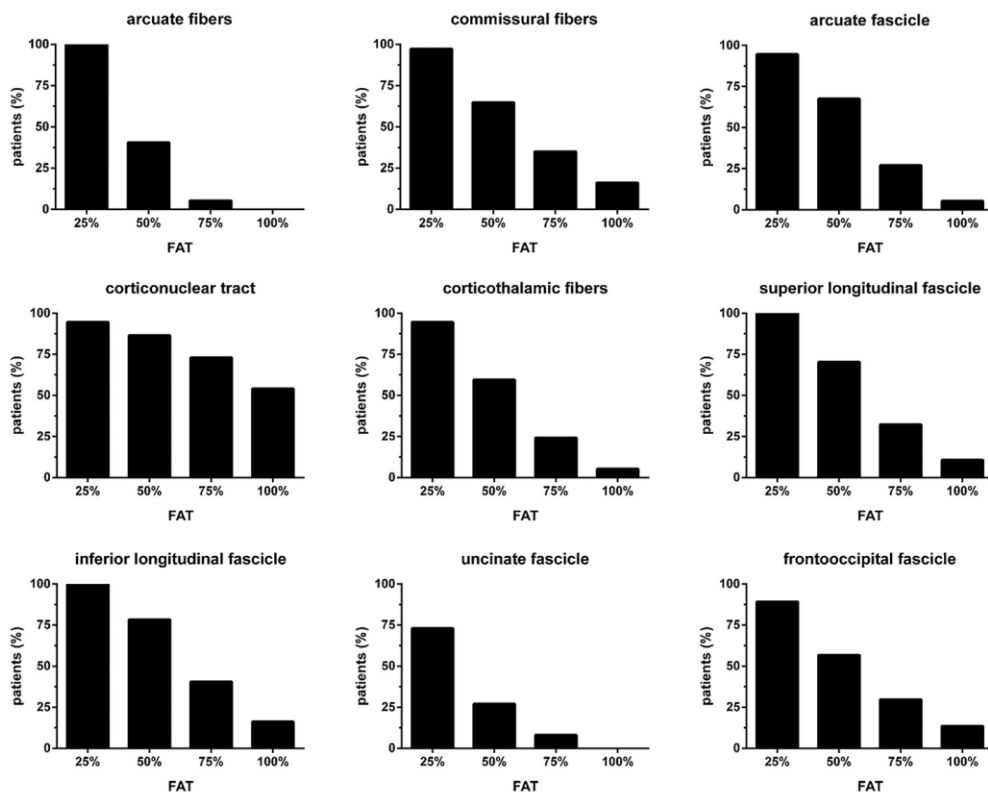


**Fig. 5.** Percentage of patients showing the different language-related pathways in relation to the fractional anisotropy threshold (FAT).

Bar graphs illustrating the percentage of patients in which a certain subcortical language-related pathway was visualized, depending on the fractional anisotropy threshold (FAT). The difference in visible tracts between DTI FT with different FATs was statistically significant for each of the 9 language pathways ( $p < 0.05$ ).

ity of the tracked fibers. Second, identification of anatomical landmarks for seeding can be difficult in subjects suffering from space-occupying brain lesions, due to a variable degree of plasticity and the likely derangement of subcortical fiber bundles (Lehericy et al., 2000; Nimsky et al., 2006; Robles et al., 2008). Although functional-based ROI seeding is typically less affected by these two shortcomings, its validity can be hampered by limitations of the underlying imaging modality. In this context, it has already been demonstrated that fMRI is likely to lack accuracy in subjects with changed intracranial oxygen levels due to brain tumors, which indicates that it might not be the optimal tool for the identification of language-related areas in such patients (Binder, 2011; Sollmann et al., 2013). In this context, recent modality comparison studies have shown that nTMS used for cortical language mapping is likely to provide more reliable and accurate data in brain tumor patients when compared to other techniques like fMRI or MEG, for instance, while it showed a good correlation with direct cortical stimulation (DCS) (Ille et al., 2015; Picht et al., 2013; Sollmann et al., 2013; Tarapore et al., 2013), which represents the gold standard with respect to mapping of language-related areas. Correspondingly, it seems to be likely that DTI FT based on nTMS results might be more reliable when compared to DTI FT originating from fMRI or MEG data since the correlation to intraoperative DCS was better for nTMS in these trials (Ille et al., 2015; Picht et al., 2013; Sollmann et al., 2013; Tarapore et al., 2013). Moreover, although nTMS-based DTI FT is dependent on the ROI size that was adjusted manually by putting an additional rim of 5 mm to the positive stimulation spots,

it might still be more suitable since the relevant hemisphere is mapped with applicable results as shown by 100% of mapping data inclusion for tracking in the present trial, whereas fMRI might even fail to identify ROIs in the lesion-affected hemisphere (Sollmann et al., 2013). However, if fMRI is able to show ROIs in the affected hemisphere, tractography of language pathways is feasible, but might not allow for detection of all tracts addressed in our present approach. Additionally, in one single case report, the technical feasibility and usefulness of nTMS-based DTI FT for language fibers was already demonstrated (Sollmann et al., 2015a). Overall, these findings motivated for the approach of the present study, and should encourage further DTI FT investigations based on functional data derived from nTMS language mapping.

Besides the aforementioned case report (Sollmann et al., 2015a), no publication up until now has been available that systematically compares nTMS-based DTI FT for language pathways to intraoperative subcortical stimulation. Yet, at least a very recent study by Conti et al. (2014) was able to prove the concordance for nTMS-based DTI FT of the CST (Conti et al., 2014), which might be able to guide similar trials in terms of nTMS-based DTI FT for language in the next future. However, since the present study is focused on feasibility, it did not systematically compare the accuracy of nTMS-based DTI FT to intraoperative stimulation techniques. Although a promising result has been highlighted in the case report (Sollmann et al., 2015a), this lack suggests that it is not yet clear whether nTMS-based DTI FT for subcortical language pathways is actually able to reflect reality in a larger cohort of brain tumor patients. Therefore,

further studies are greatly needed to confirm preoperatively gained nTMS-based DTI FT results by intraoperative subcortical stimulation.

With regard to DTI FT for the detection of language pathways in general, many studies have already investigated the accuracy of DTI FT compared to intraoperative subcortical stimulation, and these publications mostly revealed a good correlation between both techniques (Bello et al., 2008; Kuhnt et al., 2012; Leclercq et al., 2010; Nimsky et al., 2007). In a recent publication of Bello et al. (2008), for example, subcortical stimulation for the detection of subcortical language-related fiber tracts was in good accordance with preoperative DTI FT, with an overall sensitivity of 97% (Bello et al., 2008). Accordingly, DTI FT already represents a promising technique in neurosurgery, which might be further developed by using nTMS spots as seed regions as described above.

Besides these issues, the FA value, which basically reflects the direction dependence in a diffusion process, has a distinct impact on DTI FT results (Basser et al., 1994; Basser et al., 2000). When there is no standardized protocol available, this value is generally set arbitrarily to a certain score for all subjects included in one study or is simply adjusted according to the examiner's expectation about what the final DTI FT visualization should look like (Frey et al., 2012). Thus, this limits the comparability of tracking results between examiners and institutions using different FA values; DTI FT without standardized reference values such as the FAT, for example, is probably more time-consuming and less reproducible. To overcome these problems, the present study aimed to demonstrate the feasibility of nTMS-based DTI FT in the context of an already established tracking protocol (Frey et al., 2012).

In the original study, Frey et al. (2012) were able to perform DTI FT for CST reconstruction in a cohort of 50 brain tumor patients and concluded that DTI FT based on nTMS was most helpful for surgical planning when performed with 75% FAT (Frey et al., 2012). However, regarding our results, 75% as well as 100% FAT did not allow for the constant detection of the 9 language-related fiber tracts included in the analysis in each patient (Table 1 and Fig. 5). The uncinate fascicle, for example, was not detectable with 100% FAT in any case, and was only found in 3 out of 37 patients (8.1%) when DTI FT was conducted with 75% FAT (Table 1 and Fig. 5). In addition to that, the fibers/tract ratios were comparatively low for 75% FAT and 100% FAT in particular (Table 1 and Fig. 3), meaning that detectable subcortical language-related pathways only consisted of a low number of fibers. Therefore, we assume that 75% and 100% FAT do not represent adequate adjustments for the tracking of language-related fibers. However, like aforementioned, comparison of the DTI FT results to intraoperative stimulation is required to draw final conclusions about the optimal tracking protocol adjustments in the neurosurgical context.

Furthermore, concerning the two remaining FAT values tested in the present study, 25% FAT allowed for the tracking of most of the language-related tracts (Table 1 and Fig. 5), but DTI FT with this value likely resulted in the visualization of a large number of fibers and, therefore, made it more demanding to clearly identify certain fiber bundles. Low FA values also tend to facilitate the detection of aberrant fibers, which could lead to implausible fiber reconstruction (Frey et al., 2012). Compared to 75% and 100% FAT, tracking with 50% distinctly resulted in the detection of more language-related tracts (Table 1 and Fig. 5), while this adjustment allowed for clearer and easier differentiation between particular fiber bundles. However, it identified fewer tracts than 25% FAT on average, and it remains controversial if 25% or 50% FAT represents the optimal value out of the four adjustments tested in the present study. From a neurosurgical perspective, intraoperative validation should be performed within upcoming studies that go beyond the level of feasibility in order to validate these adjustments.

Regarding tracking with 75% or 100% FAT, only a minimum of fibers is displayed due to the applied protocol described above, thus making the routine visualization of all investigated tracts unlikely. However, for lower thresholds like 25% or 50% FAT, still not all language-related pathways were visualized (Table 1 and Fig. 5). Interestingly, after careful review of the anatomical MRI sequences of all patients, the missing tracts were most probably absent or not identifiable due to the locations of the tumor volumes, which were situated within the typical fiber courses or origins of the respective tracts (Fig. 1). Although missing tracts might be primarily related to the tumor locations in the present study, our approach could be refined by using tractography masks as add-ons, for instance, which might allow for better identification of language-related pathways. The combination of nTMS-based DTI FT with more elaborate tracking algorithms and masks should be the topic of upcoming studies.

Although our approach allowed for the detection of different language-related white matter tracts in all enrolled patients, we have to bear in mind some limitations of the DTI FT technique. In that context, it is still challenging to reconstruct crossing fibers because this situation interferes with the identification of a primary eigenvector of a voxel and thus the tracking of fibers (Berman et al., 2007; Krieg et al., 2012; Le Bihan et al., 2006). In addition, fibers close to tumor margins or edema are vulnerable to false-negative results, primarily due to low anisotropy, which can cause unreliable DTI FT results (Berman et al., 2007; Krieg et al., 2012). Correspondingly, more advanced MRI diffusion sequences and more complex analysis methods are currently developed with the aim of solving these DTI-related problems. Among novel model-free methods, q-space imaging (Hori et al., 2012; Yeh and Tseng, 2011) and high angular resolution diffusion imaging (HARDI) (Kuhnt et al., 2013; Tuch et al., 2002) seem to represent the most promising and best-studied advances. Both approaches allow for compensation of at least some of the inherent DTI limitations and are increasingly used in the neuroscientific context. However, application of these techniques in the neurosurgical routine still constitutes an exception in most centers although it is undoubtedly that advances in fiber tracking are crucial to overcome DTI and its limitations (Abhinav et al., 2014; Nimsky, 2014). For instance, a recent study among glioma patients has already demonstrated that application of HARDI for tracking of language-related pathways displayed more fiber bundles when compared to DTI-based results (Kuhnt et al., 2013). Moreover, it was shown that plausible fiber courses in the vicinity of the tumor were depicted by HARDI fiber tracking, and these bundles were not routinely tracked with DTI FT (Kuhnt et al., 2013). So far, the straightforward implementation of tracking results derived from such novel approaches into the neuronavigation software might have restricted the applicability in daily routine. Furthermore, MRI acquisition times are commonly longer for these novel approaches, but the use of multi-band acquisition sequences already has the potential to compensate for this limitation (Abhinav et al., 2014; Sotiropoulos et al., 2013). However, the application of such sequences has just started to become part of clinical investigations. Hence, DTI FT still represents the current standard in clinical neurosurgery for most centers until further progress allows for the reliable implementation of the outlined advances into daily routine. Accordingly, investigations regarding the DTI FT technique might still be highly relevant for the clinical setting. Thus, the present trial aimed to demonstrate the feasibility of nTMS-based DTI FT by using a standardized FAT protocol (Frey et al., 2012), and therefore, it represents one of the first approaches using nTMS language data for DTI FT in a comparatively large cohort consisting of 37 brain tumor patients. It distinctly intends to share this novel approach with the neurosurgical community for further refinement, and intraoperative stimulation for validation of

such language-related tracking results has to be the next step in a follow-up study beyond the level of feasibility.

## 5. Conclusions

The present study demonstrates that nTMS language maps can be used for DTI FT of subcortical language pathways and, furthermore, a FAT-based protocol currently seems to be a reasonable and standardized approach for nTMS-based language DTI FT. Hence, nTMS-based DTI FT might be an easy and standardized tool for the identification of various subcortical white matter tracts associated with language functions prior to surgery. Moreover, 50% or 25% of the individual FAT was shown to provide the optimal visualization of subcortical language pathways. However, the results of nTMS-based DTI FT for the detection of language-related fiber tracts should be validated by intraoperative subcortical stimulation as it was done for the CST.

## Conflict of interest

FR and SK are consultants for BrainLAB AG. SK is consultant for Nexstim Oy (Helsinki, Finland). The study was completely financed by institutional grants from the Department of Neurosurgery and the Section of Neuroradiology. The authors report no conflict of interest concerning the materials or methods used in this study or the findings specified in this manuscript.

## Acknowledgement

The first author gratefully acknowledges the support of the graduate school of our university.

## References

- Abhinav, K., Yeh, F.C., Pathak, S., Suski, V., Lacomis, D., Friedlander, R.M., Fernandez-Miranda, J.C., 2014. Advanced diffusion MRI fiber tracking in neurosurgical and neurodegenerative disorders and neuroanatomical studies: a review. *Biochim. Biophys. Acta* 1842, 2286–2297.
- Axer, H., Klingner, C.M., Prescher, A., 2013. Fiber anatomy of dorsal and ventral language streams. *Brain Lang.* 127, 192–204.
- Basser, P.J., Mattiello, J., LeBihan, D., 1994. MR diffusion tensor spectroscopy and imaging. *Biophys. J.* 66, 259–267.
- Basser, P.J., Pajevic, S., Pierpaoli, C., Duda, J., Aldroubi, A., 2000. In vivo fiber tractography using DT-MRI data. *Magn. Reson. Med.* 44, 625–632.
- Bello, L., Gambini, A., Castellano, A., Carrabba, G., Acerbi, F., Fava, E., Giussani, C., Cadioli, M., Blasi, V., Casarotti, A., Papagno, C., Gupta, A.K., Gaiini, S., Scotti, G., Falini, A., 2008. Motor and language DTI fiber tracking combined with intraoperative subcortical mapping for surgical removal of gliomas. *NeuroImage* 39, 369–382.
- Berman, J.I., Berger, M.S., Chung, S.W., Nagarajan, S.S., Henry, R.G., 2007. Accuracy of diffusion tensor magnetic resonance imaging tractography assessed using intraoperative subcortical stimulation mapping and magnetic source imaging. *J. Neurosurg.* 107, 488–494.
- Binder, J.R., 2011. Functional MRI is a valid noninvasive alternative to Wada testing. *Epilepsy Behav.* 20, 214–222.
- Catani, M., Thiebaut de Schotten, M., 2008. A diffusion tensor imaging tractography atlas for virtual in vivo dissections. *Cortex* 44, 1105–1132.
- Catani, M., Howard, R.J., Pajevic, S., Jones, D.K., 2002. Virtual in vivo interactive dissection of white matter fasciculi in the human brain. *NeuroImage* 17, 77–94.
- Chang, E.F., Raygor, K.P., Berger, M.S., 2015. Contemporary model of language organization: an overview for neurosurgeons. *J. Neurosurg.* 122, 250–261.
- Conti, A., Raffa, G., Granata, F., Rizzo, V., Germano, A., Tomasello, F., 2014. Navigated transcranial magnetic stimulation for “somatotopic” tractography of the corticospinal tract. *Neurosurgery* 10 (Suppl. 4), 542–544, discussion 54.
- Corina, D.P., Loudermilk, B.C., Detwiler, L., Martin, R.F., Brinkley, J.F., Ojemann, G., 2010. Analysis of naming errors during cortical stimulation mapping: implications for models of language representation. *Brain Lang.* 115, 101–112.
- Doek, P., Turner, R., Pekar, J., Patronas, N., Le Bihan, D., 1991. MR color mapping of myelin fiber orientation. *J. Comput. Assist. Tomogr.* 15, 923–929.
- Epstein, C.M., Lah, J.J., Meador, K., Weissman, J.D., Gaitan, L.E., Dihenia, B., 1996. Optimum stimulus parameters for lateralized suppression of speech with magnetic brain stimulation. *Neurology* 47, 1590–1593.
- Forster, M.T., Hoecker, A.C., Kang, J.S., Quick, J., Seifert, V., Hattingen, E., Hilker, R., Weise, L.M., 2015. Does navigated transcranial stimulation increase the accuracy of tractography? A prospective clinical trial based on intraoperative motor evoked potential monitoring during deep brain stimulation. *Neurosurgery* 76, 766–775, discussion 75–6.
- Frey, D., Strack, V., Wiener, E., Jussen, D., Vajkoczy, P., Picht, T., 2012. A new approach for corticospinal tract reconstruction based on navigated transcranial stimulation and standardized fractional anisotropy values. *NeuroImage* 62, 1600–1609.
- Gierhan, S.M., 2013. Connections for auditory language in the human brain. *Brain Lang.* 127, 205–221.
- Hernandez-Pavon, J.C., Makela, N., Lehtinen, H., Lioumis, P., Makela, J.P., 2014. Effects of navigated TMS on object and action naming. *Front. Hum. Neurosci.* 8, 660.
- Hori, M., Fukunaga, I., Masutani, Y., Taoka, T., Kamagata, K., Suzuki, Y., Aoki, S., 2012. Visualizing non-Gaussian diffusion: clinical application of q-space imaging and diffusional kurtosis imaging of the brain and spine. *Magn. Reson. Med. Sci.* 11, 221–233.
- Huber, W., Poeck, K., Willmes, K., 1984. The Aachen Aphasia Test. *Adv. Neurol.* 42, 291–303.
- Ille, S., Sollmann, N., Hauck, T., Maurer, S., Tanigawa, N., Obermueller, T., Negwer, C., Droese, D., Zimmer, C., Meyer, B., Ringel, F., Krieg, S.M., 2015. Combined noninvasive language mapping by navigated transcranial magnetic stimulation and functional MRI and its comparison with direct cortical stimulation. *J. Neurosurg.* 123, 212–225.
- Indefrey, P., 2011. The spatial and temporal signatures of word production components: a critical update. *Front. Psychol.* 2, 255.
- Krieg, S.M., Buchmann, N.H., Gempt, J., Shiban, E., Meyer, B., Ringel, F., 2012. Diffusion tensor imaging fiber tracking using navigated brain stimulation—a feasibility study. *Acta Neurochir.* 154, 555–563.
- Krieg, S.M., Sollmann, N., Hauck, T., Ille, S., Meyer, B., Ringel, F., 2014a. Repeated mapping of cortical language sites by preoperative navigated transcranial magnetic stimulation compared to repeated intraoperative DCS mapping in awake craniotomy. *BMC Neurosci.* 15, 20.
- Krieg, S.M., Tarapore, P.E., Picht, T., Tanigawa, N., Houde, J., Sollmann, N., Meyer, B., Vajkoczy, P., Berger, M.S., Ringel, F., Nagarajan, S., 2014b. Optimal timing of pulse onset for language mapping with navigated repetitive transcranial magnetic stimulation. *NeuroImage* 100, 219–236.
- Krieg, S.M., Sollmann, N., Tanigawa, N., Foerschler, A., Meyer, B., Ringel, F., 2015. Cortical distribution of speech and language errors investigated by visual object naming and navigated transcranial magnetic stimulation. *Brain Struct. Funct.*
- Kuhnt, D., Bauer, M.H., Becker, A., Merhof, D., Zolal, A., Richter, M., Grummich, P., Ganslandt, O., Buchfelder, M., Nimsky, C., 2012. Intraoperative visualization of fiber tracking based reconstruction of language pathways in glioma surgery. *Neurosurgery* 70, 911–919, discussion 9–20.
- Kuhnt, D., Bauer, M.H., Egger, J., Richter, M., Kapur, T., Sommer, J., Merhof, D., Nimsky, C., 2013. Fiber tractography based on diffusion tensor imaging compared with high-angular-resolution diffusion imaging with compressed sensing: initial experience. *Neurosurgery* 72 (Suppl. 1), 165–175.
- Le Bihan, D., Poupon, C., Amadon, A., Lethimonnier, F., 2006. Artifacts and pitfalls in diffusion MRI. *J. Magn. Reson. Imaging* 24, 478–488.
- Leclercq, D., Duffau, H., Delmaire, C., Capelle, L., Gatignol, P., Ducros, M., Chiras, J., Lehericy, S., 2010. Comparison of diffusion tensor imaging tractography of language tracts and intraoperative subcortical stimulations. *J. Neurosurg.* 112, 503–511.
- Lehericy, S., Duffau, H., Cornu, P., Capelle, L., Pidoux, B., Carpentier, A., Auliac, S., Clemenceau, S., Sichez, J.P., Bitar, A., Valery, C.A., Van Effenterre, R., Faillet, T., Srouf, A., Fohanno, D., Philippon, J., Le Bihan, D., Marsault, C., 2000. Correspondence between functional magnetic resonance imaging somatotopy and individual brain anatomy of the central region: comparison with intraoperative stimulation in patients with brain tumors. *J. Neurosurg.* 92, 589–598.
- Lioumis, P., Zhdanov, A., Makela, N., Lehtinen, H., Wilenius, J., Neuvonen, T., Hannula, H., Deletis, V., Picht, T., Makela, J.P., 2012. A novel approach for documenting naming errors induced by navigated transcranial magnetic stimulation. *J. Neurosci. Methods* 204, 349–354.
- Makris, N., Kennedy, D.N., McInerney, S., Sorensen, A.G., Wang, R., Caviness Jr., V.S., Pandya, D.N., 2005. Segmentation of subcomponents within the superior longitudinal fascicle in humans: a quantitative, in vivo, DT-MRI study. *Cereb. Cortex* 15, 854–869.
- Mori, S., van Zijl, P.C., 2002. Fiber tracking: principles and strategies—a technical review. *NMR Biomed.* 15, 468–480.
- Moseley, M.E., Cohen, Y., Kucharczyk, J., Mintorovitch, J., Asgari, H.S., Wendland, M.F., Tsuruda, J., Norman, D., 1990. Diffusion-weighted MR imaging of anisotropic water diffusion in cat central nervous system. *Radiology* 176, 439–445.
- Nimsky, C., 2014. Fiber tracking—we should move beyond diffusion tensor imaging. *World Neurosurg.* 82, 35–36.
- Nimsky, C., Ganslandt, O., Merhof, D., Sorensen, A.G., Fahlbusch, R., 2006. Intraoperative visualization of the pyramidal tract by diffusion-tensor-imaging-based fiber tracking. *NeuroImage* 30, 1219–1229.
- Nimsky, C., Ganslandt, O., Hastreiter, P., Wang, R., Benner, T., Sorensen, A.G., Fahlbusch, R., 2007. Preoperative and intraoperative diffusion tensor imaging-based fiber tracking in glioma surgery. *Neurosurgery* 61, 178–185, discussion 86.
- Picht, T., Krieg, S.M., Sollmann, N., Rosler, J., Niraula, B., Neuvonen, T., Savolainen, P., Lioumis, P., Makela, J.P., Deletis, V., Meyer, B., Vajkoczy, P., Ringel, F., 2013. A comparison of language mapping by preoperative navigated transcranial

- magnetic stimulation and direct cortical stimulation during awake surgery. *Neurosurgery* 72, 808–819.
- Robles, S.G., Gatignol, P., Lehericy, S., Duffau, H., 2008. Long-term brain plasticity allowing a multistage surgical approach to World Health Organization Grade II gliomas in eloquent areas. *J. Neurosurg.* 109, 615–624.
- Rogic, M., Deletis, V., Fernandez-Conejero, I., 2014. Inducing transient language disruptions by mapping of Broca's area with modified patterned repetitive transcranial magnetic stimulation protocol. *J. Neurosurg.* 120, 1033–1041.
- Salmelin, R., Helenius, P., Service, E., 2000. Neurophysiology of fluent and impaired reading: a magnetoencephalographic approach. *J. Clin. Neurophysiol.* 17, 163–174.
- Sollmann, N., Picht, T., Makela, J.P., Meyer, B., Ringel, F., Krieg, S.M., 2013. Navigated transcranial magnetic stimulation for preoperative language mapping in a patient with a left frontoopercular glioblastoma. *J. Neurosurg.* 118, 175–179.
- Sollmann, N., Tanigawa, N., Ringel, F., Zimmer, C., Meyer, B., Krieg, S.M., 2014. Language and its right-hemispheric distribution in healthy brains: an investigation by repetitive transcranial magnetic stimulation. *NeuroImage* 102 (Pt 2), 776–788.
- Sollmann, N., Gighuber, K., Tussis, L., Meyer, B., Ringel, F., Krieg, S.M., 2015a. nTMS-based DTI fiber tracking for language pathways correlates with language function and aphasia—a case report. *Clin. Neurol. Neurosurg.* 136, 25–28.
- Sollmann, N., Ille, S., Hauck, T., Maurer, S., Negwer, C., Zimmer, C., Ringel, F., Meyer, B., Krieg, S.M., 2015b. The impact of preoperative language mapping by repetitive navigated transcranial magnetic stimulation on the clinical course of brain tumor patients. *BMC Cancer* 15, 261.
- Sollmann, N., Ille, S., Obermueller, T., Negwer, C., Ringel, F., Meyer, B., Krieg, S.M., 2015c. The impact of repetitive navigated transcranial magnetic stimulation coil positioning and stimulation parameters on human language function. *Eur. J. Med. Res.* 20, 47.
- Sotiropoulos, S.N., Jbabdi, S., Xu, J., Andersson, J.L., Moeller, S., Auerbach, E.J., Glasser, M.F., Hernandez, M., Sapiro, G., Jenkinson, M., Feinberg, D.A., Yacoub, E., Lenglet, C., Van Essen, D.C., Ugurbil, K., Behrens, T.E., Consortium, W.U.-M.H., 2013. Advances in diffusion MRI acquisition and processing in the Human Connectome Project. *NeuroImage* 80, 125–143.
- Tarapore, P.E., Findlay, A.M., Honma, S.M., Mizuiri, D., Houde, J.F., Berger, M.S., Nagarajan, S.S., 2013. Language mapping with navigated repetitive TMS: proof of technique and validation. *NeuroImage* 82, 260–272.
- Tuch, D.S., Reese, T.G., Wiegell, M.R., Makris, N., Belliveau, J.W., Wedeen, V.J., 2002. High angular resolution diffusion imaging reveals intravoxel white matter fiber heterogeneity. *Magn. Reson. Med.* 48, 577–582.
- Wakana, S., Jiang, H., Nagae-Poetscher, L.M., van Zijl, P.C., Mori, S., 2004. Fiber tract-based atlas of human white matter anatomy. *Radiology* 230, 77–87.
- Wassermann, E.M., Blaxton, T.A., Hoffman, E.A., Berry, C.D., Oletsky, H., Pascual-Leone, A., Theodore, W.H., 1999. Repetitive transcranial magnetic stimulation of the dominant hemisphere can disrupt visual naming in temporal lobe epilepsy patients. *Neuropsychologia* 37, 537–544.
- Weiss, C., Tursunova, I., Neuschmelting, V., Lockau, H., Nettekoven, C., Oros-Peusquens, A.M., Stoffels, G., Rehme, A.K., Faymonville, A.M., Shah, N.J., Langen, K.J., Goldbrunner, R., Grefkes, C., 2015. Improved nTMS- and DTI-derived CST tractography through anatomical ROI seeding on anterior pontine level compared to internal capsule. *NeuroImage Clin.* 7, 424–437.
- Wheat, K.L., Cornelissen, P.L., Sack, A.T., Schuhmann, T., Goebel, R., Blomert, L., 2013. Charting the functional relevance of Broca's area for visual word recognition and picture naming in Dutch using fMRI-guided TMS. *Brain Lang.* 125, 223–230.
- Yeh, F.C., Tseng, W.Y., 2011. NTU-90: a high angular resolution brain atlas constructed by q-space diffeomorphic reconstruction. *NeuroImage* 58, 91–99.

## 11.2. Language pathway tracking: comparing nTMS-based DTI fiber tracking with a cubic ROIs-based protocol

### Language pathway tracking: comparing nTMS-based DTI fiber tracking with a cubic ROIs-based protocol

Chiara Negwer, MD,<sup>1,2</sup> Nico Sollmann, MD,<sup>1,2</sup> Sebastian Ille, MD,<sup>1,2</sup> Theresa Hauck,<sup>1,2</sup> Stefanie Maurer,<sup>1,2</sup> Jan S. Kirschke, MD,<sup>3</sup> Florian Ringel, MD,<sup>1</sup> Bernhard Meyer, MD,<sup>1</sup> and Sandro M. Krieg, MD, MBA<sup>1,2</sup>

<sup>1</sup>Department of Neurosurgery, <sup>2</sup>TUM-Neuroimaging Center, and <sup>3</sup>Section of Neuroradiology, Department of Radiology, Klinikum rechts der Isar, Technical University of Munich, Germany

**OBJECTIVE** Diffusion tensor imaging (DTI) fiber tracking (FT) has been widely used in glioma surgery in recent years. It can provide helpful information about subcortical structures, especially in patients with eloquent space-occupying lesions. This study compared the newly developed navigated transcranial magnetic stimulation (nTMS)-based DTI FT of language pathways with the most reproducible protocol for language pathway tractography, using cubic regions of interest (ROIs) for the arcuate fascicle.

**METHODS** Thirty-seven patients with left-sided perisylvian lesions underwent language mapping by repetitive nTMS. DTI FT was performed using the cubic ROIs-based protocol and the authors' nTMS-based DTI FT approach. The same minimal fiber length and fractional anisotropy were chosen (50 mm and 0.2, respectively). Both protocols were performed with standard clinical tractography software.

**RESULTS** Both methods visualized language-related fiber tracts (i.e., corticonuclear tract, arcuate fascicle, uncinate fascicle, superior longitudinal fascicle, inferior longitudinal fascicle, arcuate fibers, commissural fibers, corticothalamic fibers, and frontooccipital fascicle) in all 37 patients. Using the cubic ROIs-based protocol, 39.9% of these language-related fiber tracts were detected in the examined patients, as opposed to 76.0% when performing nTMS-based DTI FT. For specifically tracking the arcuate fascicle, however, the cubic ROIs-based approach showed better results (97.3% vs 75.7% with nTMS-based DTI FT).

**CONCLUSIONS** The cubic ROIs-based protocol was designed for arcuate fascicle tractography, and this study shows that it is still useful for this intention. However, superior results were obtained using the nTMS-based DTI FT for visualization of other language-related fiber tracts.

<http://thejns.org/doi/abs/10.3171/2016.2.JNS152382>

**KEY WORDS** cortical mapping; fiber tracking; language; navigated transcranial magnetic stimulation; space-occupying lesions; subcortical; surgical technique

**I**n modern neurooncology, resection of eloquent space-occupying lesions remains a challenge. Especially with respect to survival and quality of life, a balance is needed between gross-total resection and the preservation of neurological function, particularly motor system and language functions, to provide beneficial outcomes.<sup>6,37,38,45</sup> Various tools (e.g., neuronavigation, fluorescent dye, intraoperative neuromonitoring) have been developed to increase patient safety and improve surgical monitoring

during these neurosurgical resections. Presurgical planning mapping techniques (e.g., transcranial magnetic stimulation [TMS]) have gained particular importance because they allow surgeons to further optimize planning processes. In this field, navigated TMS (nTMS) has shown good results in previous studies, allowing the identification of motor- and language-relevant areas comparable to direct cortical stimulation (DCS), which is still defined as the gold standard.<sup>22,32,46</sup>

**ABBREVIATIONS** AF = arcuate fascicle; ArF = arcuate fibers; CST = corticospinal tract; DCS = direct cortical stimulation; DTI = diffusion tensor imaging; FA = fractional anisotropy; fMRI = functional MRI; FT = fiber tracking; MFL = minimum fiber length; nTMS = navigated transcranial magnetic stimulation; RMT = resting motor threshold; ROI = region of interest; rTMS = repetitive navigated transcranial magnetic stimulation; SLF = superior longitudinal fascicle; TMS = transcranial magnetic stimulation; UF = uncinate fascicle.

**SUBMITTED** October 14, 2015. **ACCEPTED** February 19, 2016.

**INCLUDE WHEN CITING** Published online May 27, 2016; DOI: 10.3171/2016.2.JNS152382.

Yet, the importance of eloquent subcortical structures, the role of subcortical plastic reorganization, and the ongoing shift toward a more hodotopical perspective, describing the language process as an interaction of cortico-subcortical subnetworks, cannot be ignored.<sup>9,12,14,18,21,35</sup> Diffusion tensor imaging (DTI) fiber tracking (FT), in particular, has become a frequently used technique in modern neurosurgery, both in the clinical routine and for neuroscientific research purposes. DTI FT can be based on either functional data (provided by functional MRI [fMRI], nTMS, and so on) or anatomical landmarks. One of the most reproducible language-related, anatomically based DTI FT protocols uses 3 cubic seed regions of interest (ROIs), placed according to anatomical landmarks, for visualization of the arcuate fascicle (AF) in patients with space-occupying lesions.<sup>44</sup>

Previous studies of nTMS-based DTI FT of the corticospinal tract (CST) have provided promising feasibility data,<sup>10,16,19,49</sup> and initial studies with successful repetitive nTMS (rTMS)-based DTI FT of language-related subcortical fiber tracts have been completed.<sup>39</sup> Therefore, this study investigated the feasibility and application of rTMS-based DTI FT for language-related subcortical fiber tracts in patients with left-sided perisylvian lesions, and compared rTMS-based DTI FT with a cubic ROIs-based DTI FT protocol to further investigate the benefits and potential limitations of function-based DTI FT with respect to language-related fiber tracts.

## Methods

### Ethics Approval

In conformity with the Declaration of Helsinki, the experimental protocol used in this study was certified by the local ethical committee of the Technical University of Munich. All enrolled patients gave their written informed consent to this study before language mapping by rTMS was performed.

### Study Design

The study was designed to be prospective and nonrandomized.

### Patients

From May 2011 to August 2014, 37 patients underwent preoperative language mapping by rTMS. Inclusion criteria were left-sided perisylvian lesion, age older than 18 years, and written informed consent. The general rTMS exclusion criteria (e.g., having a cochlear implant or cardiac pacemaker) were applied.

### Preoperative MRI and DTI

All enrolled patients received preoperative MRI with additional DTI sequences in 6–15 diffusion directions. The navigational MR images were acquired on a 3-T MR scanner (Achieva 3T, Philips Medical System) with an 8-channel phased-array head coil. Our standard protocol included a T2-weighted FLAIR sequence (TR/TE 12,000/140 msec; inversion time of 2500 msec; 30 slices with 1-mm gap; voxel size 0.9 × 0.9 × 4 mm; 3-minute acquisition time), an intravenous contrast administration

of gadopentetate dimeglumine, 0.1 mmol/kg body weight (Magnograf, Marotrust GmbH), and a 3D gradient echo sequence (TR/TE 9/4 msec; 1-mm<sup>3</sup> isovoxel covering the whole skull; 418-second acquisition time). DTI sequences were acquired with a single-shot spin echo planar imaging (TR/TE = 7571/55 msec) with b values of 0 and 800, and 6 orthogonal diffusion directions or in some cases 15 directions. Parallel imaging techniques were used (sensitivity encoding factor 2), and 2 averages of 73 contiguous 2-mm slices with a matrix of 112°–112 mm scanning the whole skull were taken in 135 seconds. The DTI sequences were subsequently added to a matrix of 224°–224 mm; the voxel size was 0.88°–0.88°–2 mm<sup>3</sup>. Motion artifacts of the DTI data were adjusted using the installed software on the scanner.

For navigational MRI, a 3D fast-field echo sequence was chosen, with a TR/TE of 9/4 msec and a flip angle of 8°. The complete head was covered in an isotropic resolution of 1 mm<sup>3</sup>, using a sense factor of 1.5 and a turbo factor of 164. The resulting 3D data set was transferred (via DICOM standard) to the nTMS system (eXimia, Nexstim) and to the BrainLAB iPlanNet Cranial 3.0 tractography software.

### Language Mapping by rTMS

All enrolled patients underwent language mapping using nTMS eXimia NBS version 3.2.2 and Nexstim NBS 4.3 with a NEXSPEECH module (Nexstim). A standardized, previously published protocol was used.<sup>28,32,42</sup> Subsequently, the resting motor threshold (RMT) of every patient was retrieved while performing motor mapping of the cortical representation of the contralateral abductor pollicis brevis muscle.<sup>20</sup> The obtained RMT was used afterward as a basic value for language mapping by rTMS; an object naming task, containing 131 colored pictures of common objects, was then performed.<sup>28,32,42</sup>

First, 2 baseline trials (object naming without simultaneous rTMS) were carried out. The patient was asked to identify 131 pictures of common objects in his or her native language. Each object was displayed for 700 msec (display time), and the interpicture interval was set to 2.5 seconds. These settings were not changed for subsequent language mapping. All objects that could not be named quickly and fluently in the baseline trials were discarded and thus excluded from the stimulation trials. The correct, pronounced responses were video recorded and used in the subsequent language mapping.<sup>28,43</sup>

During the actual language mapping, rTMS pulses were applied and time-locked to the randomly displayed objects. The picture-to-trigger interval (the time between the presentation of an object on the screen and the onset of the rTMS pulse) was set to 300 msec for the first 15 patients and then changed according to our current protocol to 0 msec for the following 22 patients. Even though there is evidence for both picture-to-trigger intervals,<sup>17,34,36,50</sup> we decided to adapt our protocol to 0 msec, according to a recent publication that described the potential benefits of immediate stimulation onset.<sup>23</sup> The mapping intensity and frequency were individually determined using our standard protocol.<sup>31,40,42</sup>

During language mapping by rTMS, the stimulation coil was placed tangential to the patient's skull, with

the electrical field in strict anteroposterior orientation to achieve maximum field induction.<sup>15,28,48</sup> The magnetic coil was moved between 2 displayed objects (the interpicture interval) in approximately 10-mm steps. The induced electrical field strength varied between 55 and 80 V/m. Naming performance under stimulation was video recorded, as in the prior baseline trials.<sup>28,43</sup>

For post hoc analysis, the baseline and the stimulation recordings were analyzed, compared, and systematically searched for naming errors by the same person who performed the language mapping. Language errors were categorized as no-response errors, performance errors, neologisms, phonological paraphasias, or semantic paraphasias.<sup>11,28,43</sup> Since hesitations errors were not objectified by latency recordings in our study, they were discarded. Errors due to direct muscle stimulation, noncompliance, or pain were not taken into account.

### DTI FT

Since one of our intentions in this study was to evaluate the feasibility of DTI FT using language-related areas mapped by rTMS as the ROI, we chose a deterministic algorithm. Moreover, since another leading goal was the acquisition of data for direct clinical use in the treatment plan of patients with brain tumor, we used a common deterministic tractography software for neurosurgical applications (iPlanNet 3.0, BrainLAB AG).

Language-positive stimulation spots were then imported and integrated into the deterministic tractography software using the DICOM standard. Via autosegmentation, the integrated spots were turned into individual objects and fused with DTI sequences, and the navigational T1-weighted, contrast-enhanced MRI. A 5-mm margin was added to the language-positive spots, which were then used as an ROI for the following DTI FT.

For anatomically based DTI FT, according to the cubic ROIs-based protocol, 3 cubic seed ROIs were placed along the opercular part of the inferior frontal gyrus, the inferior part of precentral gyrus, supramarginal gyrus, and the superior and medial temporal gyrus (Fig. 1). DTI FT was then performed using a minimum fiber length (MFL) of 50 mm and fractional anisotropy (FA) of 0.2; in case of poor results due to brain edema, the FA was changed to 0.15 (Fig. 2). Subsequently, the DTI FT results were analyzed and searched for visualizations of language-related fiber tracts known to be related to language processing: corticonuclear tract; arcuate fascicle; uncinate fascicle; superior longitudinal fascicle (SLF); inferior longitudinal fascicle; arcuate fibers (ArF); commissural fibers; corticothalamic fibers; frontooccipital fascicle.

Although the AF is part of the SLF, we chose to analyze them separately in this study, because impairment of the AF is highly associated with the presence of conduction aphasia. Therefore, the AF plays a major role in the surgical resection of the perisylvian space-occupying lesions of the left hemisphere.<sup>3,5,7,13</sup> The AF was defined as the part of the SLF connecting to the angular gyrus and the superior temporal gyrus.

Additionally, DTI FT was performed using 5 MFL and FA settings, which, according to a previous study, delivered the best results in visualization of language-related subcortical fibers (Negwer et al., unpublished data) (Fig. 3): MFL 70 mm, FA 0.2; MFL 80 mm, FA 0.15; MFL 90 mm, FA 0.15; MFL 100 mm, FA 0.1; and MFL 100 mm, FA 0.15. Furthermore, the number of visualized fibers for each performed DTI FT was noted.

### Statistical Analysis

Mean values  $\pm$  the standard deviation (SD), medians, minimum and maximum values, fibers per tract ratios,

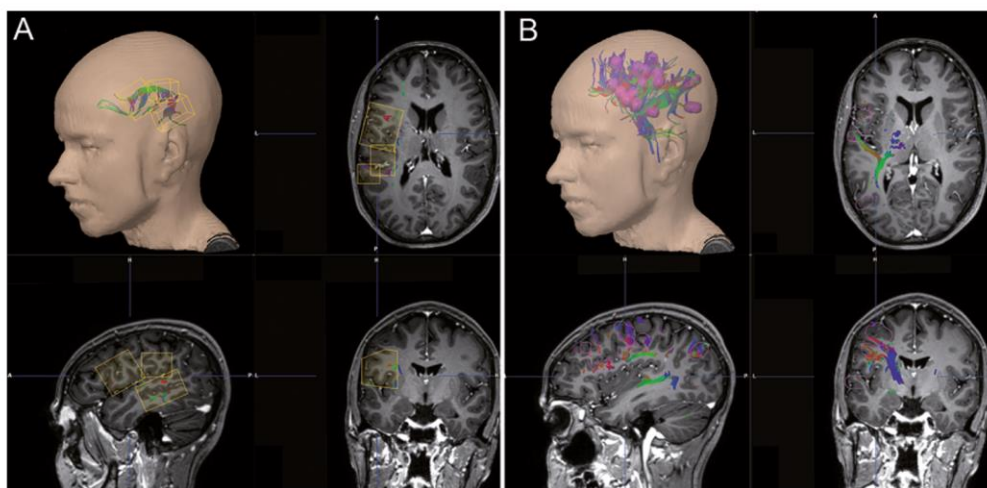
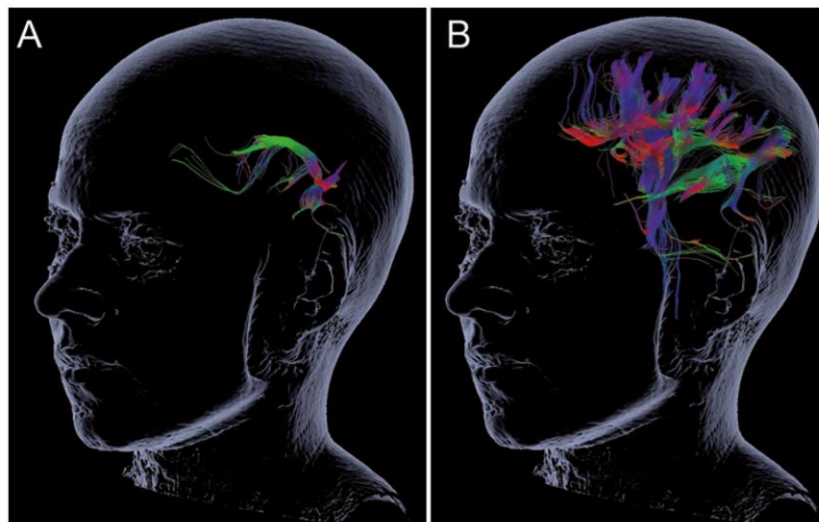


FIG. 1. Cubic ROIs seeding protocol and the nTMS-based approach. This figure shows screenshots of our tractography software (iPlanNet 3.0 Net server; BrainLAB). According the cubic ROIs-based protocol, 3 cubic ROIs were placed along the opercular part of the inferior frontal gyrus, the inferior part of the precentral gyrus, supramarginal gyrus, and superior and medial temporal gyrus (A). For our nTMS-based DTI FT, nTMS language-positive spots were imported (by DICOM standard) and then used as an ROI by enlarging the imported objects via an additional margin of 5 mm (B). Figure is available in color online only.



**FIG. 2.** Example of DTI FT using the cubic ROIs-based protocol and the nTMS-based protocol. Images show DTI FT performed on the same patient using the cubic ROIs-based protocol (A) and the nTMS-based DTI FT protocol (B). MFL and FA were set to 50 mm and 0.2, respectively, in both cases. Figure is available in color online only.

percentages of visualized language pathways, and subject-related characteristics were determined by using the GraphPad Prism software version 6.04 (GraphPad Software).

To evaluate variations between groups, the number of visualized fibers divided by the number of visualized fiber tracts (fibers/tract ratio) and the percentage of visualized language tracts out of the 9 above-outlined subcortical

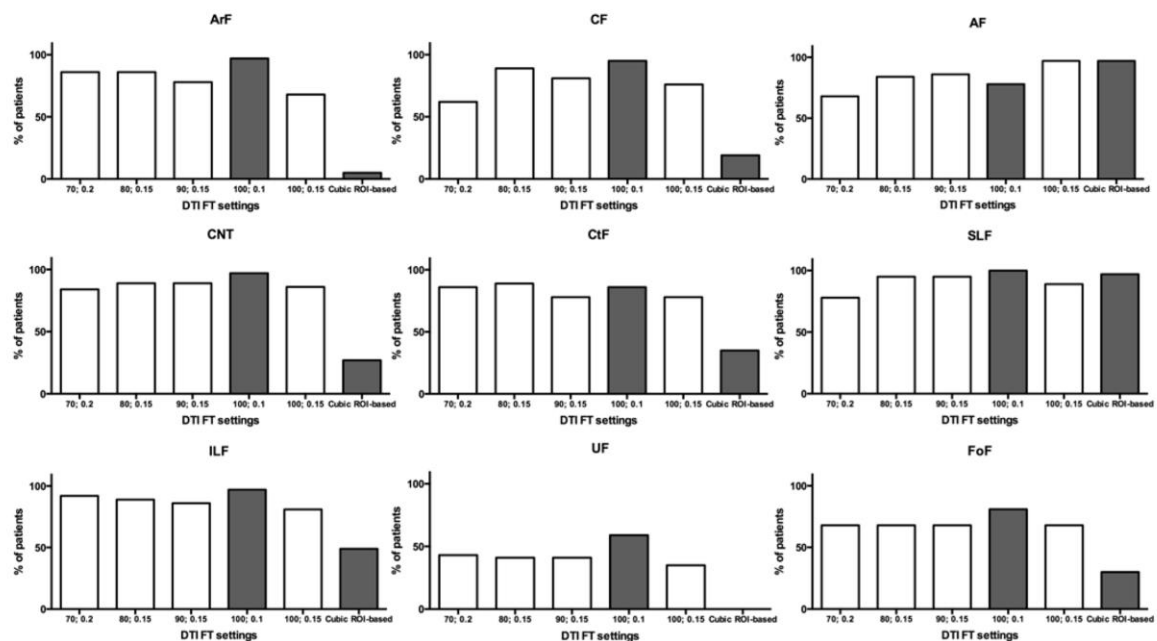


**FIG. 3.** Percentages of visualization for every individual subcortical language tract analyzed for the 5 most optimal nTMS-based DTI FT settings (MFL 70 mm, FA 0.2; MFL 80, FA 0.15; MFL 90 mm, FA 0.15; MFL 100 mm, FA 0.15; and MFL 100 mm, FA 0.1) for comparison with the cubic ROIs-based protocol. The 2 gray bars in each graph represent the results of the cubic ROIs-based protocol and the most optimal setting for nTMS-based DTI FT (MFL 100 mm; FA 0.1). CF = commissural fibers; CNT = corticonuclear tract; CtF = corticothalamic fibers; FoF = fronto-occipital fascicle; ILF = inferior longitudinal fascicle.

language tracts (percentage of tracts) were used. The fibers/tract ratio illustrates the fiber density; it is an index of DTI FT's visual portrayal and, thus, its specificity. The percentage of visualized subcortical language tracts was calculated to indicate the visualization sensitivity of the different language-related tracts via DTI FT. Additionally, Fisher's exact test was applied, measuring differences between the groups (Fig. 4). For all statistical calculations,  $p < 0.05$  was determined to be statistically significant.

## Results

### Subject and Mapping Characteristics

We enrolled 37 patients with left-sided perisylvian lesions (Table 1). Twenty-three patients were male (62.2%), and 14 were female (37.8%). Five patients (13.5%) had intracerebral vascular lesions (arteriovenous malformation, cavernoma, or hemangioblastoma), 2 had World Health Organization (WHO) Grade I astrocytoma (5.4%), 9 had WHO Grade II astrocytoma or oligoastrocytoma (24.3%), 5 had WHO Grade III astrocytoma or oligoastrocytoma (13.5%), and 16 had WHO Grade IV glioblastoma (43.3%). The median age was 39 years (range 19–65 years). Most patients had no preoperative language disorder ( $n = 23$ ; 62%), 7 patients (19%) had mild aphasia, and 6 (16%) had moderate aphasia. There was only 1 case (3%) of severe aphasia among the cohort (Table 1). To categorize the patient's aphasia, we used the previously published aphasia grading scale.<sup>35,41</sup>

Cortical language mapping by rTMS was well tolerated overall, and there were no adverse events reported during stimulation. The intensity during stimulation was  $103.0\% \pm 9.0\%$  RMT (range 80%–120% RMT), and the mean RMT was  $33.2\% \pm 7.9\%$  (range 21%–58%). Twenty-two patients (59.5%) received rTMS with 5 pulses of 5 Hz, 8 subjects (21.6%) received 5 pulses of 7 Hz, and 7 patients (18.9%) received 7 pulses of 7 Hz.

### DTI FT

Both protocols could be applied in every enrolled patient, and DTI FT was technically possible in all cases. Compared with the nTMS-based DTI FT, the cubic ROIs-based protocol had a better visualization of the AF (97.3% vs 75.7%;  $p < 0.05$ ) and of the SLF, although the latter was without statistical relevance (Table 2 and Fig. 4). For the other 7 subcortical language tracts, the nTMS-based protocol had superior results, which were statistically significant ( $p < 0.05$ ) for all of the language-related fiber tracts (Fig. 4). In particular, the shorter language tracts, such as ArFs or the uncinate fascicle (UF), were visualized more effectively using the nTMS-based approach ( $p < 0.001$ ). The UF was not detectable with the cubic ROIs-based protocol in any case (Table 2 and Fig. 4).

The fibers/tract ratio using nTMS-based DTI FT was  $236 \pm 73$ ; it was  $286 \pm 9$  using the cubic ROIs-based protocol (Table 2). These 2 values are comparable and both within the range we previously defined as ideal for a clear DTI FT result (fibers/tract 0–500; Negwer et al., unpublished data).

In addition, we performed nTMS-based DTI FT using the 5 most optimal settings and analyzed the respective percentage of visualization for the 9 subcortical language tracts (Fig. 3).

## Discussion

Besides demonstrating the reliable application of nTMS-based DTI FT for language pathways, the main goal of our study was to compare this new function-based approach to one of the best-known protocols for anatomically based DTI FT for subcortical language pathways.<sup>44</sup>

At this point, we want to emphasize that the cubic ROIs-based protocol was developed especially for SLF/AF DTI FT, so the direct comparison with our nTMS-based approach is imperfect on some points. The cubic ROIs-based

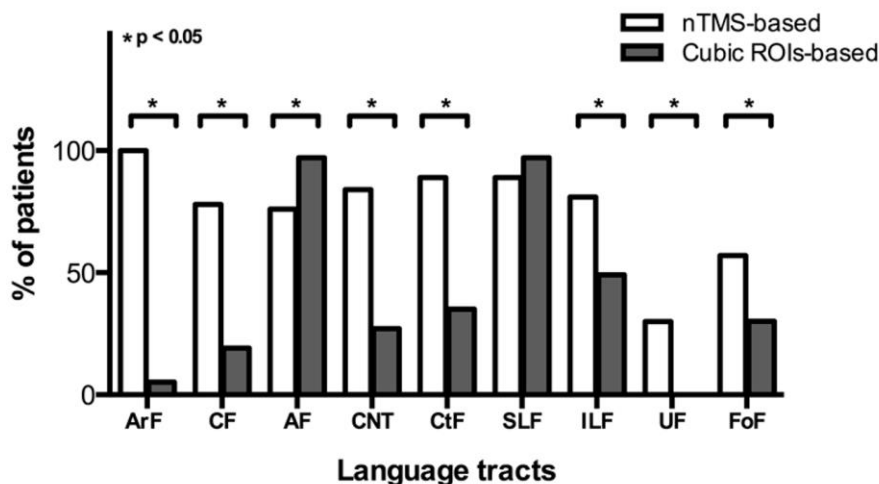


FIG. 4. Percentages of successful visualized language-related fiber tracts. The bar graph compares the visualized percentages of the 9 examined language-related fiber tracts using the cubic ROIs-based protocol (gray) and the nTMS-based protocol (white). A  $p$  value  $< 0.05$  was determined as statistically significant.

TABLE 1. Patient characteristics

Case No.	Sex	Age (yrs)	Tumor Type	Aphasia Grade*
1	F	50	GBM	1A
2	M	36	DA	0
3	M	30	GNT	0
4	M	25	aOA	1A/B
5	F	25	GC	0
6	M	62	GBM	0
7	M	46	GBM	1A
8	F	62	DA	1B
9	F	31	C	3A
10	M	42	OA	0
11	M	34	C	0
12	M	39	GBM	2B
13	M	33	GBM	0
14	F	26	AVM	0
15	F	26	DA	0
16	F	38	AA	0
17	M	51	GBM	2B
18	M	47	GBM	0
19	F	53	AVM	0
20	M	65	GBM	2A
21	F	25	DA	0
22	F	28	aOA	0
23	F	19	HB	0
24	F	47	GBM	2B
25	M	48	DA	0
26	F	43	DA	0
27	M	37	AA	0
28	M	52	GBM	1A
29	M	43	GBM	0
30	M	48	GBM	1B
31	M	26	GBM	0
32	M	38	aOA	0
33	M	27	OA	0
34	M	43	GBM	1A
35	M	23	DA	0
36	F	49	GBM	2A
37	M	48	GBM	2A/B

AA = anaplastic astrocytoma (WHO Grade III); aOA = oligoastrocytoma (WHO Grade III); AVM = arteriovenous malformation; C = cavernoma; DA = diffuse astrocytoma (WHO Grade II); GBM = glioblastoma (WHO Grade IV); GC = gangliocytoma (WHO Grade I); GNT = glioneuronal tumor (WHO Grade I); HB = hemangioblastoma (WHO Grade I); OA = diffuse oligoastrocytoma (WHO Grade II).

\* Aphasia grade: 0 = no aphasia; 1 = mild aphasia; 2 = moderate aphasia; 3 = severe aphasia; A = predominantly motor impairment; B = predominantly sensory impairment.

protocol was never meant for DTI FT of language-related subcortical fiber tracts aside from SLF/AF, so its application for other language-related fiber tracts should be considered experimental. However, this protocol is one of the first anatomically based approaches for tractography of

TABLE 2. Percentages of individually visualized fiber tracts, mean fibers per tract ratios, and mean percentages of all visualized tracts, by protocol\*

Tract	nTMS-Based Protocol (%)	Cubic ROIs-Based Protocol (%)
ArF	100	5.4
CF	78.4	18.9
AF	75.7	97.3
CNT	83.8	27
CtF	89.2	35.1
SLF	89.2	97.3
ILF	81.1	48.6
UF	29.7	0
FoF	56.8	29.7
All tracts	76	39.9
Fibers/tract ratio	236 ± 73	286 ± 9

AF = arcuate fascicle; ArF = arcuate fibers; CF = commissural fibers; CNT = corticonuclear tract; CtF = corticothalamic fibers; FoF = fronto-occipital fascicle; ILF = inferior longitudinal fascicle; SLF = superior longitudinal fascicle; UF = uncinata fascicle.

\* Minimum fiber length 50 mm, fractional anisotropy 0.2.

language-related white-matter tracts, and it has provided steady results, so an analysis of these 2 methods is certainly a subject of interest for scientific and clinical purposes.

As mentioned, there are 2 ways to place ROIs for the purpose of DTI FT. Function-based DTI FT, as the name suggests, uses functional data that can be provided by different examinations (fMRI, magnetoencephalography, nTMS), and anatomically based DTI FT relies on ROI seeding, using predefined anatomical landmarks. The biggest disadvantage of anatomically based DTI FT is that anatomy may be altered by the tumor mass and/or the surrounding edema; thus, even for a trained examiner, precise ROI seeding might be cumbersome.<sup>27,30,33</sup> Moreover, the results depend on the examiner's expertise and experience, so there is a high interobserver variability,<sup>8,47</sup> whereas a previous study analyzing interobserver differences in the application of anatomically and nTMS-based DTI FT for the CST showed significantly less interobserver variability for nTMS-based DTI FT.<sup>19</sup>

However, function-based DTI FT has its own limitations, which mainly depend on the reliability and accuracy of the chosen modality. For example, fMRI data, in particular the blood oxygenation-dependent signal, may be altered by tumor surrounding edemas and by changed oxygen levels, leading to inaccurate results.<sup>4,42</sup>

After providing promising and reliable data in previous studies, nTMS gained importance in neuroscience research and modern neurosurgery, showing good correlation with DCS results, and certainly still represents the gold standard for the detection of language-related brain areas.<sup>22,32,46</sup> Furthermore, the results of the application of nTMS-based DTI FT of the CST were promising and could be confirmed by intraoperative subcortical stimulation.<sup>10,16,19,49</sup> Recent reports analyzing nTMS-based DTI FT for language-related tracts also showed convincing results that correlated with clinical status.<sup>39</sup> Thus, nTMS-

based DTI FT has the potential to become a helpful tool for preoperative planning and intraoperative application in modern neurosurgery.

In this study, the results of the nTMS-based DTI FT protocol showed overall superior results to those of the anatomically based approach using cubic ROIs. The AF was more reliably visualized using the cubic ROIs-based protocol than using our nTMS-based DTI FT. However, if the results of our nTMS-based protocol are further analyzed using the 5 most optimal settings mentioned, the successful visualization of the AF was possible in up to 97.3% of the enrolled cohort (range 67.2%–97.3%) (Fig. 3). Therefore, this particular advantage of the cubic ROIs-based protocol can be discarded. Visualization of the SLF, using the cubic ROIs-based protocol, showed slightly better results, but these were without statistical significance (97.3% cubic ROIs-based protocol vs 89.2% nTMS-based protocol;  $p = 0.36$ ) (Table 2 and Fig. 4). When using an MFL of 100 mm and FA of 0.1 (1 of the 5 most optimal settings), the visualization increased to 100% for the nTMS-based approach (Fig. 3). To better compare the obtained results, we used the same MFL and FA settings as in the cubic ROIs-based protocol (MFL 50 mm; FA 0.2); these, however, do not correspond with the optimal settings for nTMS-based DTI FT for language-related subcortical fiber tracts (Negwer et al., unpublished data). Nevertheless, even with this suboptimal combination, our new protocol showed superior results. The cubic ROIs-based protocol did not allow constant visualization of the other analyzed subcortical fiber tracts, the UF was not detectable in any of the patients, and the ArF were only detectable in 5.4% of the patients (Table 2 and Fig. 4). The cubic ROIs were placed using anatomical landmarks along the expected fiber course of the AF/SLF, so the DTI FT of other subcortical fiber tracts in different anatomical regions was suboptimal, and sometimes impossible, as expected.

Reviewing the results, DTI FT, especially of the AF/SLF, is feasible and successful using the cubic ROIs-based protocol, keeping in mind that it was designed for this purpose. However, by using the 5 most optimal parameters, we achieved an improved visualization of the different subcortical fiber tracts using nTMS-based DTI FT compared with using the predefined settings (MFL 50; FA 0.2) of the ROIs-based protocol<sup>14</sup> (Fig. 3). The best results were seen using MFL of 100 mm and FA of 0.1, so this setting is recommended for optimal results.

From our point of view, it is essential to analyze the individual subcortical language pathways and their interrelations to further investigate language function and potential subcortical plasticity. For this purpose, our protocol seems to be an applicable tool, as it focuses on many subcortical fiber bundles and not just the major subcortical fiber tracts, such as the AF/SLF, with high percentage of visualization.

### Limitations

One major limitation of this technique is the challenge of reconstructing crossing fibers because the technique inhibits the identification of a voxel's primary eigenvector, thus impeding FT.<sup>2,19,25</sup> Furthermore, DTI FT, especially in patients with space-occupying lesions, can provide false-

negative and other inaccurate results in regions close to the lesion or edema, because of low anisotropy.<sup>2,19</sup>

As mentioned, previous studies have analyzed DTI FT using intraoperative subcortical stimulations and have provided promising results.<sup>1,24,26,29</sup> Furthermore, nTMS-based DTI FT of the CST could be validated using subcortical stimulation, encouraging new approaches in this field.<sup>10</sup>

In our study, we enhanced the TMS-positive spots by a rim of 5 mm because, rather than considering cortical language located in 1 spot, we prefer the theory of a language-positive area on the cortical surface. Certainly this approach is experimental, and it remains unclear in which dimension the enlargement affects the following DTI FT.

In this study, the nTMS-based protocol showed better results, especially in tracking a multitude of language-relevant white-matter tracts, as opposed to the anatomical-based approach. These results do not ensure the superiority of the protocol, because what is certainly more important than a higher number of tracked fibers is the question of their functionality.

Until now, there have been no studies examining the correlation of nTMS-based DTI FT for subcortical language tracts, so it remains unclear whether the provided results can be objectified by subcortical stimulation. Thus, this should be the next step in future studies.

### Conclusions

This study demonstrates the feasibility of nTMS-based DTI FT and its superiority to the cubic ROIs-based DTI FT approach, with the exception of AF. These results are encouraging and could further accelerate the spread of nTMS-based DTI FT, which is a reasonable and standardized approach for the visualization of language-related white-matter tracts.

Besides its scientific applications, nTMS-based DTI FT also seems to be feasible for clinical use, especially for preoperative planning in patients with brain tumor. However, these results need to be validated by intraoperative subcortical stimulation in future studies prior to routine clinical use.

### References

- Bello L, Gambini A, Castellano A, Carrabba G, Acerbi F, Fava E, et al: Motor and language DTI Fiber Tracking combined with intraoperative subcortical mapping for surgical removal of gliomas. *Neuroimage* **39**:369–382, 2008
- Berman JI, Berger MS, Chung SW, Nagarajan SS, Henry RG: Accuracy of diffusion tensor magnetic resonance imaging tractography assessed using intraoperative subcortical stimulation mapping and magnetic source imaging. *J Neurosurg* **107**:488–494, 2007
- Bernal B, Ardila A: The role of the arcuate fasciculus in conduction aphasia. *Brain* **132**:2309–2316, 2009
- Binder JR: Functional MRI is a valid noninvasive alternative to Wada testing. *Epilepsy Behav* **20**:214–222, 2011
- Breier JI, Hasan KM, Zhang W, Men D, Papanicolaou AC: Language dysfunction after stroke and damage to white matter tracts evaluated using diffusion tensor imaging. *AJNR Am J Neuroradiol* **29**:483–487, 2008
- Capelle L, Fontaine D, Mandonnet E, Taillandier L, Golmard JL, Bauchet L, et al: Spontaneous and therapeutic prognostic factors in adult hemispheric World Health Organization

- Grade II gliomas: a series of 1097 cases: clinical article. **J Neurosurg** **118**:1157–1168, 2013
7. Catani M, Mesulam M: The arcuate fasciculus and the disconnection theme in language and aphasia: history and current state. **Cortex** **44**:953–961, 2008
  8. Catani M, Thiebaut de Schotten M: A diffusion tensor imaging tractography atlas for virtual in vivo dissections. **Cortex** **44**:1105–1132, 2008
  9. Chan-Seng E, Moritz-Gasser S, Duffau H: Awake mapping for low-grade gliomas involving the left sagittal stratum: anatomofunctional and surgical considerations. **J Neurosurg** **120**:1069–1077, 2014
  10. Conti A, Raffa G, Granata F, Rizzo V, Germanò A, Tomasello F: Navigated transcranial magnetic stimulation for “somatotopic” tractography of the corticospinal tract. **Neurosurgery** **10** (Suppl 4):542–554, 2014
  11. Corina DP, Loudermilk BC, Detwiler L, Martin RF, Brinkley JF, Ojemann G: Analysis of naming errors during cortical stimulation mapping: implications for models of language representation. **Brain Lang** **115**:101–112, 2010
  12. Duffau H: Surgical neurooncology is a brain networks surgery: a “connectomic” perspective. **World Neurosurg** **82**:e405–e407, 2014
  13. Duffau H, Capelle L, Sichez N, Denvil D, Lopes M, Sichez JP, et al: Intraoperative mapping of the subcortical language pathways using direct stimulations. An anatomic-functional study. **Brain** **125**:199–214, 2002
  14. Duffau H, Moritz-Gasser S, Mandonnet E: A re-examination of neural basis of language processing: proposal of a dynamic hodotopical model from data provided by brain stimulation mapping during picture naming. **Brain Lang** **131**:1–10, 2014
  15. Epstein CM, Lah JJ, Meador K, Weissman JD, Gaitan LE, Dihenia B: Optimum stimulus parameters for lateralized suppression of speech with magnetic brain stimulation. **Neurology** **47**:1590–1593, 1996
  16. Frey D, Strack V, Wiener E, Jussen D, Vajkoczy P, Picht T: A new approach for corticospinal tract reconstruction based on navigated transcranial stimulation and standardized fractional anisotropy values. **Neuroimage** **62**:1600–1609, 2012
  17. Indefrey P: The spatial and temporal signatures of word production components: a critical update. **Front Psychol** **2**:255, 2011
  18. Ius T, Angelini E, Thiebaut de Schotten M, Mandonnet E, Duffau H: Evidence for potentials and limitations of brain plasticity using an atlas of functional resectability of WHO grade II gliomas: towards a “minimal common brain.” **Neuroimage** **56**:992–1000, 2011
  19. Krieg SM, Buchmann NH, Gempt J, Shiban E, Meyer B, Ringel F: Diffusion tensor imaging fiber tracking using navigated brain stimulation—a feasibility study. **Acta Neurochir (Wien)** **154**:555–563, 2012
  20. Krieg SM, Shiban E, Buchmann N, Gempt J, Foerschler A, Meyer B, et al: Utility of presurgical navigated transcranial magnetic brain stimulation for the resection of tumors in eloquent motor areas. **J Neurosurg** **116**:994–1001, 2012
  21. Krieg SM, Sollmann N, Hauck T, Ille S, Foerschler A, Meyer B, et al: Functional language shift to the right hemisphere in patients with language-eloquent brain tumors. **PLoS One** **8**:e75403, 2013
  22. Krieg SM, Sollmann N, Hauck T, Ille S, Meyer B, Ringel F: Repeated mapping of cortical language sites by preoperative navigated transcranial magnetic stimulation compared to repeated intraoperative DCS mapping in awake craniotomy. **BMC Neurosci** **15**:20, 2014
  23. Krieg SM, Tarapore PE, Picht T, Tanigawa N, Houde J, Sollmann N, et al: Optimal timing of pulse onset for language mapping with navigated repetitive transcranial magnetic stimulation. **Neuroimage** **100**:219–236, 2014
  24. Kuhnt D, Bauer MH, Becker A, Merhof D, Zolal A, Richter M, et al: Intraoperative visualization of fiber tracking based reconstruction of language pathways in glioma surgery. **Neurosurgery** **70**:911–920, 2012
  25. Le Bihan D, Poupon C, Amadon A, Lethimonnier F: Artifacts and pitfalls in diffusion MRI. **J Magn Reson Imaging** **24**:478–488, 2006
  26. Leclercq D, Duffau H, Delmaire C, Capelle L, Gatignol P, Ducros M, et al: Comparison of diffusion tensor imaging tractography of language tracts and intraoperative subcortical stimulations. **J Neurosurg** **112**:503–511, 2010
  27. Lehericy S, Duffau H, Cornu P, Capelle L, Pidoux B, Carpentier A, et al: Correspondence between functional magnetic resonance imaging somatotopy and individual brain anatomy of the central region: comparison with intraoperative stimulation in patients with brain tumors. **J Neurosurg** **92**:589–598, 2000
  28. Lioumis P, Zhdanov A, Mäkelä N, Lehtinen H, Wilenius J, Neuvonen T, et al: A novel approach for documenting naming errors induced by navigated transcranial magnetic stimulation. **J Neurosci Methods** **204**:349–354, 2012
  29. Nimsky C, Ganslandt O, Hastreiter P, Wang R, Benner T, Sorensen AG, et al: Preoperative and intraoperative diffusion tensor imaging-based fiber tracking in glioma surgery. **Neurosurgery** **61** (1 Suppl):178–186, 2007
  30. Nimsky C, Ganslandt O, Merhof D, Sorensen AG, Fahlbusch R: Intraoperative visualization of the pyramidal tract by diffusion-tensor-imaging-based fiber tracking. **Neuroimage** **30**:1219–1229, 2006
  31. Pascual-Leone A, Gates JR, Dhuna A: Induction of speech arrest and counting errors with rapid-rate transcranial magnetic stimulation. **Neurology** **41**:697–702, 1991
  32. Picht T, Krieg SM, Sollmann N, Rösler J, Niraula B, Neuvonen T, et al: A comparison of language mapping by preoperative navigated transcranial magnetic stimulation and direct cortical stimulation during awake surgery. **Neurosurgery** **72**:808–819, 2013
  33. Robles SG, Gatignol P, Lehericy S, Duffau H: Long-term brain plasticity allowing a multistage surgical approach to World Health Organization Grade II gliomas in eloquent areas. **J Neurosurg** **109**:615–624, 2008
  34. Rogić M, Deletis V, Fernández-Conejero I: Inducing transient language disruptions by mapping of Broca’s area with modified patterned repetitive transcranial magnetic stimulation protocol. **J Neurosurg** **120**:1033–1041, 2014
  35. Rösler J, Niraula B, Strack V, Zdunczyk A, Schilt S, Savolainen P, et al: Language mapping in healthy volunteers and brain tumor patients with a novel navigated TMS system: evidence of tumor-induced plasticity. **Clin Neurophysiol** **125**:526–536, 2014
  36. Salmelin R, Helenius P, Service E: Neurophysiology of fluent and impaired reading: a magnetoencephalographic approach. **J Clin Neurophysiol** **17**:163–174, 2000
  37. Sanai N, Berger MS: Glioma extent of resection and its impact on patient outcome. **Neurosurgery** **62**:753–764, 264–266, 2008
  38. Smith JS, Chang EF, Lamborn KR, Chang SM, Prados MD, Cha S, et al: Role of extent of resection in the long-term outcome of low-grade hemispheric gliomas. **J Clin Oncol** **26**:1338–1345, 2008
  39. Sollmann N, Giglhuber K, Tussis L, Meyer B, Ringel F, Krieg SM: nTMS-based DTI fiber tracking for language pathways correlates with language function and aphasia – a case report. **Clin Neurol Neurosurg** **136**:25–28, 2015
  40. Sollmann N, Hauck T, Hapfelmeier A, Meyer B, Ringel F, Krieg SM: Intra- and interobserver variability of language mapping by navigated transcranial magnetic brain stimulation. **BMC Neurosci** **14**:150, 2013
  41. Sollmann N, Ille S, Hauck T, Maurer S, Negwer C, Zimmer C, et al: The impact of preoperative language mapping by

- repetitive navigated transcranial magnetic stimulation on the clinical course of brain tumor patients. **BMC Cancer** 15:261, 2015
42. Sollmann N, Picht T, Mäkelä JP, Meyer B, Ringel F, Krieg SM: Navigated transcranial magnetic stimulation for preoperative language mapping in a patient with a left frontoopercular glioblastoma. **J Neurosurg** 118:175–179, 2013
  43. Sollmann N, Tanigawa N, Ringel F, Zimmer C, Meyer B, Krieg SM: Language and its right-hemispheric distribution in healthy brains: an investigation by repetitive transcranial magnetic stimulation. **Neuroimage** 102:776–788, 2014
  44. Henning Stieglitz L, Seidel K, Wiest R, Beck J, Raabe A: Localization of primary language areas by arcuate fascicle fiber tracking. **Neurosurgery** 70:56–65, 2012
  45. Stummer W, Reulen HJ, Meinel T, Pichlmeier U, Schumacher W, Tonn JC, et al: Extent of resection and survival in glioblastoma multiforme: identification of and adjustment for bias. **Neurosurgery** 62:564–576, 2008
  46. Tarapore PE, Findlay AM, Honma SM, Mizuiri D, Houde JF, Berger MS, et al: Language mapping with navigated repetitive TMS: proof of technique and validation. **Neuroimage** 82:260–272, 2013
  47. Wakana S, Jiang H, Nagae-Poetscher LM, van Zijl PC, Mori S: Fiber tract-based atlas of human white matter anatomy. **Radiology** 230:77–87, 2004
  48. Wassermann EM, Blaxton TA, Hoffman EA, Berry CD, Oletsky H, Pascual-Leone A, et al: Repetitive transcranial magnetic stimulation of the dominant hemisphere can disrupt visual naming in temporal lobe epilepsy patients. **Neuropsychologia** 37:537–544, 1999
  49. Weiss C, Tursunova I, Neuschmelting V, Lockau H, Netekoven C, Oros-Peusquens AM, et al: Improved nTMS- and DTI-derived CST tractography through anatomical ROI seeding on anterior pontine level compared to internal capsule. **Neuroimage Clin** 7:424–437, 2015
  50. Wheat KL, Cornelissen PL, Sack AT, Schuhmann T, Goebel R, Blomert L: Charting the functional relevance of Broca's area for visual word recognition and picture naming in Dutch using fMRI-guided TMS. **Brain Lang** 125:223–230, 2013

---

#### Disclosure

Dr. Krieg is a consultant for BrainLAB and Nexstim. Drs. Krieg and Ringel are consultants for BrainLAB AG. The study was completely financed by institutional grants from the Department of Neurosurgery and the Section of Neuroradiology, Technical University of Munich.

#### Author Contributions

Conception and design: Krieg. Acquisition of data: Negwer, Sollmann, Ille, Hauck, Maurer, Kirschke. Analysis and interpretation of data: Negwer. Drafting the article: Krieg, Negwer. Critically revising the article: Krieg, Kirschke. Reviewed submitted version of manuscript: Krieg, Sollmann, Ille, Hauck, Maurer, Ringel, Meyer. Approved the final version of the manuscript on behalf of all authors: Krieg. Statistical analysis: Krieg, Negwer. Administrative/technical/material support: Krieg, Ringel, Meyer. Study supervision: Krieg, Ringel, Meyer.

#### Correspondence

Sandro M. Krieg, Department of Neurosurgery, Klinikum rechts der Isar, Technische Universität München, Ismaninger Str. 22, Munich 81675, Germany. email: sandro.krieg@tum.de.

# 11.3. Interhemispheric connectivity revealed by diffusion tensor imaging fiber tracking derived from navigated transcranial magnetic stimulation maps as a sign of language function at risk in patients with brain tumors

## Interhemispheric connectivity revealed by diffusion tensor imaging fiber tracking derived from navigated transcranial magnetic stimulation maps as a sign of language function at risk in patients with brain tumors

\*Nico Sollmann, MD,<sup>1,2</sup> Chiara Negwer, MD,<sup>1,2</sup> Lorena Tussis, BSc,<sup>1,2</sup> Theresa Hauck,<sup>1,2</sup> Sebastian Ille, MD,<sup>1,2</sup> Stefanie Maurer,<sup>1,2</sup> Katrin Gighlhuber,<sup>1,2</sup> Jan S. Bauer, MD,<sup>3</sup> Florian Ringel, MD,<sup>1</sup> Bernhard Meyer, MD,<sup>1</sup> and Sandro M. Krieg, MD, MBA<sup>1,2</sup>

<sup>1</sup>Department of Neurosurgery, <sup>2</sup>TUM-Neuroimaging Center, and <sup>3</sup>Section of Neuroradiology, Department of Radiology, Klinikum rechts der Isar, Technische Universität München, Germany

**OBJECTIVE** Resection of brain tumors in language-eloquent areas entails the risk of postoperative aphasia. It has been demonstrated via navigated transcranial magnetic stimulation (nTMS) that language function can partially shift to the unaffected hemisphere due to tumor-induced plasticity. Therefore, this study was designed to evaluate whether interhemispheric connectivity (IC) detected by nTMS-based diffusion tensor imaging–fiber tracking (DTI-FT) can be used to predict surgery-related aphasia in patients with brain tumors.

**METHODS** Thirty-eight patients with left-sided perisylvian brain lesions underwent cortical language mapping of both hemispheres by nTMS prior to awake surgery. Then, nTMS-based DTI-FT was conducted with a fractional anisotropy (FA) of 0.01 and 0.2 to visualize nTMS-based IC. Receiver operating characteristics were calculated for the prediction of a postoperative (irrespective of the preoperative state) and a new surgery-related aphasia by the presence of detectable IC.

**RESULTS** Language mapping by nTMS was possible in all patients. Seventeen patients (44.7%) suffered from surgery-related worsening of language performance (transient aphasia according to 3-month follow-up in 16 subjects [42.1%]; new permanent aphasia according to 3-month follow-up in 1 patient [2.6%]). Regarding the correlation of aphasia to nTMS-based IC, statistically significant differences were revealed for both evaluated FA values. However, better results were observed for tractography with an FA of 0.2, which led to a specificity of 93% (postoperative aphasia) and 90% (surgery-related aphasia). For postoperative aphasia, the corresponding OR was 0.1282 (95% CI 0.0143–1.1520), and for surgery-related aphasia the OR was 0.1184 (95% CI 0.0208–0.6754).

**CONCLUSIONS** According to these results, IC detected by preoperative nTMS-based DTI-FT might be regarded as a risk factor for surgery-related aphasia, with a specificity of up to 93%. However, because the majority of enrolled patients suffered from transient aphasia postoperatively, it has to be evaluated whether this approach distinctly leads to similar results among patients with permanent language deficits. Despite this restriction, this approach might contribute to individualized patient consultation prior to tumor resection in clinical practice.

<http://thejns.org/doi/abs/10.3171/2016.1.JNS152053>

**KEY WORDS** aphasia; brain tumor; diffusion tensor imaging; fiber tracking; interhemispheric connectivity; transcranial magnetic stimulation; oncology

**ABBREVIATIONS** CC = corpus callosum; DCS = direct cortical stimulation; DTI = diffusion tensor imaging; EHI = Edinburgh Handedness Inventory; FA = fractional anisotropy; fMRI = functional MRI; FN = false-negative; FP = false-positive; FT = fiber tracking; IC = interhemispheric connectivity; NPV = negative predictive value; nTMS = navigated transcranial magnetic stimulation; O1 = first object, O2 = second object; PPV = positive predictive value; PTI = picture-to-trigger interval; RMT = resting motor threshold; ROC = receiver operating characteristic; ROI = region of interest; TN = true-negative; TP = true-positive.

**SUBMITTED** August 31, 2015. **ACCEPTED** January 14, 2016.

**INCLUDE WHEN CITING** Published online April 1, 2016; DOI: 10.3171/2016.1.JNS152053.

\* Drs. Sollmann and Negwer contributed equally to this work.

**T**HE resection of brain tumors that are located within so-called eloquent areas entails the inherent risk of causing a functional deficit that reduces the patient's quality of life. Regarding tumors that are located within language-eloquent brain regions, the risk of surgery-related aphasia is one of the main factors that can limit the overall extent of resection significantly and therefore has to be considered during patient counseling. To achieve a reasonable balance between resection and preservation of neurological function, the application of pre- and intraoperative neuroimaging and mapping methods is essential.<sup>7,9,10,46</sup> Regarding mapping of human language, navigated transcranial magnetic stimulation (nTMS) has already proven to be a helpful and reliable tool that correlates well with direct cortical stimulation (DCS), the gold standard in terms of functional mapping.<sup>21,36,37,56</sup> Furthermore, the use of nTMS mapping data for diffusion tensor imaging–fiber tracking (DTI-FT) principally allows for the detection of subcortical language-related pathways.<sup>50</sup> In this context, nTMS-based DTI-FT represents a combination of functional and structural neuroimaging that is able to provide individualized information on cortical and subcortical functional anatomy.

These data can be used during surgery by implementation in the neuronavigation; they can also be used to evaluate patients by visualizing their individual functional anatomy in the vicinity of the tumor. Yet, these data could also be of value to allow for the assessment of patients' risk for surgery-related aphasia in surgical decision making. In this context, various studies have already investigated language reorganization within the human brain due to intracranial pathologies, and language plasticity was reported to occur as a partial shift of language function to the unaffected hemisphere.<sup>3,6,20,42,60</sup> Such a compensatory shift between hemispheres has to be mediated somehow, and it seems obvious that the corpus callosum (CC), which represents interhemispheric connectivity (IC) as the largest white matter structure that connects homologous and nonhomologous brain regions,<sup>13,14,58</sup> might play a crucial role in this context. Indeed, there are initial studies using functional MRI (fMRI) available that report on enhanced IC both in the context of motor and language compensation mechanisms,<sup>31,39</sup> which underlines the presumable involvement and modulation of IC in the context of plastic brain reshaping due to intracranial pathologies in general.

Additionally, there is evidence specifically derived from recent nTMS trials showing that language function can partially shift to the unaffected hemisphere during the course of tumor-induced plasticity,<sup>20,42</sup> indicating that the healthy hemisphere seems to be able to partially take over language function from its impaired homolog, most likely emerging from the attempt to compensate for a potential loss of function. Thus, IC detected by nTMS could be an essential factor that might be altered in the course of such an interhemispheric shift. If so, preoperative assessment of nTMS-based IC would allow for functional evaluation and surgical risk stratification in the individual patient. Thus, the present study was designed to evaluate whether IC detected by nTMS-based DTI-FT correlates with surgery-related aphasia in patients undergoing left-sided perisylvian brain tumor resection during awake surgery.

## Methods

### Ethics Considerations

The present study was approved by the local institutional review board and was conducted in accordance with the Declaration of Helsinki. Written informed consent was obtained from all patients.

### Patient Selection

Overall, 38 patients were enrolled in the present investigation between 2011 and 2014. Patients were eligible for participation if they were over 18 years old and were diagnosed with a tumor localized within perisylvian areas of the left hemisphere (i.e., classic language-eloquent regions). Exclusion criteria were general nTMS exclusion criteria (e.g., the presence of a cochlear implant or cardiac pacemaker). In addition, patients with severe aphasia that did not allow for nTMS language mapping were not included.

### Study Design

All patients underwent MRI, preoperative repetitive nTMS for cortical language mapping of the left and right hemispheres, and nTMS-based DTI-FT. Tumor resection was performed during awake surgery including intraoperative neuronavigation, intraoperative DCS, and subcortical language mapping.<sup>21,35,36,47,55</sup> Aphasia was assessed during the preoperative, postoperative (on the 5th postoperative day), and follow-up examinations (3 months after surgery) using a modified grading scale as published earlier (0 = no aphasia, 1 = mild aphasia, 2 = moderate aphasia, 3 = severe aphasia, A = nonfluent aphasia, and B = fluent aphasia).<sup>21,52</sup> Postoperative aphasia was defined as any grade of language impairment at the 5th postoperative day, regardless of preoperative language function. Surgery-related aphasia was defined as any change in language performance when comparing pre- and postoperative language function (Table 1). All aphasia grading was done by a medical doctor with neurosurgical training.

### Imaging Parameters

Scanning was conducted with a 3-T MR scanner (Achieva 3T, Philips Medical Systems) through the use of an 8-channel phased-array head coil. Imaging included a T2-weighted FLAIR (TR/TE 12,000/140 msec, voxel size  $0.9 \times 0.9 \times 4 \text{ mm}^3$ , acquisition time 3 min) and a 3D T1-weighted gradient echo sequence (TR/TE 9/4 msec,  $1 \text{ mm}^3$  isovoxel covering the whole head, acquisition time 6 min 58 sec) with and without intravenous application of gadopentetate dimeglumine (Magnograf, Marotrust GmbH) for contrast enhancement. Furthermore, DTI sequences were acquired with 6 (TR/TE 7571/55 msec, spatial resolution of  $2 \times 2 \times 2 \text{ mm}^3$ , b-values of 0 and 800, acquisition time 2 min 15 sec) or 15 (TR/TE 10,737/55 msec, spatial resolution of  $2 \times 2 \times 2 \text{ mm}^3$ , b-values of 0 and 800, acquisition time 6 min 26 sec) orthogonal diffusion directions.

In each subject, motion artifacts of the acquired DTI data were adjusted using the software of the MR scanner. The contrast-enhanced 3D gradient echo sequences and

TABLE 1. Characteristics of 38 patients with brain tumors\*

Case No.	Sex	Age, Yrs	Entity†	EOR	Aphasia‡			nTMS				DTI-FT (FA = 0.01)		DTI-FT (FA = 0.2)	
					Preop	Postop	FU	RMT LH, %	RMT RH, %	Int, % RMT	Freq, Hz/Pulses	IC	No. of Fibers	IC	No. of Fibers
1	M	65	GBM	GTR	2A	1A	1A	33	33	110	5/5				
2	M	27	GBM	GTR	0	0	0	35	22	100	7/5				
3	M	24	Astrocytoma II	GTR	1A	1A	1A	33	35	100	5/5				
4	M	49	GBM	GTR	2AB	1AB	0	32	32	100	7/5				
5	M	39	Astrocytoma III	STR	0	0	0	33	33	100	7/7				
6	M	31	Astrocytoma I	GTR	0	0	0	29	29	110	7/7				
7	M	38	Astrocytoma III	STR	0	1A	0	23	23	110	7/5	X	90		
8	M	47	GBM	STR	1A	0	0	25	25	120	5/5				
9	F	26	Astrocytoma II	STR	0	0	0	27	27	120	7/5				
10	M	49	GBM	STR	1B	2B	1B	29	29	100	7/5				
11	M	49	Astrocytoma II	STR	0	1B	0	46	46	100	7/5	X	1		
12	F	27	AVM	GTR	0	1A	0	36	32	100	5/5				
13	M	43	Astrocytoma II	STR	0	2A	0	21	21	100	5/5				
14	M	47	GBM	GTR	0	0	0	30	30	110	5/5				
15	F	32	AVM	GTR	3A	0	0	33	33	100	7/7	X	3		
16	M	53	GBM	GTR	1A	2A	1A	41	41	100	5/5	X	12		
17	M	33	GBM	GTR	0	3A	0	37	37	100	5/5				
18	F	63	Astrocytoma II	STR	1B	2B	1B	36	36	120	7/7	X	237	X	165
19	M	34	AVM	GTR	0	0	0	43	43	120	5/5				
20	M	40	GBM	STR	2B	0	0	39	39	120	5/5				
21	M	51	GBM	STR	2B	2B	2B	25	25	100	7/7	X	1		
22	M	43	GBM	GTR	1A	1A	1A	58	58	80	5/5	X	1		
23	F	43	Astrocytoma II	GTR	0	0	0	34	34	100	7/5				
24	M	37	Astrocytoma II	STR	0	1A	0	37	37	100	5/5				
25	F	26	Astrocytoma I	GTR	0	1AB	0	21	21	120	7/7	X	50	X	31
26	M	28	Astrocytoma II	STR	0	2AB	1AB	42	42	100	5/5	X	3	X	2
27	M	25	Astrocytoma III	GTR	1AB	2AB	1AB	43	43	100	5/5	X	2	X	2
28	F	20	AVM	GTR	0	0	0	27	27	100	5/5				
29	F	38	Astrocytoma III	STR	0	1B	0	26	26	100	5/5	X	1217	X	184
30	M	43	GBM	STR	0	0	0	30	30	100	5/5				
31	F	26	Astrocytoma II	GTR	0	1A	0	35	30	100	5/5				
32	M	74	GBM	GTR	0	1A	0	28	22	100	5/5	X	42	X	14
33	F	34	Astrocytoma III	GTR	0	1A	0	35	33	100	5/5	X	533	X	264
34	F	51	GBM	GTR	2A	1A	1A	27	27	110	7/7				
35	F	50	Metastasis	STR	2A	2A	2A	35	31	100	7/7				

CONTINUED ON PAGE 4 »

» CONTINUED FROM PAGE 3  
**TABLE 1. Characteristics of 38 patients with brain tumors\***

Case No.	Sex	Age, Yrs	Entity†	EOR	Aphasia‡			nTMS			DTI-FT (FA = 0.01)		DTI-FT (FA = 0.2)		
					Preop	Postop	FU	RMT LH, %	RMT RH, %	Int, % RMT	Freq, Hz/Pulses	IC	No. of Fibers	IC	No. of Fibers
36	M	70	GBM	STR	2AB	1AB	1AB	33	33	100	7/7	X	701	X	55
37	M	31	AVM	GTR	0	1B	0	29	33	100	5/5	X	1015	X	332
38	M	35	AVM	GTR	0	0	0	35	35	100	5/5	X	260	X	61

AVM = arteriovenous malformation; EOR = extent of resection; Freq = mapping frequency; FU = grading during follow-up 3 months after surgery; GBM = glioblastoma multiforme; GTR = gross-total resection; Int = mapping intensity as a percentage of the RMT; LH = left hemisphere; Postop = grading on the 5th postoperative day; Preop = preoperative grading; RH = right hemisphere; STR = subtotal resection.  
 \* Overview of subject-related characteristics including sex, age (in years), tumor entity, extent of resection, and aphasia gradings. Postoperative aphasia was defined as any grade of language impairment at the 5th postoperative day, regardless of preoperative language function. Surgery-related aphasia was defined as any change in language performance when comparing pre- and postoperative language function. In addition, nTMS mapping parameters (RMT for the left and right hemisphere; mapping intensity as a percentage of the RMT; mapping frequency) and DTI-FT results (detectability of nTMS-based IC; number of nTMS-based IC fibers) for tractography with FA values of 0.01 and 0.2 are shown.  
 † Roman numeral = WHO grade.  
 ‡ 0 = no, 1 = mild, 2 = moderate, 3 = severe, A = nonfluent, and B = fluent aphasia.

DTI sequences were transferred to the Nexstim eXimia NBS system (version 3.2.2 or version 4.3, Nexstim Oy) and to a Brainlab iPlan Net server (version 3.0.1, Brainlab AG).

**Navigated Transcranial Magnetic Stimulation**

Language mapping of both hemispheres was performed with the eXimia NBS system, version 3.2.2 or 4.3, in combination with a NEXSPEECH module (Nexstim Oy). First, a contrast-enhanced 3D gradient echo sequence of the patient was uploaded to the system's software because it was needed for individualized neuronavigation. The head position of each patient was then tracked by reflectors fastened to the head with an elastic strap and an infrared tracking camera (Polaris Spectra). Moreover, the coil position was followed by reflectors fixed to the back side of the magnetic coil. This setup allowed for controlled coil movement and coil detection during nTMS.<sup>24,44</sup> In this context, the current approach for nTMS language-mapping trials has been repeatedly described.<sup>15,22,23,30,41,42,54,56</sup>

Briefly, the resting motor threshold (RMT) was first determined to be able to individually adjust the stimulation intensity during language mapping. Muscle electrodes (Neuroline 720, Ambu) were placed over the abductor pollicis brevis muscle. We identified the most excitable spot in the precentral gyrus to assess the exact RMT value, which is commonly defined as the lowest stimulation intensity that elicits motor evoked potentials greater than 50 µV in amplitude in 50% of stimulation trials.<sup>43</sup> We determined the RMT separately for each hemisphere because both hemispheres were examined.

During language mapping, the patients were instructed to name everyday objects as quickly and precisely as possible.<sup>22,30,42,54</sup> The objects were displayed on a screen and the assortment was similar to the objects of Snodgrass and Vanderwart.<sup>49</sup> Initially, the subjects had to perform the object-naming task twice without stimulation, and objects that were misnamed or did not elicit clear responses were discarded.<sup>22,30,42,54</sup> The remaining objects constituted the baseline and were used in the mapping session, and they were presented in randomized order during stimulation. If a patient was not able to sufficiently perform baseline testing due to aphasia or incomppliance according to the evaluation of the examiner and at least 1 medical doctor with profound nTMS experience, he or she was excluded from the present study.

Each mapping was performed according to a protocol that has proven to be reliable in recent nTMS investigations.<sup>21,22,30,36,51,54,56</sup> The nTMS pulses were applied time-locked to the objects (display time 700 msec, interpicture interval 2500 msec), and the picture-to-trigger interval (PTI) was 300 msec in the first 10 patients and 0 msec in the remaining 28 patients. There is evidence for both PTIs,<sup>17,41,45,62</sup> but we decided to switch to 0 msec with regard to a recent evaluation of the advantages of 0 msec for nTMS language mapping when compared with awake mapping.<sup>23</sup> Both hemispheres were examined in consecutive order, and each stimulation target was stimulated 3 times before moving the coil to the next stimulation spot during the interpicture interval. A video camera recorded both the baseline testing and the language mapping for later offline analysis.<sup>22,30,42,54</sup>

The stimulation videos were systematically searched for naming errors by comparing them to the corresponding baseline recordings as described previously.<sup>15,22,30,36,54</sup> This was done by at least 1 experienced and trained investigator, and a linguist was available for support in unclear cases. All detected naming errors were classified as no-response errors (complete lack of naming response), performance errors (articulatory or language production errors), neologisms (production of nonexistent words), phonological paraphasias (unintended phonemic modification of the target word), or semantic paraphasias (substitution of a semantically related word for the target word). These error categories are most frequently used during nTMS analyses and have been described precisely in recent publications.<sup>22,30,42,54</sup> Each stimulation point at which a naming error of 1 of these categories was elicited was defined as a language-positive spot.

After analysis of nTMS mapping data, we transferred all left- and right-sided language-positive spots to an external Brainlab iPlan Net server via the DICOM standard. Hence, all language-positive spots derived from preoperative nTMS mapping were implemented into the neuronavigation system, and these functional landmarks were used for resection planning and intraoperative resection guidance in all patients. Tumor resection was then performed during an awake surgery approach, which included intraoperative neuronavigation, intraoperative DCS, and intraoperative subcortical stimulation, according to current practice.<sup>21,35,36,47,55</sup>

### Diffusion Tensor Imaging–Fiber Tracking

As described above, all language-positive spots (stimulation spots at which naming errors of the described categories were elicited) were transferred to an external Brainlab iPlan Net server to allow for neuronavigation planning and DTI-FT. Only error points were uploaded to the server, whereas language-negative spots (stimulation spots at which no naming errors were elicited during nTMS) were not taken into account. The software performs DTI-FT based on a deterministic tracking approach, which reconstructs subcortical white matter fibers on the basis of the fiber assignment by continuous tracking (FACT) principle.<sup>32</sup> This software has been used repeatedly for nTMS-based DTI-FT and represents one of the most common and well-distributed clinical tractography tools in neurosurgery.<sup>12,19,50</sup> First, the left-hemispheric and right-hemispheric language-positive nTMS spots were uploaded as 2 separate data files, and both were fused with the same preoperatively obtained FLAIR, gradient echo, and DTI sequences. Eddy current correction was applied throughout. The stack of merged data was then used for intraoperative neuronavigation, and it constituted the basis for later DTI-FT. Each imported nTMS spot was displayed as a column consisting of 3 solitary points belonging to the same language-positive nTMS spot at 0, 5, and 10 mm from the cortical surface in the data set.

Next, objects eligible for subsequent DTI-FT had to be determined for the software. Thus, the file containing all left-hemispheric language-positive spots was displayed, and the whole group of these individual spots was defined as the first object (O1). The same was done with the right-

hemispheric language-positive spots in an analogous way: the corresponding file was opened, and the entire group of right-hemispheric spots was defined as the second object (O2). Consequently, 2 single objects (O1 and O2) were created. Then, 2 separate regions of interest (ROIs) were generated from these objects by simply defining each object as a single ROI. Accordingly, O1, which was previously generated from the left-hemispheric data file, became the left-hemispheric ROI, whereas O2 became the right-hemispheric ROI (Fig. 1). During the step of ROI definition, an additional rim of 5 mm was added to each language-positive spot. As a result, 2 ROIs were visualized: The first ROI solely consisted of left-hemispheric language-positive spots, whereas the second one only included right-hemispheric points derived from the nTMS data. The immediate definition of O1 and O2 as ROIs replaces the conventional drawing method for ROI definition.

Subsequently, tracking of white matter fibers that were connecting these 2 ROIs was performed with a minimum fiber length of 40 mm. Regarding the fractional anisotropy (FA), tracking was conducted separately with 2 values (0.01 and 0.2) until predefined stop criteria were reached (FA value, fiber angulation > 30°). In this context, 0.01 represents the lowest FA value technically possible for DTI-FT, whereas 0.2 led to reliable results in nTMS-based tractography of motor pathways in recent trials.<sup>12,19</sup> With respect to these adjustments, the DTI-FT algorithm calculated all fibers in between the 2 ROIs. If no fibers were tracked, the condition was defined as IC– (no IC detectable; Fig. 1 left), whereas the visualization of at least 1 fiber connecting the 2 ROIs was defined as IC+ (IC detectable; Fig. 1 right). In cases of IC+, the software's output consisted of a directionally encoded color map of white matter fibers, which all originated from either the left- or right-hemispheric ROI and went to the contralateral ROI. By definition, for later correlation with clinical data, nTMS-based IC was present when there was at least 1 fiber visualized that connected the left-hemispheric ROI with the right-hemispheric ROI (IC+), whereas there was no nTMS-based IC registered when there were no fibers present between these 2 ROIs (IC–). Furthermore, the software displayed the overall number of tracked fibers. If no nTMS-based IC was present (IC–), the corresponding fiber number was 0.

To additionally evaluate the quality of DTI scans (especially in cases where no nTMS-based IC was revealed), DTI-FT was performed separately with a manually drawn ROI at the CC without the language-positive nTMS spots to track callosal fibers.

In addition to the language-positive nTMS spots that were displayed during intraoperative neuronavigation, DTI-FT results in the affected hemisphere were also accessible during surgery. However, the results of the nTMS-based IC assessment were not provided before or during tumor resection.

### Statistical Analysis

All statistical data analyses were performed using GraphPad Prism (GraphPad Prism 6.04). Regarding patient and mapping-related characteristics as well as fiber numbers, the mean ± SD, median, minimum, and maximum values are reported. Differences between left- and

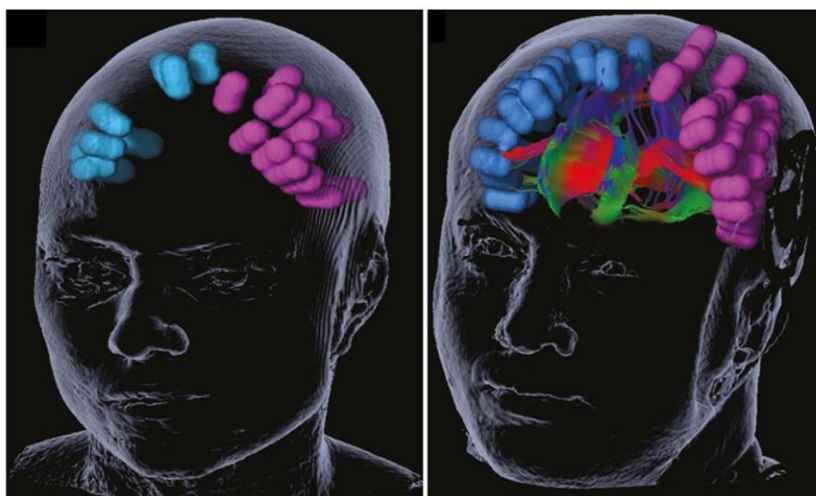


**FIG. 1.** Illustrative cases of DTI-FT based on nTMS mapping results. The **left** panel shows unsuccessful DTI-FT for detection of IC (no IC detectable = IC-), whereas the **right** panel shows a case in which DTI-FT led to visualization of IC (IC detected = IC+). In the right panel, detected IC is visualized by directionally encoded subcortical white matter fibers between the left- and right-hemispheric ROIs. Left-hemispheric language-positive nTMS spots constituted the left-hemispheric ROI (shown in purple), whereas the right-hemispheric ROI consists of all right-hemispheric language-positive nTMS points (depicted in blue). Language-positive nTMS spots are specific cortical points that were prone to a certain kind of naming error during nTMS mapping in combination with an object-naming task. Figure is available in color online only.

right-hemispheric mapping parameters were tested by an independent samples t-test (statistical significance  $p < 0.05$ ).

Regarding aphasia, contingency tables were generated based on the total number of patients diagnosed with or without aphasia preoperatively, on the 5th postoperative day, and during follow-up after 3 months in relation to the detectability of IC by nTMS-based DTI-FT. To assess whether nTMS-based IC could serve as a predictive parameter for aphasia in patients with brain tumors, the OR and the corresponding 95% CI were calculated. Moreover, a chi-square test revealed whether differences in these characteristics were significant or not (statistical significance  $p < 0.05$ ).

In addition, we calculated receiver operating characteristics (sensitivity, specificity, positive predictive value [PPV], and negative predictive value [NPV]) based on the obtained DTI-FT results.<sup>26</sup> In this context, aphasia represented the ground truth, and the following conditions were defined as follows: 1) true-positive (TP)—IC was detected and aphasia was found; 2) true-negative (TN)—no IC was detected and no aphasia was found; 3) false-positive (FP)—IC was detected and no aphasia was found; and 4) false-negative (FN)—no IC was detected and aphasia was found.

Based on these 4 conditions, the potential influence of the PTI on the obtained tracking results was examined because 2 different PTIs were used during language mapping in the present study (300 msec and 0 msec). This was done by additional contingency analyses systematically comparing these conditions between the patients who were mapped with 300 msec and 0 msec. Again, a chi-square test was used to assess statistical significance (statistical significance  $p < 0.05$ ).

## Results

### Patient Characteristics

The median age of the cohort, which consisted of 12 women (31.6%) and 26 men (68.4%), was 39 years (range 20–74 years). According to the Edinburgh Handedness Inventory (EHI), 35 subjects (92.1%) were right-handed (EHI  $80.1 \pm 21.5$ ), whereas the remaining 3 patients (7.9%) were left-handed or ambidextrous (EHI  $-63.0 \pm 47.8$ ). All enrolled patients were considered suitable for nTMS language mapping.

Seventeen patients (44.7%) suffered from surgery-related worsening of language performance. Of these 17 patients, 16 (42.1%) were diagnosed with transient aphasia, meaning that language function resolved at least to the preoperative state during the 3-month follow-up interval. Furthermore, 1 patient (2.6%) was diagnosed with a new permanent aphasia that did not resolve to the initial preoperative status during the 3-month follow-up interval. Table 1 gives an overview of subject-related characteristics, including tumor entities and aphasia grades for each patient.

### Navigated TMS Mapping

Left-hemispheric and right-hemispheric cortical language mapping by nTMS was achieved successfully in all patients enrolled. Each patient had at least 1 language-positive point on each hemisphere with respect to the definition of language-positive nTMS spots given in the *Methods* section, and language-positive spots were found close to the tumor in all patients with surgery-related worsening of language function. Furthermore, left-hemispheric nTMS resulted in language-positive spots in all left-handed or ambidextrous patients, and left-hemispheric intraoperative

DCS elicited clear naming errors in these cases as well. During nTMS mapping, no adverse events were observed.

Furthermore, the mean left-hemispheric RMT was  $33.2\% \pm 7.4\%$  (range 21%–58%) and the analogous right-hemispheric RMT was  $32.4\% \pm 7.7\%$  on average (range 21%–58%;  $p = 0.6712$ ). The mapping intensity related to the individual RMT ranged from 80% to 120% RMT according to the mapping protocol, with a mean of  $104.0\% \pm 9.0\%$ . Table 1 summarizes nTMS mapping parameters for all individuals separately.

### Diffusion Tensor Imaging–Fiber Tracking

Using an FA value of 0.01, nTMS-based IC was detected in 16 of 38 patients (IC+ 42.1%), whereas no connectivity was found in the remaining 22 patients (IC– 57.9%). During DTI-FT with the CC as the ROI, numerous fibers were detected in all patients. Within the group of patients in whom connectivity was identified, the mean number of visualized interhemispheric fibers was  $260.5 \pm 394.7$  (range 1–1217 fibers; Table 1).

Furthermore, tracking with an FA value of 0.2 resulted in detection of nTMS-based IC in 10 of 38 patients (IC+ 26.3%), whereas no connectivity was revealed in 28 patients (IC– 73.7%). The corresponding mean number of visualized interhemispheric fibers was  $111.0 \pm 118.2$  (range 2–332 fibers; Table 1).

Table 2 compares the number of patients suffering from aphasia with the number of patients in whom no aphasia was found in relation to the presence of nTMS-based IC for both FA values used. Regarding the comparison for postoperative and surgery-related aphasia for FA = 0.01, there were statistically significant differences (postoperative aphasia:  $p = 0.0161$ , OR 0.1429, 95% CI 0.0261–0.7831; surgery-related aphasia:  $p = 0.0111$ , OR 0.1705, 95% CI 0.0415–0.7008).

TABLE 2. Interhemispheric connectivity and aphasia\*

Aphasia	FA = 0.01			FA = 0.2		
	IC+	IC–	p Value	IC+	IC–	p Value
Preop			0.6456			0.4752
No	9	14		7	16	
Yes	7	8		3	12	
Postop			0.0161			0.0404
No	2	11		1	13	
Yes	14	11		9	15	
Follow-up			0.1687			0.5045
No	9	17		6	20	
Yes	7	5		4	8	
Surgery-related			0.0111			0.0090
No	5	16		2	19	
Yes	11	6		8	9	

\* Comparison between the number of patients suffering from aphasia and the number of patients in whom no aphasia was found correlated to the presence of IC (IC detected = IC+; no IC detectable = IC–) for both FA values used in the present study. The analysis differentiates between preoperative, postoperative, follow-up, and surgery-related aphasia. There were statistically significant differences for the postoperative (FA = 0.01,  $p = 0.0161$ ; FA = 0.2,  $p = 0.0404$ ) and surgery-related aphasia (FA = 0.01,  $p = 0.0111$ ; FA = 0.2,  $p = 0.0090$ ).

Concerning the corresponding results of the second FA adjustment used in the present study (FA = 0.2), there were also statistically significant differences found for postoperative and surgery-related aphasia (postoperative aphasia:  $p = 0.0404$ , OR 0.1282, 95% CI 0.0143–1.1520; surgery-related aphasia:  $p = 0.0090$ , OR 0.1184, 95% CI 0.0208–0.6754; Table 2).

Sensitivity, specificity, PPV, and NPV for the 2 FA values to predict postoperative and surgery-related aphasia by preoperative nTMS-based IC are displayed in Table 3 and Fig. 2. The figure shows that all data points are clearly above the line  $y = x$  (random performance) and are located within the left or upper-left part of the graph, reflecting comparatively high TP rates in combination with rather low FP rates.

Regarding a potential influence of the PTI on tractography results, we compared TP, TN, FP, and FN values between the patients that were mapped with 300 msec and 0 msec for both FA values used in the present study. Based on these 4 conditions, the comparison between 300 msec and 0 msec for FA = 0.01 was not significant for postoperative aphasia ( $p = 0.1107$ ), but it became statistically significant for surgery-related aphasia ( $p = 0.0387$ ). Concerning tracking with FA = 0.2, the comparisons for postoperative and surgery-related aphasia were not statistically significant ( $p = 0.1557$  and  $p = 0.1072$ , respectively).

## Discussion

### Navigated TMS–Based DTI-FT Related to Aphasia

The present study explores whether IC detected by nTMS-based DTI-FT can be used to predict surgery-related aphasia in patients with brain tumors. With regard to language function on the 5th postoperative day of our patient cohort, there were statistically significant differences revealed for both DTI-FT adjustments (Table 2). Furthermore, nTMS-based IC was found to a variable degree but less frequently in patients without postoperative aphasia compared with the group of patients suffering from postoperative aphasia. A similar correlation of nTMS-based IC and aphasia was also found for surgery-related language impairment. However, all patients who were diagnosed with postoperative worsening of language function suffered from transient aphasia, except for 1 patient who suffered from permanent aphasia (Table 1). This finding seems to restrict the implications of our findings to transient aphasia.

Because nTMS-based IC was not detected in each enrolled patient, we have to be aware of the fact that structural connection between hemispheres is, of course, present in all patients regardless of their grades of language deficits, which was proven by DTI-FT with the CC as the ROI for DTI scan quality assessment in the present trial. In this context, the present study does not claim that anatomical IC is not present in patients where nTMS-based IC was not detectable. Instead, it shows that no detectable IC exclusively based on DTI-FT using individually assessed language mapping data might allow one to draw conclusions about the individual aphasia risk.

Many studies using different neuroimaging modalities have reported on language reorganization within the hu-

**TABLE 3. Sensitivity, specificity, PPV, and NPV\***

Characteristic	FA = 0.01		FA = 0.2	
	% w/ Postop Aphasia	% w/ Surgery-Related Aphasia	% w/ Postop Aphasia	% w/ Surgery-Related Aphasia
PPV	88	69	90	80
NPV	50	73	46	68
Sensitivity	56	65	38	47
Specificity	85	76	93	90

\* This table shows the sensitivity, specificity, PPV, and NPV for the 2 FA groups to predict postoperative and surgery-related aphasia by preoperative IC based on nTMS data. Regarding surgery-related aphasia, 16 patients (42.1%) suffered from a transient deficit, whereas 1 patient (2.6%) was diagnosed with a new permanent surgery-related aphasia.

man brain due to intracranial pathologies.<sup>3,6,20,42,60</sup> In this context, language plasticity was reported to occur as a partial shift of language function to the unaffected brain hemisphere. This principally suggests an interhemispheric reorganization of language function to compensate for impaired cerebral language function.<sup>3,6,20,42,60</sup> At least since the early split-brain examinations, it has been known that the CC as the main anatomical correlate of structural IC plays an important role, especially for the integrity of language functions.<sup>13,14</sup>

As an interpretation, the detectability of nTMS-based IC might reflect the manifestation of early compensatory mechanisms for recovery of language function via an interhemispheric functional shift when language function is already at risk prior to surgery, because data for DTI-FT are solely based on individual functional data in the present study. Basically, this hypothesis is in good agreement with the aforementioned literature on interhemi-

spheric language reorganization.<sup>3,6,20,42,60</sup> Moreover, there are initial fMRI-based studies that report enhanced IC in the context of motor and language compensation mechanisms.<sup>31,39</sup>

Regarding the motor system, it was recently shown that motor recovery after stroke is associated with an enhancement of resting-state IC between motor cortices, suggesting compensatory or reactive neural plasticity.<sup>31</sup> With respect to the present study, the finding that task-dependent IC of the language network was increased preoperatively within a cohort of patients with epilepsy might be more important.<sup>39</sup> In this context, a decline during postoperative language tests correlated positively with the strength of preoperative IC, meaning that patients who showed the greatest worsening of language function after surgery were those who previously showed the strongest functional IC.<sup>39</sup> Hence, stronger preoperative IC appeared to be an unfavorable prognostic biomarker, and one could speculate that a correlate in the form of nTMS-based IC was identified in the present study among patients with brain tumors.

However, it is still a topic of debate how the CC mediates information transfer between hemispheres.<sup>58</sup> In this context, theories of inhibition and excitation exist, and both seem to be probable candidates to adequately describe callosal function.<sup>58</sup> With respect to our approach, it could be the case that inhibitory fibers are primarily detected by nTMS-based DTI-FT, which might explain postoperative language worsening due to interhemispheric inhibition. This is speculative and cannot be demonstrated by our present results, but it reflects a hypothetical explanation from a neuroanatomical perspective.

Whereas postoperative aphasia includes both tumor-induced (preoperative) and surgery-related language deficits, surgery-related aphasia solely depicts new or aggravated language impairment due to tumor resection itself. Thus, for these categories, IC detected by nTMS-based DTI-FT could be regarded as a risk factor for the occurrence of at least transient aphasia in patients with brain tumors with a comparatively high specificity, depending on the FA value (Table 3, Fig. 2). However, we are not aware of other literature distinctly investigating IC as a potential aphasia risk factor in patients with brain tumors. Thus, this interpretation has to be confirmed by future studies that include more patients.

We have to note that the reorganization of language function does not seem to be able to compensate for all

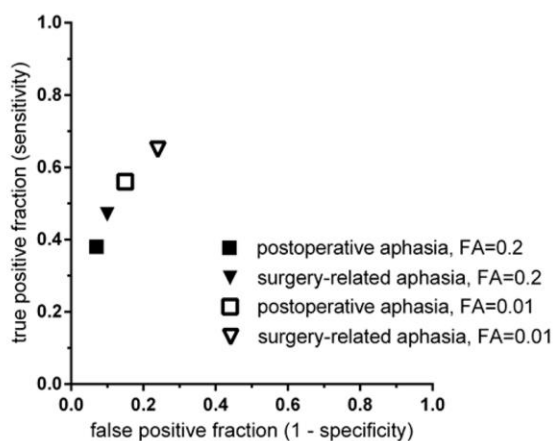


**FIG. 2.** The TP versus FP fraction for DTI-FT of IC. In this figure, the results for sensitivity are plotted against 1 – specificity for DTI-FT performed with an FA of 0.01 and 0.2 in relation to postoperative and surgery-related aphasia, respectively. For sensitivity, specificity, PPV, and NPV, the following criteria were defined: 1) TP—IC was detected and aphasia was found; 2) TN—no IC was detected and no aphasia was found; 3) FP—IC was detected and no aphasia was found; and 4) FN—no IC was detected and aphasia was found. All 4 data points are above  $y = x$  (random performance) and are located within the left or upper-left part of the graph, which indicates comparatively high TP rates in combination with low FP rates.

functional impairments in every case.<sup>20,42</sup> This finding might be reflected by the occurrence of aphasia in some patients in whom nTMS-based IC was not revealed (Table 2). In this context, we should be aware of investigations showing that language shift to the unaffected hemisphere could also lead to a reduction of language abilities in subgroups of patients.<sup>48</sup> This demonstrates that an ideal correlation or corresponding OR between nTMS-based IC and aphasia might not be achievable per se.

### Significance of the Present Study

In general, the creation of ROIs can be performed according to either anatomical or functional data. However, ROI seeding based on anatomical structures depends on the anatomical knowledge of the examiner and is therefore likely to vary from one operator to another.<sup>4,59</sup> More importantly, correct identification of anatomical landmarks is challenging in patients suffering from intracranial lesions due to the spatial derangement of subcortical fiber pathways.<sup>29,34,40</sup> For these reasons, the placement of ROIs based on functional data can be favored, and nTMS mapping is a new modality that can generate data technically suitable for subsequent DTI-FT. In this context, some studies have already successfully used cortical nTMS maps as a source for DTI-FT.<sup>5,11,12,19,50,61</sup>

As described initially, all language-positive spots derived from preoperative nTMS mapping were implemented into the neuronavigation system and were accessible during surgery. Although the present study does not focus on the correlation between preoperative nTMS maps and intraoperative DCS results, it should be mentioned that a good correlation of nTMS and DCS language maps has been demonstrated.<sup>16,21,36,53,56</sup> Interestingly, the overall agreement between nTMS and DCS language maps was higher when compared with corresponding results of fMRI or magnetoencephalography versus DCS.<sup>16,53,56</sup> However, nTMS performed with the current stimulation protocols has been shown to be more sensitive and less specific when compared with DCS.<sup>16,36</sup>

Furthermore, there are hints that nTMS language mapping might have a positive impact on clinical parameters because it has been shown to be associated with smaller craniotomies and lower postoperative deficit rates.<sup>52</sup> The present study explored whether nTMS-based DTI-FT can be used to predict surgery-related aphasia, thereby providing further evidence that nTMS might potentially expand its role as a beneficial tool in neuro-oncological patients.

Overall, the majority of patients with new language deficits were diagnosed with transient aphasia (Table 1). Therefore, we may only be able to state that IC detected by nTMS-based DTI-FT correlates with transient aphasia. This is because only 1 patient suffered from a new permanent aphasia, whereas all other patients showed no new or only transient language impairment. This observation does not imply that our approach is inapplicable to permanent aphasia in general, but rather suggests that larger patient cohorts or multicenter studies are needed to enroll enough patients with permanent deficits to confirm our results. In the present study, the single patient with permanent deficits showed IC, which could be a motivating factor for performing future investigations.

Moreover, although the aphasia grading used in the present study is regarded as sufficiently accurate for most neurosurgical patients,<sup>21,52</sup> it still seems to be comparatively rough from a more linguistic point of view. Language function is complex, and most postoperative neurosurgical classifications might not cover all aspects of language during the testing period. In other words, some patients might be diagnosed with no impairment even though there is a certain degree of slight or subclinical deficit present. Such impairment is not likely to be relevant for the overall neurosurgical evaluation, but we hypothesize that the use of more sensitive assessments could improve the specificity of our approach. The functional outcome of the patient is important and becomes increasingly crucial for the evaluation of the neurosurgeon's success within the context of the individual onco-functional balance.<sup>10</sup> Thus, predictive tools such as our approach, in combination with finer-grained clinical assessments, seem to be gaining increased importance.

Although IC might primarily be regarded as a risk factor for transient aphasia, it can still be beneficial in daily clinical practice from both the neurosurgeon's and the patient's perspective. From both viewpoints, preoperative risk stratification is valuable because it is intended to inherently support decision making. For the neurosurgeon, detection of nTMS-based IC might create awareness of language function being at risk even in patients for whom mere anatomical imaging may not have suggested it. The result could be more careful and thorough intraoperative stimulation to preserve function. Additionally, preoperative patient consultation might be improved because any statements about the functional outcome could be supported by clinical data derived from individual nTMS-based DTI-FT. Moreover, from the patient's perspective, preoperative knowledge about the presumable postoperative status might influence the decision for or against surgery, in a more enlightened state. The present approach mainly provided data for transient deficits, but prediction of this kind of temporary impairment could strengthen the postoperative acceptance of transient impairments among patients. Although a specificity of up to 93% was shown in the present study (Table 3 and Fig. 2), further potential benefits of our approach should be carefully tested in upcoming studies.

Although the ROC and corresponding ORs do not reach optimal values, they still allow for functional assessment and consultation of each patient via individualized functional data. In this context, the data points in Fig. 2, which graphically depicts the results of sensitivity against 1 – specificity, can be found above  $y = x$  (diagonal line reflecting random performance). Generally, each data point is characterized by a TP–FP rate pair, and high TP rates in combination with low FP rates symbolize perfect classification.<sup>26</sup> Thus, the upper triangular region above  $y = x$  contains spots with high TP–low FP values. All of our data points are localized within this area (Fig. 2), indicating comparatively high quality of our testing approach. We are not aware of any previous trials to investigate the surgery-related aphasia risk in patients with brain tumors, based on individual functional data. Hence, the present study represents an encouraging first approach for presurgical

risk stratification in such patients. As aforementioned, this additional information might contribute to individual decision making and the preservation of neurological function as the crucial goal in neurosurgery.<sup>10</sup>

### Limitations of DTI-FT

Although our results are promising and should be valuable for individual assessment of the postoperative aphasia risk, we must be aware of some limitations of the DTI-FT technique. With regard to crossing or kissing white matter fiber bundles, it has been demonstrated that reliable reconstruction of such fiber courses can be challenging (or even impossible) for the tracking algorithms. This is because DTI is still unable to resolve more than a single fiber direction within each imaging voxel.<sup>2,8,19,27</sup> Especially when the FA value is set comparatively low and, therefore, a high number of fibers is visualized, this limitation can influence the correct fiber visualization. The tracking result might then not necessarily reflect reality. However, new technical approaches, such as q-ball imaging, may compensate for the problem of fiber crossings.<sup>33,57</sup>

Furthermore, DTI-FT of fiber tracts in the vicinity of a brain tumor or within tumor-related edema can be vulnerable to FN results, mainly due to low anisotropy values.<sup>2,19</sup> In an area where tumor infiltration can be found, the normal white matter architecture of the brain is disordered. More than 1 fiber population probably occupies the same voxel, which makes it complicated to reliably reconstruct white matter pathways.<sup>2,18,38</sup> Yet, our study shows increases in fiber tracts when tumor infiltration is close to functional pathways. Thus, reducing this shortcoming of reduced fiber reconstruction in the vicinity of intracerebral lesions might even increase the PPV and specificity of our presented approach.

Moreover, as already discussed, the majority of patients who showed new language deficits postoperatively were diagnosed with transient aphasia (Table 1). As a consequence, we might only be able to state that IC detected by nTMS-based DTI-FT correlates with transient aphasia, although 1 patient with a permanent deficit and IC was detected. In addition to nTMS-based IC, which might act as a risk factor for surgery-related aphasia in the present study, other parameters may also contribute to surgery-related language deficits. Although the present study enrolled a rather large cohort of patients with brain tumors, it did not systematically account for other factors (e.g., the tumor entity or tumor size) within the scope of a multivariate analysis. To perform this type of statistical evaluation, further studies that enroll more patients are needed.

Regarding a potential influence of the PTI on tractography results, the comparison concerning postoperative aphasia between patients mapped with 300 msec and 0 msec for FA = 0.01 and the comparison for postoperative and surgery-related aphasia for FA = 0.2 were not statistically significant, according to our results. Overall, these analyses suggest that results to predict whether IC detected by nTMS-based DTI-FT correlates with aphasia are not significantly dependent on the PTI used. However, the comparison regarding surgery-related aphasia for FA = 0.01 was statistically significant. Because surgery-related aphasia was comparatively less common among the pa-

tients mapped with 300 msec (Table 1), we suppose that this difference was primarily due to unequal aphasia distribution between the patients mapped with 300 msec and 0 msec.

Although these analyses might show that the results presented in this study are not significantly dependent on the 2 PTIs, we believe it is important to state that there is only 1 nTMS PTI comparison study for preoperative mapping available,<sup>23</sup> and the distinct impact of different PTIs on the intrasubject level has yet to be investigated. As aforementioned, clear evidence for both PTIs is available,<sup>17,41,45,62</sup> but data on the impact of the PTI on tracking results are lacking. Hence, further studies are probably needed to refine our approach.

### Challenges of nTMS-Based DTI-FT

For detection of language-eloquent cortical and subcortical areas, intraoperative stimulation techniques represent the current gold standard in neurosurgery. Numerous studies have tested the accuracy and reliability of DTI-FT for identification of language pathways in comparison with intraoperative mapping, and a good overall correlation between the modalities has been reported.<sup>1,25,28,33</sup> However, the question remains whether tractography that is exclusively derived from nTMS language-positive spots accurately reflects reality. Because the present study focused on the prediction of aphasia, this circumstance should not limit the significance of our work. However, further studies are needed to confirm preoperatively gained nTMS-based DTI-FT results by intraoperative subcortical stimulation.

Besides intraoperative validation, further work investigating optimal tracking parameters for nTMS-based DTI-FT is needed. In this context, our study has shown that the number of visualized fibers and specificity as well as sensitivity values clearly depend on the FA value used for tractography, which could be compensated for by the introduction of an optimal tracking protocol for nTMS-based DTI-FT of subcortical fibers associated with language function.

### Conclusions

In general, IC detected by preoperative nTMS-based DTI-FT can be regarded as a risk factor for aphasia in patients with brain tumors with a specificity of up to 93%. However, because the majority of enrolled patients suffered from transient aphasia postoperatively, it has to be evaluated whether our approach leads to similar results among patients with permanent language deficits. Despite this restriction and the limitations of the DTI technique, this novel approach might allow for individual patient consultation prior to tumor resection in clinical practice.

### Acknowledgments

We gratefully acknowledge the support of the Technische Universität München Graduate School's Faculty Graduate Center of Medicine. This study was completely financed by institutional grants from the Department of Neurosurgery and the Section of Neuroradiology.

### References

1. Bello L, Gambini A, Castellano A, Carrabba G, Acerbi F,

- Fava E, et al: Motor and language DTI Fiber Tracking combined with intraoperative subcortical mapping for surgical removal of gliomas. **Neuroimage** **39**:369–382, 2008
2. Berman JI, Berger MS, Chung SW, Nagarajan SS, Henry RG: Accuracy of diffusion tensor magnetic resonance imaging tractography assessed using intraoperative subcortical stimulation mapping and magnetic source imaging. **J Neurosurg** **107**:488–494, 2007
  3. Briganti C, Sestieri C, Mattei PA, Esposito R, Galzio RJ, Tartaro A, et al: Reorganization of functional connectivity of the language network in patients with brain gliomas. **AJNR Am J Neuroradiol** **33**:1983–1990, 2012
  4. Catani M, Thiebaut de Schotten M: A diffusion tensor imaging tractography atlas for virtual in vivo dissections. **Cortex** **44**:1105–1132, 2008
  5. Conti A, Raffa G, Granata F, Rizzo V, Germanò A, Tomasello F: Navigated transcranial magnetic stimulation for “somatotopic” tractography of the corticospinal tract. **Neurosurgery** **10** (Suppl 4):542–554, 2014
  6. Cousin E, Baciú M, Pichat C, Kahane P, Le Bas JF: Functional MRI evidence for language plasticity in adult epileptic patients: Preliminary results. **Neuropsychiatr Dis Treat** **4**:235–246, 2008
  7. De Witt Hamer PC, Robles SG, Zwinderman AH, Duffau H, Berger MS: Impact of intraoperative stimulation brain mapping on glioma surgery outcome: a meta-analysis. **J Clin Oncol** **30**:2559–2565, 2012
  8. Duffau H: Diffusion tensor imaging is a research and educational tool, but not yet a clinical tool. **World Neurosurg** **82**:e43–e45, 2014
  9. Duffau H, Capelle L, Denvil D, Sichez N, Gatignol P, TAILLANDIER L, et al: Usefulness of intraoperative electrical subcortical mapping during surgery for low-grade gliomas located within eloquent brain regions: functional results in a consecutive series of 103 patients. **J Neurosurg** **98**:764–778, 2003
  10. Duffau H, Mandonnet E: The “onco-functional balance” in surgery for diffuse low-grade glioma: integrating the extent of resection with quality of life. **Acta Neurochir (Wien)** **155**:951–957, 2013
  11. Forster MT, Hoecker AC, Kang JS, Quick J, Seifert V, Hattinen E, et al: Does navigated transcranial stimulation increase the accuracy of tractography? A prospective clinical trial based on intraoperative motor evoked potential monitoring during deep brain stimulation. **Neurosurgery** **76**:766–776, 2015
  12. Frey D, Strack V, Wiener E, Jussen D, Vajkoczy P, Picht T: A new approach for corticospinal tract reconstruction based on navigated transcranial stimulation and standardized fractional anisotropy values. **Neuroimage** **62**:1600–1609, 2012
  13. Gazzaniga MS: Forty-five years of split-brain research and still going strong. **Nat Rev Neurosci** **6**:653–659, 2005
  14. Gazzaniga MS, Sperry RW: Language after section of the cerebral commissures. **Brain** **90**:131–148, 1967
  15. Hernandez-Pavon JC, Mäkelä N, Lehtinen H, Lioumis P, Mäkelä JP: Effects of navigated TMS on object and action naming. **Front Hum Neurosci** **8**:660, 2014
  16. Ille S, Sollmann N, Hauck T, Maurer S, Tanigawa N, Obermüller T, et al: Combined noninvasive language mapping by navigated transcranial magnetic stimulation and functional MRI and its comparison with direct cortical stimulation. **J Neurosurg** **123**:212–225, 2015
  17. Indefrey P: The spatial and temporal signatures of word production components: a critical update. **Front Psychol** **2**:255, 2011
  18. Jones DK: Determining and visualizing uncertainty in estimates of fiber orientation from diffusion tensor MRI. **Magn Reson Med** **49**:7–12, 2003
  19. Krieg SM, Buchmann NH, Gempt J, Shiban E, Meyer B, Ringel F: Diffusion tensor imaging fiber tracking using navigated brain stimulation—a feasibility study. **Acta Neurochir (Wien)** **154**:555–563, 2012
  20. Krieg SM, Sollmann N, Hauck T, Ille S, Foerschler A, Meyer B, et al: Functional language shift to the right hemisphere in patients with language-eloquent brain tumors. **PLoS One** **8**:e75403, 2013
  21. Krieg SM, Sollmann N, Hauck T, Ille S, Meyer B, Ringel F: Repeated mapping of cortical language sites by preoperative navigated transcranial magnetic stimulation compared to repeated intraoperative DCS mapping in awake craniotomy. **BMC Neurosci** **15**:20, 2014
  22. Krieg SM, Sollmann N, Tanigawa N, Foerschler A, Meyer B, Ringel F: Cortical distribution of speech and language errors investigated by visual object naming and navigated transcranial magnetic stimulation. **Brain Struct Funct** [epub ahead of print], 2015
  23. Krieg SM, Tarapore PE, Picht T, Tanigawa N, Houde J, Sollmann N, et al: Optimal timing of pulse onset for language mapping with navigated repetitive transcranial magnetic stimulation. **Neuroimage** **100**:219–236, 2014
  24. Krings T, Chiappa KH, Foltys H, Reinges MH, Cosgrove GR, Thron A: Introducing navigated transcranial magnetic stimulation as a refined brain mapping methodology. **Neurosurg Rev** **24**:171–179, 2001
  25. Kuhnt D, Bauer MH, Becker A, Merhof D, Zolal A, Richter M, et al: Intraoperative visualization of fiber tracking based reconstruction of language pathways in glioma surgery. **Neurosurgery** **70**:911–920, 2012
  26. Lasko TA, Bhagwat JG, Zou KH, Ohno-Machado L: The use of receiver operating characteristic curves in biomedical informatics. **J Biomed Inform** **38**:404–415, 2005
  27. Le Bihan D, Poupon C, Amadon A, Lethimonnier F: Artifacts and pitfalls in diffusion MRI. **J Magn Reson Imaging** **24**:478–488, 2006
  28. Leclercq D, Duffau H, Delmaire C, Capelle L, Gatignol P, Ducros M, et al: Comparison of diffusion tensor imaging tractography of language tracts and intraoperative subcortical stimulations. **J Neurosurg** **112**:503–511, 2010
  29. Lehéricy S, Duffau H, Cornu P, Capelle L, Pidoux B, Carpentier A, et al: Correspondence between functional magnetic resonance imaging somatotopy and individual brain anatomy of the central region: comparison with intraoperative stimulation in patients with brain tumors. **J Neurosurg** **92**:589–598, 2000
  30. Lioumis P, Zhdanov A, Mäkelä N, Lehtinen H, Wilenius J, Neuvonen T, et al: A novel approach for documenting naming errors induced by navigated transcranial magnetic stimulation. **J Neurosci Methods** **204**:349–354, 2012
  31. Liu J, Qin W, Zhang J, Zhang X, Yu C: Enhanced interhemispheric functional connectivity compensates for anatomical connection damages in subcortical stroke. **Stroke** **46**:1045–1051, 2015
  32. Mori S, van Zijl PC: Fiber tracking: principles and strategies—a technical review. **NMR Biomed** **15**:468–480, 2002
  33. Nimsky C, Ganslandt O, Hastreiter P, Wang R, Benner T, Sorensen AG, et al: Preoperative and intraoperative diffusion tensor imaging-based fiber tracking in glioma surgery. **Neurosurgery** **61** (1 Suppl):178–186, 2007
  34. Nimsky C, Ganslandt O, Merhof D, Sorensen AG, Fahlbusch R: Intraoperative visualization of the pyramidal tract by diffusion-tensor-imaging-based fiber tracking. **Neuroimage** **30**:1219–1229, 2006
  35. Picht T, Kombos T, Gramm HJ, Brock M, Suess O: Multimodal protocol for awake craniotomy in language cortex tumour surgery. **Acta Neurochir (Wien)** **148**:127–138, 2006
  36. Picht T, Krieg SM, Sollmann N, Rösler J, Niraula B, Neuvonen T, et al: A comparison of language mapping by preoperative navigated transcranial magnetic stimulation and

- direct cortical stimulation during awake surgery. **Neurosurgery** 72:808–819, 2013
37. Picht T, Mularski S, Kuehn B, Vajkoczy P, Kombos T, Suess O: Navigated transcranial magnetic stimulation for preoperative functional diagnostics in brain tumor surgery. **Neurosurgery** 65 (6 Suppl):93–99, 2009
  38. Pierpaoli C, Jezzard P, Basser PJ, Barnett A, Di Chiro G: Diffusion tensor MR imaging of the human brain. **Radiology** 201:637–648, 1996
  39. Pravatà E, Sestieri C, Colicchio G, Colosimo C, Romani GL, Caulo M: Functional connectivity MRI and post-operative language performance in temporal lobe epilepsy: initial experience. **Neuroradiol J** 27:158–162, 2014
  40. Robles SG, Gatignol P, Lehericy S, Duffau H: Long-term brain plasticity allowing a multistage surgical approach to World Health Organization Grade II gliomas in eloquent areas. **J Neurosurg** 109:615–624, 2008
  41. Rogić M, Deletis V, Fernández-Conejero I: Inducing transient language disruptions by mapping of Broca's area with modified patterned repetitive transcranial magnetic stimulation protocol. **J Neurosurg** 120:1033–1041, 2014
  42. Rösler J, Niraula B, Strack V, Zdunczyk A, Schilt S, Savolainen P, et al: Language mapping in healthy volunteers and brain tumor patients with a novel navigated TMS system: evidence of tumor-induced plasticity. **Clin Neurophysiol** 125:526–536, 2014
  43. Rossini PM, Barker AT, Berardelli A, Caramia MD, Caruso G, Cracco RQ, et al: Non-invasive electrical and magnetic stimulation of the brain, spinal cord and roots: basic principles and procedures for routine clinical application. Report of an IFCN committee. **Electroencephalogr Clin Neurophysiol** 91:79–92, 1994
  44. Ruohonen J, Karhu J: Navigated transcranial magnetic stimulation. **Neurophysiol Clin** 40:7–17, 2010
  45. Salmelin R, Helenius P, Service E: Neurophysiology of fluent and impaired reading: a magnetoencephalographic approach. **J Clin Neurophysiol** 17:163–174, 2000
  46. Sanai N, Berger MS: Intraoperative stimulation techniques for functional pathway preservation and glioma resection. **Neurosurg Focus** 28(2):E1, 2010
  47. Sanai N, Mirzadeh Z, Berger MS: Functional outcome after language mapping for glioma resection. **N Engl J Med** 358:18–27, 2008
  48. Saur D, Lange R, Baumgaertner A, Schraknepper V, Willmes K, Rijntjes M, et al: Dynamics of language reorganization after stroke. **Brain** 129:1371–1384, 2006
  49. Snodgrass JG, Vanderwart M: A standardized set of 260 pictures: norms for name agreement, image agreement, familiarity, and visual complexity. **J Exp Psychol Hum Learn** 6:174–215, 1980
  50. Sollmann N, Giglhuber K, Tussis L, Meyer B, Ringel F, Krieg SM: nTMS-based DTI fiber tracking for language pathways correlates with language function and aphasia – A case report. **Clin Neurol Neurosurg** 136:25–28, 2015
  51. Sollmann N, Hauck T, Hapfelmeier A, Meyer B, Ringel F, Krieg SM: Intra- and interobserver variability of language mapping by navigated transcranial magnetic brain stimulation. **BMC Neurosci** 14:150, 2013
  52. Sollmann N, Ille S, Hauck T, Maurer S, Negwer C, Zimmer C, et al: The impact of preoperative language mapping by repetitive navigated transcranial magnetic stimulation on the clinical course of brain tumor patients. **BMC Cancer** 15:261, 2015
  53. Sollmann N, Picht T, Mäkelä JP, Meyer B, Ringel F, Krieg SM: Navigated transcranial magnetic stimulation for preoperative language mapping in a patient with a left frontoopercular glioblastoma. **J Neurosurg** 118:175–179, 2013
  54. Sollmann N, Tanigawa N, Ringel F, Zimmer C, Meyer B, Krieg SM: Language and its right-hemispheric distribution in healthy brains: An investigation by repetitive transcranial magnetic stimulation. **Neuroimage** 102 (Pt 2):776–788, 2014
  55. Szelényi A, Bello L, Duffau H, Fava E, Feigl GC, Galanda M, et al: Intraoperative electrical stimulation in awake craniotomy: methodological aspects of current practice. **Neurosurg Focus** 28(2):E7, 2010
  56. Tarapore PE, Findlay AM, Honma SM, Mizuiri D, Houde JF, Berger MS, et al: Language mapping with navigated repetitive TMS: proof of technique and validation. **Neuroimage** 82:260–272, 2013
  57. Tuch DS, Reese TG, Wiegell MR, Wedeen VJ: Diffusion MRI of complex neural architecture. **Neuron** 40:885–895, 2003
  58. van der Knaap LJ, van der Ham IJ: How does the corpus callosum mediate interhemispheric transfer? A review. **Behav Brain Res** 223:211–221, 2011
  59. Wakana S, Jiang H, Nagae-Poetscher LM, van Zijl PC, Mori S: Fiber tract-based atlas of human white matter anatomy. **Radiology** 230:77–87, 2004
  60. Wang L, Chen D, Yang X, Olson JJ, Gopinath K, Fan T, et al: Group independent component analysis and functional MRI examination of changes in language areas associated with brain tumors at different locations. **PLoS One** 8:e59657, 2013
  61. Weiss C, Tursunova I, Neuschmelting V, Lockau H, Nettekoven C, Oros-Peusquens AM, et al: Improved nTMS- and DTI-derived CST tractography through anatomical ROI seeding on anterior pontine level compared to internal capsule. **Neuroimage Clin** 7:424–437, 2015
  62. Wheat KL, Cornelissen PL, Sack AT, Schuhmann T, Goebel R, Blomert L: Charting the functional relevance of Broca's area for visual word recognition and picture naming in Dutch using fMRI-guided TMS. **Brain Lang** 125:223–230, 2013

## Disclosures

Drs. Krieg and Ringel are consultants for Brainlab AG. Dr. Krieg is also a consultant for Nexstim Oy.

## Author Contributions

Conception and design: Krieg, Sollmann, Negwer, Tussis, Hauck, Ille, Maurer, Giglhuber, Bauer. Analysis and interpretation of data: Krieg, Sollmann, Negwer, Tussis. Drafting the article: Krieg, Sollmann. Critically revising the article: Krieg, Sollmann. Reviewed submitted version of manuscript: Krieg, Hauck, Ille, Maurer, Giglhuber, Bauer, Ringel, Meyer. Approved the final version of the manuscript on behalf of all authors: Krieg. Statistical analysis: Krieg, Sollmann, Negwer. Administrative/technical/material support: Krieg, Ringel, Meyer. Study supervision: Krieg, Meyer.

## Correspondence

Sandro M. Krieg, Department of Neurosurgery, Klinikum rechts der Isar, Technische Universität München, Ismaninger Str. 22, Munich 81675, Germany. email: sandro.krieg@tum.de.